

Air-route(supplementary material)

The 'Active' status of aircraft route carrier.

**Here's an explanation of each column in the provided dataset:**

1. Index: This column seems to represent the index or identifier for each entry in the dataset.
2. Airline ID: An ID assigned to each airline. It uniquely identifies an airline within this dataset.
3. Name: The name of the airline. This column contains the full name of the airline company.
4. Alias: Any alias or alternative name used for the airline. It might contain alternative names or abbreviations.
5. IATA: International Air Transport Association (IATA) code. It's a two-character code assigned to each airline, helping to uniquely identify airlines in the airline industry.
6. ICAO: International Civil Aviation Organization (ICAO) code. Similar to IATA codes, ICAO codes are unique identifiers for airlines. They consist of three or four characters.
7. Callsign: The radio callsign used by the airline. It's the specific name used by pilots and air traffic control when communicating with a particular airline.
8. Country: The country associated with the airline. It indicates the country where the airline is based or registered.
9. Active: Indicates whether the airline is currently active or not. It contains 'Y' for active airlines and 'N' for inactive ones.

This dataset appears to contain information about various airlines, including their names, identification codes, country of operation, and active status. Each row represents a different airline, with specific details about its identification, location, and operational status.

#### LOGISTIC-EQUATION:

Accuracy: 0.8282009724473258

Coefficients: [0.0014888837900653693, 0.0014888837900653693, 0.002940846694653343, -0.0019009857228614222, 0.001450212602931048, 0.0020058713734052765, 0.0025775741975943844, 0.0010261230545502685]

Intercept: -0.0002163885304761421

Logistic Equation:

$$P(\text{Active}=1) = 1 / (1 + e^{-( -0.0002163885304761421 + 0.001488884 * \text{index} + 0.001488884 * \text{Airline ID} + 0.002940847 * \text{Name} + -0.001900986 * \text{Alias} + 0.001450213 * \text{IATA} + 0.002005871 * \text{ICAO} + 0.002577574 * \text{Callsign} + 0.001026123 * \text{Country})})$$

Accuracy: 0.8346839546191248

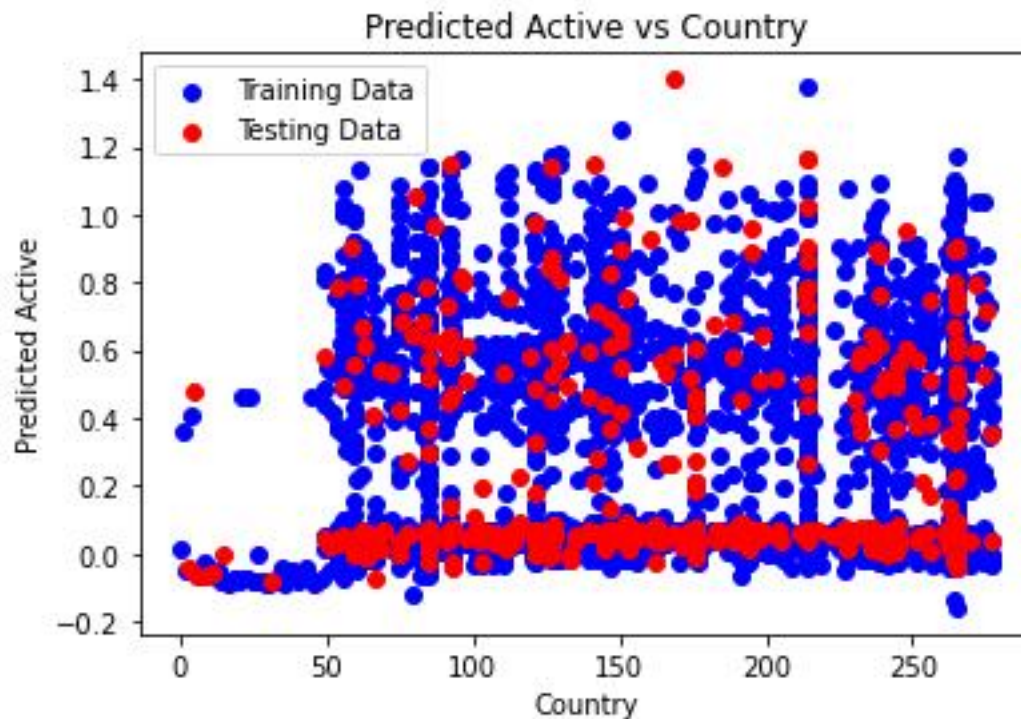
Coefficients: [0.002342848464305821, 0.002342848464305821, 0.0042163501969052705, -0.0016509220835420107, 0.0006884642979800578, 0.003068166564539872, 0.004143627517591879, 0.0011242492366517753]

Intercept: -0.00045813723866787795

Logistic Equation:

$$P(\text{Active}=1) = 1 / (1 + e^{-( -0.00045813723866787795 + 0.002342848 * \text{index} + 0.002342848 * \text{Airline ID} + 0.004216350 * \text{Name} + -0.001650922 * \text{Alias} + 0.000688464 * \text{IATA} + 0.003068167 * \text{ICAO} + 0.004143628 * \text{Callsign} + 0.001124249 * \text{Country})})$$

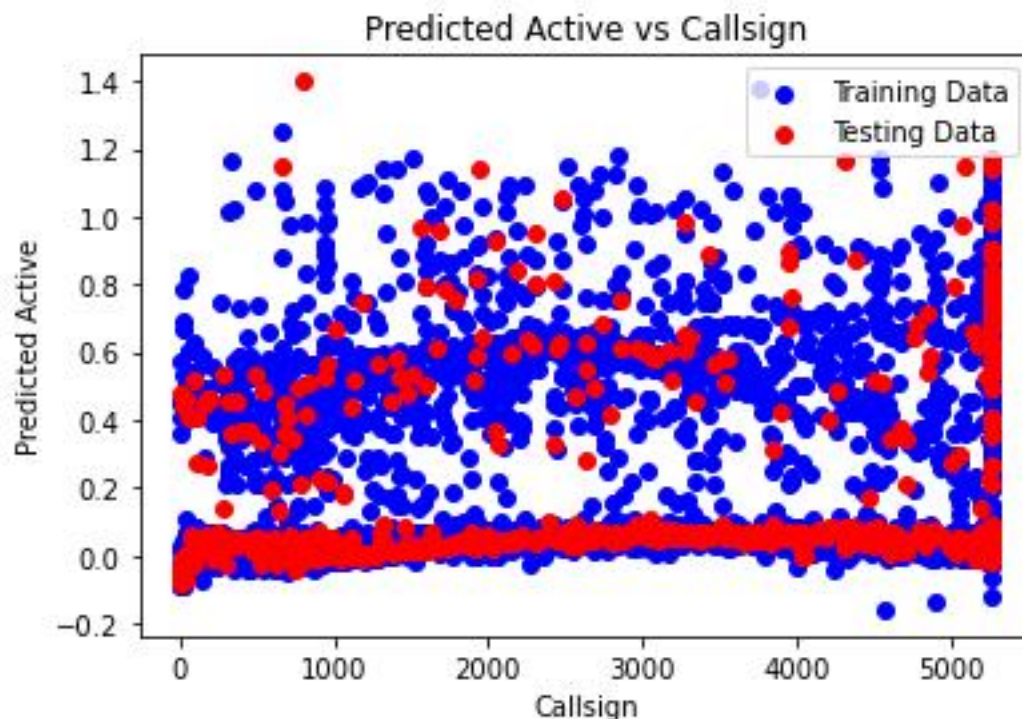
Logistic Equation:  $\sigma(z) = 1/(1+e^{-z})$



The provided scatter plot juxtaposes a model's predicted active cases against actual testing data for various countries. The x-axis, labeled "Country," lacks a numerical scale. Meanwhile, the y-axis, labeled "Predicted Active," spans from 0 to 1.4. The plot comprises two datasets.

A discernible positive correlation exists between the predicted active cases and the testing data, although the fit is not entirely precise. This indicates that the model generally forecasts higher values of active cases for countries with elevated actual active cases. However, considerable dispersion in the data implies that the model's predictions are not consistently accurate. Instances exist where the model overestimated active cases for countries with low actual counts and underestimated them for countries with high actual counts.

In summation, the plot intimates that while the model demonstrates some success in predicting active cases, it is not flawless. There remains scope for refinement and enhancement in its predictive accuracy.



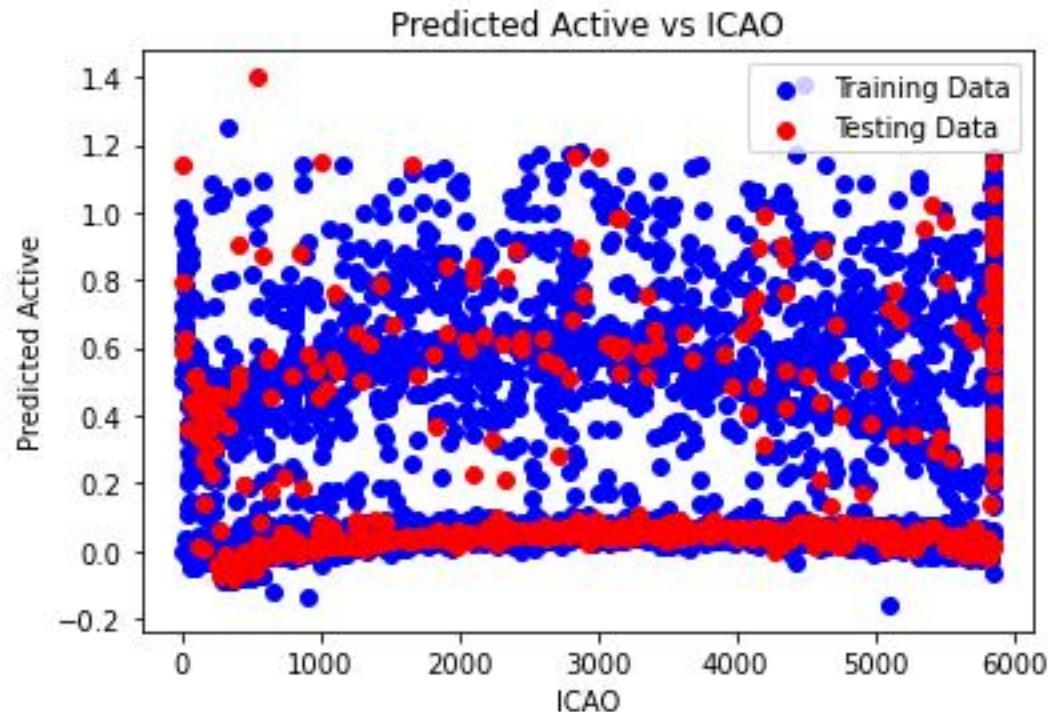
The provided scatter plot depicts the performance of a model in predicting the number of active calls, with the x-axis labeled "Callsign" ranging from 0 to 5000, and the y-axis labeled "Predicted Active" spanning from -0.2 to 1.4. Two datasets are visualized: a red line representing the model's predicted number of active calls and a blue line representing the actual number of calls in the training dataset.

The plot suggests that the model's predictions generally approximate the actual number of calls in the training dataset. However, notable scatter in the data indicates occasional discrepancies between the model's predictions and the actual counts. Instances exist where the model overestimates or underestimates the number of active calls relative to the actual counts associated with specific callsigns.

Additionally, the accompanying text atop the plot clarifies that the red line denotes the model's predictions for the training dataset, while the blue line signifies the actual call counts in the testing dataset. The discernible separation between the two lines implies that the model struggles to generalize effectively to unseen data, potentially indicative of overfitting to the training data.

In summary, while the plot illustrates some success in predicting the number of active calls, it also underscores limitations in the model's generalization capabilities to new data. There exists variability in

the accuracy of predictions, and caution is warranted in relying solely on the model's outputs for decision-making purposes.

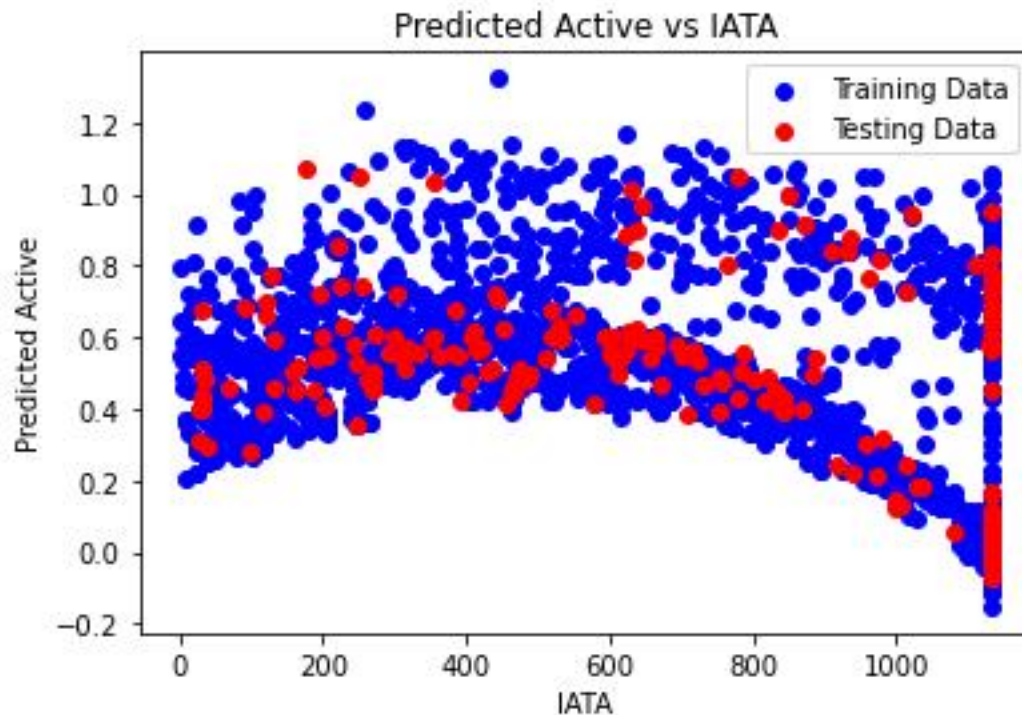


The provided scatter plot illustrates the disparity between a model's predicted and actual active cases across different countries, presumably identified by their ICAO codes. The x-axis is denoted as "ICAO" without a discernible scale, while the y-axis is labeled "Predicted Active - Testing Data," ranging from -0.2 to 1.4. Two datasets are represented: red dots depicting the variance between the model's predicted active cases and the actual testing data.

The scatter plot reveals no discernible trend, indicating that the model's predictions neither consistently overestimate nor underestimate the number of active cases. Instances occur where the model overestimates (positive y-axis values) or underestimates (negative y-axis values) the actual number of active cases for various countries.

It's crucial to acknowledge that the plot solely displays the discrepancy between predicted and actual values, precluding direct insights into the model's accuracy in absolute terms. Without visibility into the actual values, the plot cannot ascertain whether the model consistently tends to overestimate or underestimate active cases.

In summary, while the scatter plot highlights discrepancies between the model's predictions and actual data, it fails to discern a systematic pattern in the errors. Further analysis is imperative to comprehensively evaluate the model's performance and ascertain the factors contributing to prediction inaccuracies.

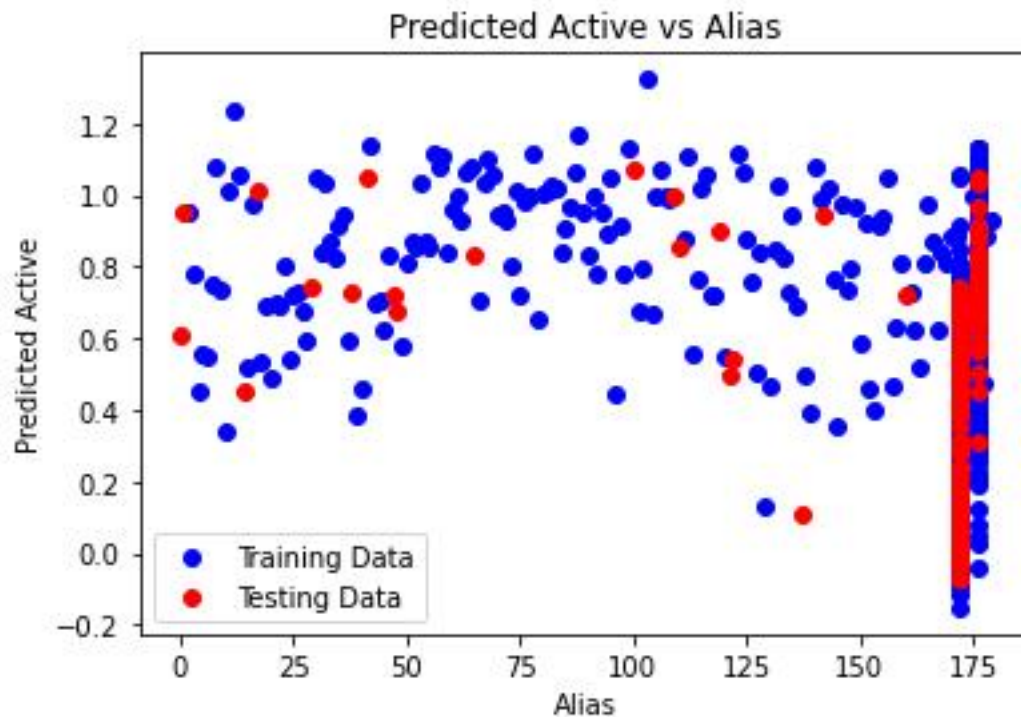


The provided scatter plot compares a model's predicted active cases to actual IATA training data across different countries. The x-axis is labeled "IATA" with a scale ranging from 0 to 1000, while the y-axis is labeled "Predicted Active" and spans from 0 to 1.2. Two datasets are depicted: red dots representing the model's predicted active cases, and blue text along the bottom axis indicating the IATA training data.

A discernible positive correlation is observed between the predicted active cases and the training data, indicating that the model generally predicts higher values for countries with higher IATA values in the training dataset. However, the relationship is not entirely precise, as evidenced by the considerable scatter in the data. This implies that the model's predictions occasionally deviate from the actual values. For instance, instances occur where the model predicts a high number of active cases despite corresponding low IATA values, and vice versa.

Overall, while the plot suggests some success in predicting active cases based on IATA training data, it also highlights areas for enhancement. The model's predictive accuracy could be further refined to minimize discrepancies between predicted and actual values. Continued optimization may lead to more reliable predictions in the future.





The provided scatter plot illustrates the relationship between predicted active cases and an unspecified variable referred to as "Alias." The plot features a red line representing predicted active cases and a blue line representing testing data. The x-axis is labeled "Alias" without a discernible scale, while the y-axis is labeled "Predicted Active," ranging from 0 to 1.4.

A positive correlation is observed between predicted active cases and the testing data, indicating that higher values of active cases are generally associated with higher values of the unspecified "Alias" variable in the testing data. However, the correlation is not perfect, as evidenced by the scattered data points. This variability suggests that the model's predictions do not consistently align with the actual testing data. Notably, instances exist where the model overestimates or underestimates the number of active cases relative to the corresponding values in the testing data.

Given the ambiguity surrounding the nature of the "Alias" variable, precise interpretation of the plot is challenging. However, the overall trend implies that the model exhibits some success in predicting active cases based on the "Alias" data, albeit with room for improvement. Further refinement of the model may enhance its predictive accuracy and reduce discrepancies between predicted and actual values.

The provided scatter plot illustrates the performance of a model for predicting active cases, with the x-axis labeled "Name" and the y-axis labeled "Predicted Active." The y-axis ranges from 0 to 1.2. The plot

features two datasets: red dots representing the model's predicted active cases and blue text along the bottom axis representing the training data.

A weak positive correlation is observed between the predicted active cases and the training data, indicating that the model tends to predict higher values of active cases for entities (countries or other units represented by "Name") with higher values in the training data. However, significant scatter in the data suggests that the model's predictions are not consistently accurate. Instances exist where the model overestimates or underestimates the number of active cases relative to the corresponding values in the training data.

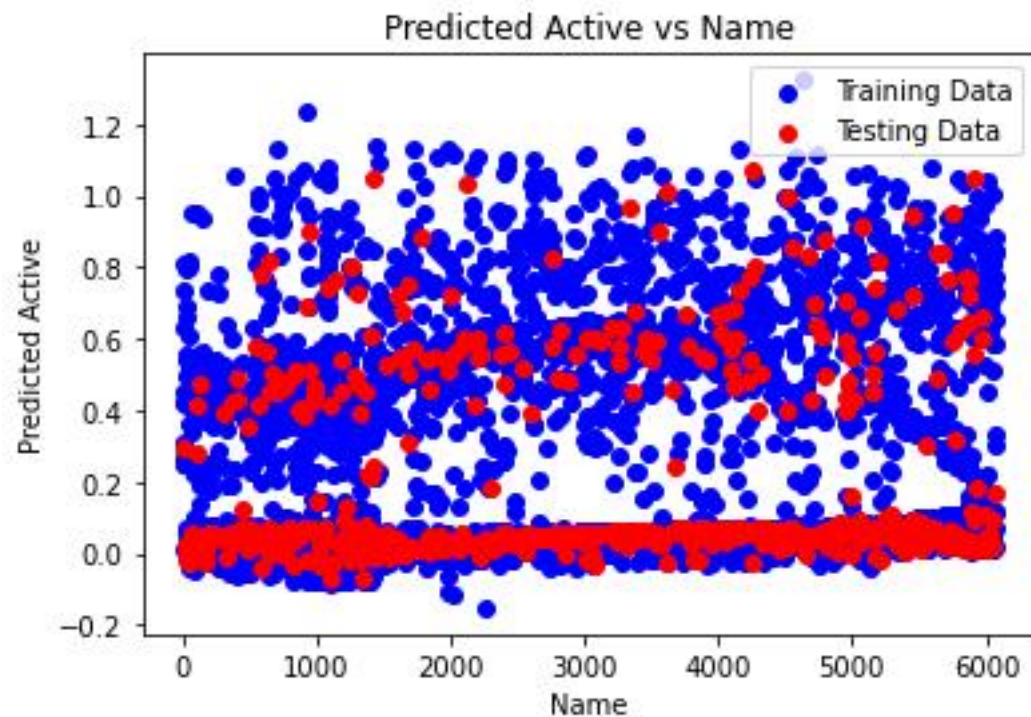
The text at the top of the plot clarifies that the blue labels on the x-axis represent the training data, indicating that the model's performance is evaluated based on this dataset. Ideally, a close alignment between the red dots and the blue labels would indicate strong performance on the training data. However, the presence of scatter suggests that the model's performance is imperfect, indicating potential limitations in its predictive accuracy on the training data.

It's essential to note that the plot does not provide insight into the model's performance on unseen data. Further analysis would be required to assess the model's generalization capabilities beyond the training data.

In summary, the plot suggests that the model exhibits some ability to predict active cases based on the training data, albeit with limited accuracy. Additional analysis is necessary to evaluate the model's



performance on unseen data and identify potential areas for



improvement.

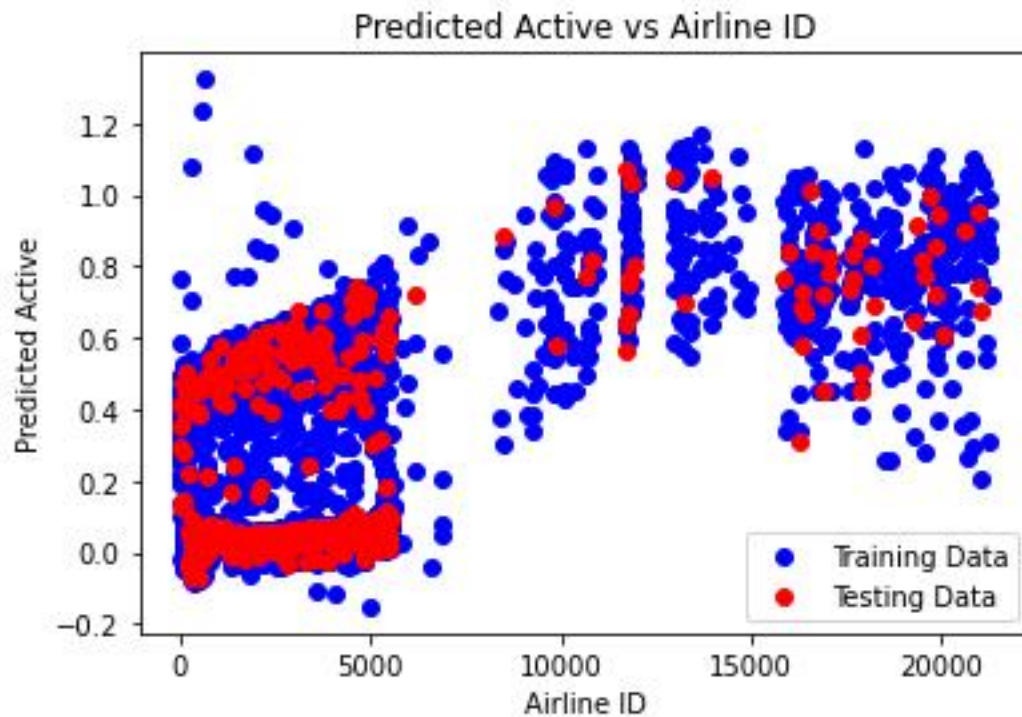
The provided scatter plot illustrates the performance of a predictive model for estimating active cases, with the x-axis labeled "Name" and the y-axis labeled "Predicted Active." The y-axis ranges from 0 to 1.2. The plot contains two datasets: red dots representing the model's predicted active cases and blue text along the bottom axis representing the training data.

A weak positive correlation is observed between the predicted active cases and the training data, indicating that the model tends to predict higher values of active cases for entities (countries or other units represented by "Name") with higher values in the training data. However, significant scatter in the data suggests that the model's predictions are not consistently accurate. Instances exist where the model overestimates or underestimates the number of active cases relative to the corresponding values in the training data.

The text at the top of the plot clarifies that the blue labels on the x-axis represent the training data, indicating that the model's performance is evaluated based on this dataset. Ideally, a close alignment between the red dots and the blue labels would indicate strong performance on the training data. However, the presence of scatter suggests that the model's performance is imperfect, indicating potential limitations in its predictive accuracy on the training data.

It's essential to note that the plot does not provide insight into the model's performance on unseen data. Further analysis would be required to assess the model's generalization capabilities beyond the training data.

In summary, the plot suggests that the model exhibits some ability to predict active cases based on the training data, albeit with limited accuracy. Additional analysis is necessary to evaluate the model's performance on unseen data and identify potential areas for improvement.

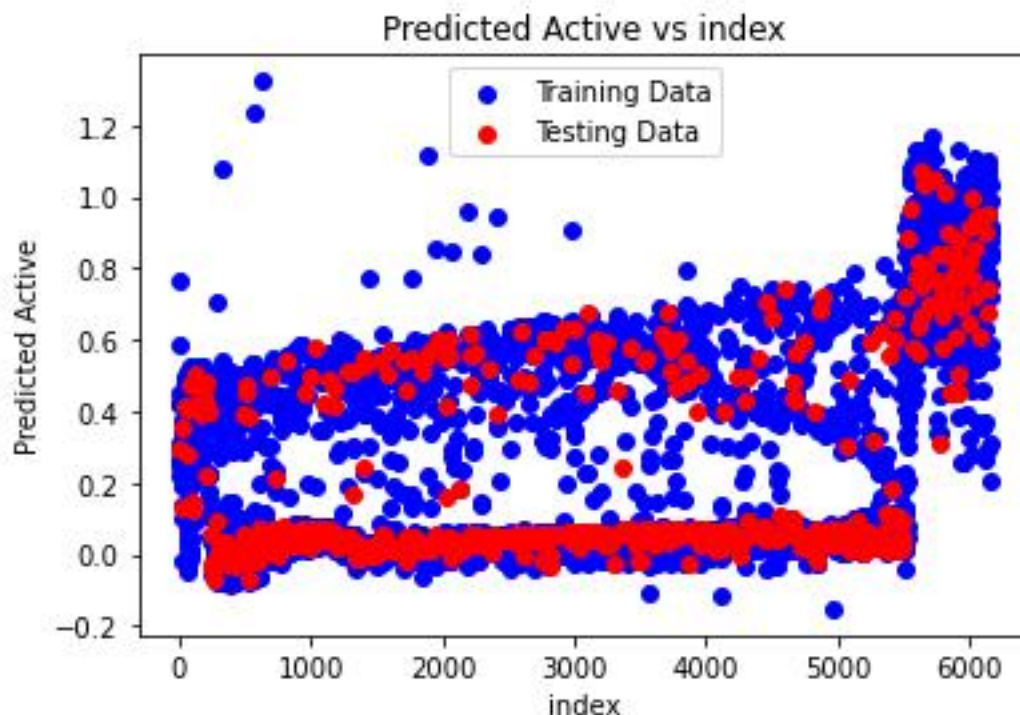


The provided scatter plot illustrates the relationship between a model's predicted active cases and airline ID. The x-axis is labeled "Airline ID," ranging from 0 to 20000, while the y-axis is labeled "Predicted Active," ranging from 0 to 1.2. Two datasets are plotted on the graph.

A positive correlation is observed between the predicted active cases and the testing data, indicating that the model tends to predict higher values for airlines with higher numbers of active cases in the testing data. However, significant scatter in the data suggests that the model's predictions are not consistently accurate. Instances exist where the model overestimates or underestimates the number of active cases relative to the corresponding values in the testing data.

The text at the top of the plot states "Predicted Active vs Airline ID," clarifying the variables being compared. Additionally, the presence of two datasets (red and blue dots) indicates the model's performance on unseen data, with the blue dots representing airline IDs not seen during training. Ideally, a close alignment between the red and blue dots would indicate strong generalization to unseen data. However, the observed scatter suggests imperfect generalization.

In summary, the plot suggests that the model exhibits some ability to predict active cases for airlines, although its accuracy is limited, and its generalization to unseen data is not perfect. Further analysis is necessary to evaluate the model's performance comprehensively and identify potential areas for improvement.

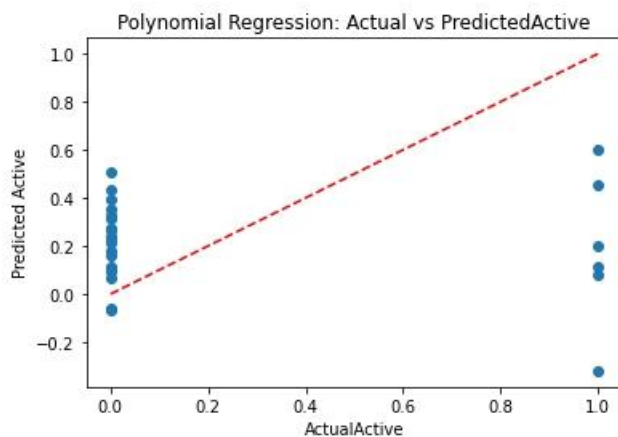


The plot is a scatter plot depicting the performance of a model in predicting active cases. The x-axis is labeled "Index," ranging from 0 to 6000, while the y-axis is labeled "Predicted Active," ranging from 0 to 1.4. It comprises two datasets.

A positive correlation between the predicted active cases and the testing data is observed, indicating that the model generally predicts higher values for entities (indexed by "Index") with higher values in the testing data. However, the correlation is not perfect, as evidenced by the significant scatter in the data. This implies that the model's predictions often deviate from the actual values. Instances exist where the model overestimates or underestimates the number of active cases relative to the corresponding values in the testing data.

The text at the top of the plot clarifies that it represents "Predicted Active vs Index \*Testing Data\*," indicating that the blue line represents the testing data, not the training data. Ideally, close alignment between the red dots and the blue line would signify strong performance of the model on unseen data. However, the presence of scatter indicates that the model's performance is not optimal on the testing data.

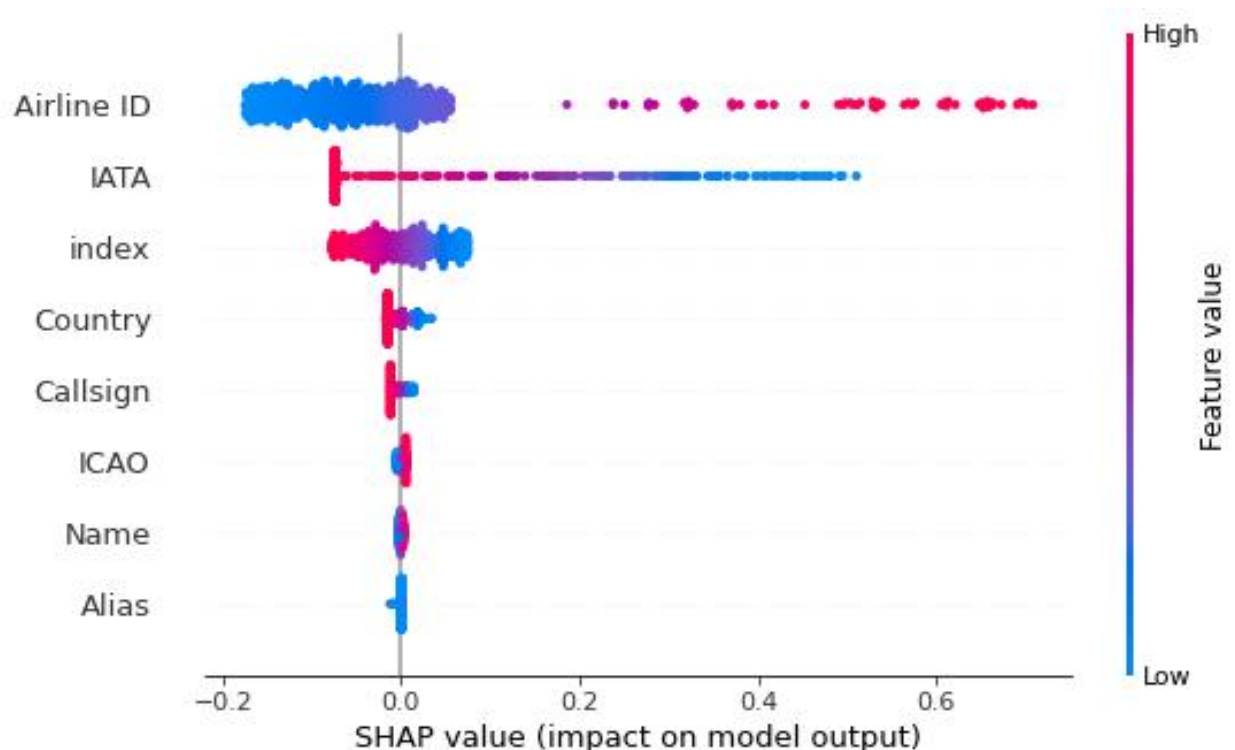
In summary, while the plot suggests that the model possesses some ability to predict active cases based on the testing data, its accuracy is limited. Further analysis is warranted to comprehensively assess the model's performance and identify potential areas for improvement.



The plot a polynomial regression which shows the relationship between predicted active and actual active. The red line represents the predicted active, and the blue line represents the actual active.

In general, a good fit is indicated by a close correspondence between the red line (predicted values) and the blue line (actual values). The closer the two lines are throughout the range of the x-axis, the better the model is at predicting the actual values.

In this specific plot, it appears that the polynomial regression model fits the data well at higher values of actual active (on the right side of the axis), but not as well for lower values (on the left side of the axis). There seems to be a more significant spread of the blue points around the red line on the left side. This suggests that the model may be less accurate at predicting low values of active.



The provided image is a SHAP (SHapley Additive exPlanations) feature importance plot, which illustrates the influence of various features on a machine learning model. The model aims to predict a certain outcome, with the features representing different characteristics of airlines.

Maintenance of Radar system:

describe each feature present in the dataset:

1. index: This column represents the index or identifier of each record in the dataset.
2. X: The X-coordinate or longitude of the antenna structure location.
3. Y: The Y-coordinate or latitude of the antenna structure location.
4. FID: A unique identifier for each antenna structure.
5. REGNUM: Registration number or code associated with the antenna structure.
6. FILENUM: File number associated with the antenna structure.
7. ISSUEDATE: Date when regulatory approval or other significant event related to the antenna structure occurred.
8. ENTITY: Entity or company that owns or operates the antenna structure.
9. LAT\_DMS: Latitude in degrees, minutes, and seconds.
10. LAT\_DIR: Direction indicator for latitude (N for north or S for south).
11. LON\_DMS: Longitude in degrees, minutes, and seconds.

12. LON\_DIR: Direction indicator for longitude (E for east or W for west).
13. DD\_TEMP: Elevation or altitude of the antenna structure.
14. DD\_TEMP0: Additional information related to elevation or altitude.
15. STRUCHT: Type or category of the antenna structure (e.g., tower, mast, rooftop installation).
16. STRUCADD: Address of the antenna structure.
17. STRUCCITY: City where the antenna structure is located.
18. STRUCSTATE: State where the antenna structure is located.
19. FAASTUDY: FAA study number associated with the antenna structure.
20. FAACIRC: FAA circular number associated with the antenna structure.
21. LICID: License ID associated with the antenna structure.
22. CONTNAME: Name of the contact person or entity associated with the antenna structure.
23. CONTADD: Address of the contact person or entity associated with the antenna structure.
24. CONTPO: Post office box or other postal information of the contact person or entity.
25. CONTCITY: City of the contact person or entity associated with the antenna structure.



26. CONTSTATE: State of the contact person or entity associated with the antenna structure.

27. CONTZIP: ZIP code of the contact person or entity associated with the antenna structure.

These features provide comprehensive information about the location, ownership, regulatory compliance, and contact details of antenna structures in the dataset.

#### LIME-INTERPRETATION:

##### Feature Value

DD_TEMPO	-81.99
X	-81.99
LAT_DMS	77472.00
ISSUEDATE	2993.00
FAASTUDY	109814.00
CONTSTATE	52.00
CONTCITY	5243.00
STRUCHT	76.80
FAACIRC	10.00
FILENUM	115741.00
FID	32815.00
index	31814.00
LICID	2555.00
Y	41.20
LON_DMS	47563.00
STRUCSTATE	44.00
CONTPO	0.00
STRUCCITY	9487.00
STRUCADD	47693.00
CONTZIP	7707.00

CONTADD 13987.00

CONTNAME 4999.00

ENTITY 14244.00

REGNUM 1054571.00

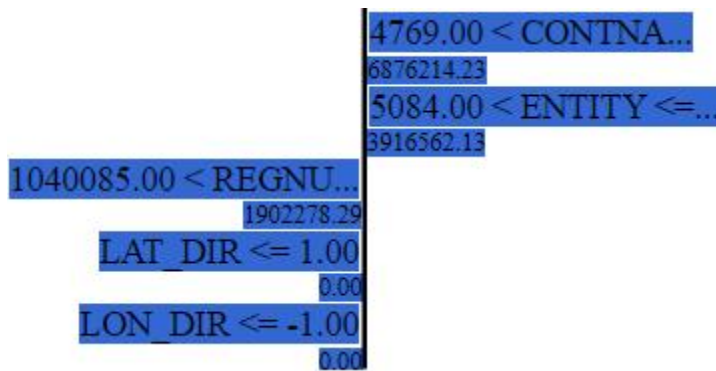
LAT\_DIR 1.00

LON\_DIR -1.00

negative

positive

DD_TEMP0 > -82.52	X > -82.52
1582.66	733178
53334.00 < LAT_DM...	2218.00 < ISSUEDA...
293700771.94	218109184.02
FAASTUDY > 89243.00	
216468516.29	
CONTSTATE > 45.00	
169536776.52	
	CONTCITY > 5062.00
	164533706.79
	67.00 < STRUCHT <= ...
	156943029.64
	0.00 < FAACIRC <= ...
	144437532.33
FILENUM > 93593.00	
130853131.03	
31206.00 < FID <= 6...	
104252370.63	
	31215.00 < index <= 6...
	98385763.67
	1458.00 < LICID <= ...
	88611001.84
37.29 < Y <= 41.26	
87762610.48	
	29569.00 < LON_DM...
	73397976.18
34.00 < STRUCSTATE...	
45134324.55	
CONTPO <= 0.00	
32795021.62	
	6801.00 < STRUCCIT...
	28381478.31
	29857.00 < STRUCAD...
	21518669.28
	CONTZIP > 7332.00
	13450115.86
	8307.00 < CONTADD ...
	11864431.88
	4769.00 < CONTNA...
	6876214.23
	5084.00 < ENTITY <= ...



#### EQUATIONS:

$DD\_TEMP = -0.000012059667171 + -0.261829001805310 * X + 1.000000004981352 * Y +$   
 $0.000000000003293 * FID + 0.000000000000055 * REGNUM + 0.000000000000130 * FILENUM +$   
 $0.0000000000005968 * ISSUEDATE + -0.000000000002411 * ENTITY + -0.0000000000032615 * LAT\_DMS +$   
 $0.000002784904611 * LAT\_DIR + -0.000000000003766 * LON\_DMS + -0.000000475028544 * LON\_DIR +$   
 $0.261828997616792 * DD\_TEMPO + -0.000000000414901 * STRUCHT + 0.000000000000823 *$   
 $STRUCADD + -0.000000000000130 * STRUCCITY + -0.000000000097739 * STRUCSTATE +$   
 $0.000000000000110 * FAASTUDY + 0.000000000734967 * FAACIRC + 0.00000000001024 * LICID + -$   
 $0.000000000000816 * CONTNAME + 0.000000000000069 * CONTADD + 0.000000000008185 * CONTPO$   
 $+ -0.000000000009477 * CONTCITY + -0.000000001392464 * CONTSTATE + 0.000000000018000 *$   
 $CONTZIP$

#### ENCODING ONLY CATEGORICAL VARIABLES:

coefficient [-2.85937016e-03 5.26026629e-04 2.00064940e-01 9.24303619e-04

2.73070578e-05 -5.52084300e-05 -2.24224761e-05 4.41098847e-05  
 -2.67890341e-03 2.88533240e-06 -9.18019324e-04 4.56569199e-05  
 5.32466316e-04 2.85022909e-03 -1.44635458e-07 -9.40433790e-07  
 -1.54855636e-05 2.08190523e-05 5.53185336e-03 4.34067606e-04  
 4.50876951e-05 6.04134929e-05 4.78824311e-04 -1.74995865e-03  
 1.29813163e-04 2.10799229e-03 -1.52655666e-16 1.19542489e-05  
 -8.40296613e-14 -4.85722573e-17 5.55111512e-17 5.55111512e-17  
 2.43186547e-16 1.73472348e-18 2.30718222e-16 1.42968497e-03  
 2.77555756e-17 7.03356828e-09 -1.19542519e-05 3.42323283e-15  
 5.83300769e-17 3.72965547e-17 1.54490610e-14 -1.34441069e-17

-1.12167008e-14 -8.93382590e-17 1.83880688e-16 1.20129601e-16  
2.83898339e-16 2.19008839e-17 -5.10429847e-15 1.71737624e-16  
2.32364591e-03 -2.03431999e-04 -1.27497782e-05 -3.68218772e-07  
3.48808141e-08 7.97121012e-06 -1.59477521e-06 3.14591584e-06  
-2.72730567e-04 -1.03975762e-06 1.67973059e-06 -1.68748264e-06  
-7.35583782e-04 1.17037429e-07 -1.70771551e-07 1.09511748e-04  
1.03068816e-07 -4.44008038e-05 4.47539584e-06 5.65133755e-06  
-1.48972398e-06 6.00045441e-07 3.51764261e-06 1.53401578e-04  
3.42867601e-05 -4.11475445e-09 5.67662347e-14 -1.75887493e-13  
-6.16732007e-14 -6.67530816e-13 -2.43690376e-13 2.28607655e-12  
3.99967342e-01 -1.66370164e-13 2.82277026e-05 2.03428412e-04  
-8.37226565e-11 -1.20916122e-14 -1.76425291e-14 -3.58194314e-10  
8.91694962e-14 2.63237941e-10 2.83271956e-13 7.57752812e-13  
-3.34941640e-13 -3.22991990e-12 3.48999342e-13 -2.73544758e-10  
5.96683681e-12 -6.59194921e-17 6.93889390e-17 4.51028104e-17  
2.27682456e-18 3.59955121e-17 -1.90819582e-17 -4.62151710e-04  
-7.97972799e-17 -6.31867159e-09 1.27497814e-05 -7.17178731e-15  
4.85722573e-17 -1.03216047e-16 1.61793474e-14 6.93889390e-18  
1.86385994e-14 1.39536820e-16 5.89805982e-17 1.75640752e-17  
-1.69731850e-16 6.03900610e-17 -1.86810118e-14 4.12430506e-16  
9.71445147e-17 4.16333634e-17 4.33680869e-17 -1.99493200e-17  
5.55111512e-17 -1.36535269e-05 -2.42861287e-17 -9.98612050e-12  
3.68218832e-07 -1.94733552e-15 3.46944695e-17 6.24500451e-17  
-8.24579798e-16 1.17961196e-16 3.16198585e-15 -1.34441069e-17  
8.67361738e-19 -3.20923843e-17 -4.42354486e-17 -3.59955121e-17  
1.45126559e-15 -5.33427469e-17 1.31838984e-16 -8.04478012e-17  
-1.12757026e-17 0.00000000e+00 2.76042046e-05 2.42861287e-17  
9.63121457e-12 -3.48808260e-08 8.76347063e-16 0.00000000e+00  
1.00613962e-16 -3.89767971e-15 4.85722573e-17 -1.08556361e-14

-5.20417043e-18 -4.33680869e-18 -2.60208521e-17 2.64274280e-17  
-1.09287579e-16 1.19292393e-15 -9.32413868e-17 -5.37757501e-16  
7.25060203e-19 1.25116931e-16 1.12111656e-05 8.15252271e-17  
-2.79583430e-10 -7.97121230e-06 7.68440233e-15 -7.09068221e-17  
-1.79570985e-18 8.33206801e-15 -9.10729825e-18 -7.19495136e-14  
1.02389343e-17 -3.83028299e-17 -3.65240607e-18 6.12909864e-16  
-4.17194220e-16 3.78096771e-14 5.69907484e-16 3.42607887e-17  
4.07660017e-17 -2.20549291e-05 1.30104261e-18 -2.20640831e-12  
1.59477553e-06 -6.92174043e-16 -8.67361738e-18 -7.52436308e-17  
-8.34046852e-15 -5.20417043e-17 2.14893918e-14 5.93600689e-17  
-4.51299154e-17 -8.46219796e-17 4.53789431e-17 -3.52094656e-17  
9.09067607e-15 -1.27366650e-16 4.85722573e-17 1.33945166e-03  
-8.32667268e-17 -1.50134176e-07 -3.14591630e-06 6.23087939e-15  
4.16333634e-17 1.38777878e-17 6.05226183e-14 -6.93889390e-18  
-5.76807368e-14 -1.04083409e-17 -5.46437895e-17 5.46437895e-17  
5.37296715e-16 3.10081821e-17 4.95512055e-14 -6.48569740e-16  
4.94137455e-06 4.59009669e-04 8.99217964e-05 -2.56508785e-04  
-1.42510691e-03 7.23146257e-08 4.70215044e-07 7.75091966e-06  
-1.04095281e-05 -2.76592612e-03 -2.17033838e-04 -2.25439121e-05  
-3.02067302e-05 -2.39412134e-04 8.74979277e-04 -6.49061108e-05  
-1.05399650e-03 5.03069808e-17 -7.67253176e-08 1.03975778e-06  
-2.76862714e-15 1.73472348e-17 2.27682456e-17 -5.08477690e-15  
1.14491749e-16 -4.12463223e-16 -7.15573434e-18 3.45453917e-17  
-1.10588622e-17 3.49113100e-17 -9.37834879e-18 -9.27975416e-17  
1.53245201e-16 8.99218429e-05 4.02346811e-06 -1.41246157e-08  
5.36801433e-12 3.32738233e-11 -8.85960232e-07 2.68682069e-12  
2.02968018e-08 8.76214329e-11 1.50841087e-10 -9.89803290e-12  
2.98149063e-10 1.17888930e-10 1.87698560e-08 8.29136223e-10  
-2.32195897e-03 7.35583961e-04 -1.17037444e-07 1.70771565e-07

-1.09511682e-04 -1.03068841e-07 4.44009251e-05 -4.47539689e-06  
-5.65133893e-06 1.48972438e-06 -6.00045564e-07 -3.51764366e-06  
-1.53401690e-04 -3.42867677e-05 -1.14507321e-13 1.02804897e-15  
1.23790032e-15 -1.31541990e-12 -8.64651233e-17 7.41357661e-13  
1.38517306e-15 2.34734027e-15 3.66628756e-15 2.36716537e-14  
1.00951504e-16 1.16759870e-13 1.90998476e-15 1.17961196e-16  
2.77555756e-17 -6.30006166e-16 6.93889390e-18 -2.85410991e-15  
-2.16840434e-17 -6.07153217e-17 -8.71698547e-17 6.45642394e-17  
-9.49761103e-17 3.91146263e-16 -7.11236625e-17 -5.42101086e-17  
1.58840976e-15 -1.56125113e-17 -1.80084549e-15 -4.01154804e-17  
-6.36697726e-17 -6.28295159e-17 -2.50467643e-17 -1.09463762e-16  
-1.41437943e-15 -5.33800163e-17 5.64290815e-12 3.20012436e-16  
9.98544536e-12 1.19958916e-14 -2.57581512e-15 1.64372884e-15  
-2.28724333e-14 -2.05634524e-14 2.42636750e-12 1.18032153e-13  
7.63278329e-17 1.46821017e-15 -1.82145965e-17 -4.38017678e-17  
-6.41847686e-17 -6.58991633e-18 -8.45677695e-17 -3.80175492e-16  
-1.09829680e-16 5.40026822e-11 1.06521502e-14 -7.71418006e-15  
-1.03991560e-14 -9.78716726e-14 3.63855696e-14 7.58441304e-12  
2.12285270e-14 6.54316011e-17 3.12521276e-17 -3.37186876e-17  
1.34909055e-16 -1.42979161e-17 -3.19855597e-15 2.81350464e-16  
-3.93023288e-19 -6.07153217e-18 1.40406722e-16 -1.34644357e-17  
1.39991790e-14 7.59551384e-17 1.54498810e-17 -1.46405410e-17  
-1.17148045e-16 -3.16431890e-15 -3.37728977e-17 -2.29464592e-15  
-4.20353653e-16 -1.21046919e-14 6.74305989e-17 3.38406603e-17  
9.84862616e-14 -5.68935090e-17 2.17262903e-12 -1.74136847e-14  
4.37184197e-16]

intercept -2.273924814488737e-05

Equation: DD\_TEMP= -0.00002273924814488737 + 0.00052602662865129158 \* X +  
0.20006493980471073968 \* Y + 0.00092430361918688126 \* FID + 0.00002730705779010603 \*



REGNUM + -0.00005520843000511943 \* FILENUM + -0.00002242247612391914 \* ISSUEDATE +  
0.00004410988473880875 \* ENTITY + -0.00267890340813844692 \* LAT\_DMS +  
0.00000288533240143518 \* LAT\_DIR + -0.00091801932394075048 \* LON\_DMS +  
0.00004565691993775503 \* LON\_DIR + 0.00053246631642591682 \* DD\_TEMP0 +  
0.00285022909392752084 \* STRUCHT + -0.00000014463545756414 \* STRUCADD + -  
0.00000094043378957588 \* STRUCCITY + -0.00001548556362174028 \* STRUCSTATE +  
0.00002081905226988767 \* FAASTUDY + 0.00553185335872829857 \* FAACIRC +  
0.00043406760602561327 \* LICID + 0.00004508769506283045 \* CONTNAME +  
0.00006041349291266583 \* CONTADD + 0.00047882431058625467 \* CONTPO + -  
0.00174995864639957083 \* CONTCITY + 0.00012981316272389130 \* CONTSTATE +  
0.00210799229236807630 \* CONTZIP + -0.00000000000000015266 \* index^2 +  
0.00001195424891011961 \* index^1\*X^1 + -0.000000000000008402966 \* index^1\*Y^1 + -  
0.0000000000000004857 \* index^1\*FID^1 + 0.0000000000000005551 \* index^1\*REGNUM^1 +  
0.0000000000000005551 \* index^1\*FILENUM^1 + 0.0000000000000024319 \* index^1\*ISSUEDATE^1  
+ 0.0000000000000000173 \* index^1\*ENTITY^1 + 0.0000000000000023072 \* index^1\*LAT\_DMS^1 +  
0.00142968497110787323 \* index^1\*LAT\_DIR^1 + 0.0000000000000002776 \* index^1\*LON\_DMS^1 +  
0.00000000703356827742 \* index^1\*LON\_DIR^1 + -0.00001195425185188876 \*  
index^1\*DD\_TEMP0^1 + 0.00000000000000342323 \* index^1\*STRUCHT^1 + 0.0000000000000005833  
\* index^1\*STRUCADD^1 + 0.0000000000000003730 \* index^1\*STRUCCITY^1 +  
0.00000000000001544906 \* index^1\*STRUCSTATE^1 + -0.0000000000000001344 \*  
index^1\*FAASTUDY^1 + -0.00000000000001121670 \* index^1\*FAACIRC^1 + -0.0000000000000008934  
\* index^1\*LICID^1 + 0.00000000000000018388 \* index^1\*CONTNAME^1 + 0.00000000000000012013 \*  
index^1\*CONTADD^1 + 0.00000000000000028390 \* index^1\*CONTPO^1 + 0.0000000000000002190 \*  
index^1\*CONTCITY^1 + -0.000000000000000510430 \* index^1\*CONTSTATE^1 +  
0.00000000000000017174 \* index^1\*CONTZIP^1 + 0.00232364591494893698 \* X^2 + -  
0.00020343199924590519 \* X^1\*Y^1 + -0.00001274977824306984 \* X^1\*FID^1 + -  
0.00000036821877173742 \* X^1\*REGNUM^1 + 0.00000003488081407746 \* X^1\*FILENUM^1 +  
0.00000797121011887128 \* X^1\*ISSUEDATE^1 + -0.00000159477520685104 \* X^1\*ENTITY^1 +  
0.00000314591584200732 \* X^1\*LAT\_DMS^1 + -0.00027273056732701333 \* X^1\*LAT\_DIR^1 + -  
0.00000103975761941967 \* X^1\*LON\_DMS^1 + 0.00000167973059180217 \* X^1\*LON\_DIR^1 + -  
0.00000168748263650914 \* X^1\*DD\_TEMP0^1 + -0.00073558378185098971 \* X^1\*STRUCHT^1 +  
0.00000011703742923890 \* X^1\*STRUCADD^1 + -0.00000017077155143172 \* X^1\*STRUCCITY^1 +  
0.00010951174783339585 \* X^1\*STRUCSTATE^1 + 0.00000010306881639325 \* X^1\*FAASTUDY^1 + -  
0.00004440080378704384 \* X^1\*FAACIRC^1 + 0.00000447539583854924 \* X^1\*LICID^1 +  
0.00000565133755019818 \* X^1\*CONTNAME^1 + -0.00000148972398407419 \* X^1\*CONTADD^1 +  
0.00000060004544064387 \* X^1\*CONTPO^1 + 0.00000351764260591636 \* X^1\*CONTCITY^1 +  
0.00015340157808438505 \* X^1\*CONTSTATE^1 + 0.00003428676006253668 \* X^1\*CONTZIP^1 + -  
0.00000000411475444936 \* Y^2 + 0.00000000000005676623 \* Y^1\*FID^1 + -  
0.00000000000017588749 \* Y^1\*REGNUM^1 + -0.00000000000006167320 \* Y^1\*FILENUM^1 + -  
0.000000000000066753082 \* Y^1\*ISSUEDATE^1 + -0.00000000000024369038 \* Y^1\*ENTITY^1 +  
0.000000000000228607655 \* Y^1\*LAT\_DMS^1 + 0.39996734207588441334 \* Y^1\*LAT\_DIR^1 + -  
0.00000000000016637016 \* Y^1\*LON\_DMS^1 + 0.00002822770264378638 \* Y^1\*LON\_DIR^1 +  
0.00020342841236839048 \* Y^1\*DD\_TEMP0^1 + -0.00000000008372265649 \* Y^1\*STRUCHT^1 + -  
0.00000000000001209161 \* Y^1\*STRUCADD^1 + -0.0000000000001764253 \* Y^1\*STRUCCITY^1 + -

0.00000000035819431406 \* Y^1\*STRUCSTATE^1 + 0.00000000000008916950 \* Y^1\*FAASTUDY^1 +  
0.00000000026323794065 \* Y^1\*FAACIRC^1 + 0.00000000000028327196 \* Y^1\*LICID^1 +  
0.00000000000075775281 \* Y^1\*CONTNAME^1 + -0.00000000000033494164 \* Y^1\*CONTADD^1 + -  
0.000000000000322991990 \* Y^1\*CONTPO^1 + 0.00000000000034899934 \* Y^1\*CONTCITY^1 + -  
0.00000000027354475836 \* Y^1\*CONTSTATE^1 + 0.0000000000059683681 \* Y^1\*CONTZIP^1 + -  
0.0000000000000006592 \* FID^2 + 0.0000000000000006939 \* FID^1\*REGNUM^1 +  
0.00000000000000004510 \* FID^1\*FILENUM^1 + 0.0000000000000000228 \* FID^1\*ISSUEDATE^1 +  
0.00000000000000003600 \* FID^1\*ENTITY^1 + -0.00000000000000001908 \* FID^1\*LAT\_DMS^1 + -  
0.00046215170957877985 \* FID^1\*LAT\_DIR^1 + -0.00000000000000007980 \* FID^1\*LON\_DMS^1 + -  
0.00000000631867159023 \* FID^1\*LON\_DIR^1 + 0.00001274978143280560 \* FID^1\*DD\_TEMP0^1 + -  
0.000000000000000717179 \* FID^1\*STRUCHT^1 + 0.00000000000000004857 \* FID^1\*STRUCADD^1 + -  
0.000000000000000010322 \* FID^1\*STRUCCITY^1 + 0.00000000000001617935 \* FID^1\*STRUCSTATE^1  
+ 0.00000000000000000694 \* FID^1\*FAASTUDY^1 + 0.00000000000001863860 \* FID^1\*FAACIRC^1 +  
0.000000000000000013954 \* FID^1\*LICID^1 + 0.00000000000000005898 \* FID^1\*CONTNAME^1 +  
0.000000000000000001756 \* FID^1\*CONTADD^1 + -0.000000000000000016973 \* FID^1\*CONTPO^1 +  
0.000000000000000006039 \* FID^1\*CONTCITY^1 + -0.00000000000001868101 \* FID^1\*CONTSTATE^1 +  
0.000000000000000041243 \* FID^1\*CONTZIP^1 + 0.00000000000000009714 \* REGNUM^2 +  
0.00000000000000004163 \* REGNUM^1\*FILENUM^1 + 0.00000000000000004337 \*  
REGNUM^1\*ISSUEDATE^1 + -0.00000000000000001995 \* REGNUM^1\*ENTITY^1 +  
0.000000000000000005551 \* REGNUM^1\*LAT\_DMS^1 + -0.00001365352685793215 \*  
REGNUM^1\*LAT\_DIR^1 + -0.000000000000000002429 \* REGNUM^1\*LON\_DMS^1 + -  
0.000000000000998612050 \* REGNUM^1\*LON\_DIR^1 + 0.00000036821883173389 \*  
REGNUM^1\*DD\_TEMP0^1 + -0.0000000000000000194734 \* REGNUM^1\*STRUCHT^1 +  
0.000000000000000003469 \* REGNUM^1\*STRUCADD^1 + 0.00000000000000006245 \*  
REGNUM^1\*STRUCCITY^1 + -0.000000000000000082458 \* REGNUM^1\*STRUCSTATE^1 +  
0.0000000000000000011796 \* REGNUM^1\*FAASTUDY^1 + 0.00000000000000316199 \*  
REGNUM^1\*FAACIRC^1 + -0.000000000000000001344 \* REGNUM^1\*LICID^1 +  
0.00000000000000000087 \* REGNUM^1\*CONTNAME^1 + -0.000000000000000003209 \*  
REGNUM^1\*CONTADD^1 + -0.000000000000000004424 \* REGNUM^1\*CONTPO^1 + -  
0.000000000000000003600 \* REGNUM^1\*CONTCITY^1 + 0.000000000000000145127 \*  
REGNUM^1\*CONTSTATE^1 + -0.000000000000000005334 \* REGNUM^1\*CONTZIP^1 +  
0.0000000000000000013184 \* FILENUM^2 + -0.00000000000000008045 \* FILENUM^1\*ISSUEDATE^1 + -  
0.000000000000000001128 \* FILENUM^1\*ENTITY^1 + 0.00000000000000000000 \*  
FILENUM^1\*LAT\_DMS^1 + 0.00002760420458983083 \* FILENUM^1\*LAT\_DIR^1 +  
0.000000000000000002429 \* FILENUM^1\*LON\_DMS^1 + 0.00000000000963121457 \*  
FILENUM^1\*LON\_DIR^1 + -0.00000003488082597957 \* FILENUM^1\*DD\_TEMP0^1 +  
0.000000000000000087635 \* FILENUM^1\*STRUCHT^1 + 0.00000000000000000000 \*  
FILENUM^1\*STRUCADD^1 + 0.000000000000000010061 \* FILENUM^1\*STRUCCITY^1 + -  
0.0000000000000000389768 \* FILENUM^1\*STRUCSTATE^1 + 0.00000000000000004857 \*  
FILENUM^1\*FAASTUDY^1 + -0.00000000000001085564 \* FILENUM^1\*FAACIRC^1 + -  
0.00000000000000000520 \* FILENUM^1\*LICID^1 + -0.00000000000000000434 \*  
FILENUM^1\*CONTNAME^1 + -0.000000000000000002602 \* FILENUM^1\*CONTADD^1 +  
0.000000000000000002643 \* FILENUM^1\*CONTPO^1 + -0.00000000000000010929 \*  
FILENUM^1\*CONTCITY^1 + 0.000000000000000119292 \* FILENUM^1\*CONTSTATE^1 + -

0.00000000000000009324 \* FILENUM^1\*CONTZIP^1 + -0.00000000000000053776 \* ISSUEDATE^2 +  
0.00000000000000000073 \* ISSUEDATE^1\*ENTITY^1 + 0.00000000000000012512 \*  
ISSUEDATE^1\*LAT\_DMS^1 + 0.00001121116556185008 \* ISSUEDATE^1\*LAT\_DIR^1 +  
0.000000000000000008153 \* ISSUEDATE^1\*LON\_DMS^1 + -0.00000000027958343037 \*  
ISSUEDATE^1\*LON\_DIR^1 + -0.00000797121230317001 \* ISSUEDATE^1\*DD\_TEMP0^1 +  
0.000000000000000768440 \* ISSUEDATE^1\*STRUCHT^1 + -0.0000000000000007091 \*  
ISSUEDATE^1\*STRUCADD^1 + -0.0000000000000000180 \* ISSUEDATE^1\*STRUCCITY^1 +  
0.000000000000000833207 \* ISSUEDATE^1\*STRUCSTATE^1 + -0.0000000000000000911 \*  
ISSUEDATE^1\*FAASTUDY^1 + -0.00000000000007194951 \* ISSUEDATE^1\*FAACIRC^1 +  
0.00000000000000001024 \* ISSUEDATE^1\*LICID^1 + -0.0000000000000003830 \*  
ISSUEDATE^1\*CONTNAME^1 + -0.0000000000000000365 \* ISSUEDATE^1\*CONTADD^1 +  
0.000000000000000061291 \* ISSUEDATE^1\*CONTPO^1 + -0.00000000000000041719 \*  
ISSUEDATE^1\*CONTCITY^1 + 0.00000000000003780968 \* ISSUEDATE^1\*CONTSTATE^1 +  
0.000000000000000056991 \* ISSUEDATE^1\*CONTZIP^1 + 0.00000000000000003426 \* ENTITY^2 +  
0.000000000000000004077 \* ENTITY^1\*LAT\_DMS^1 + -0.00002205492908471865 \*  
ENTITY^1\*LAT\_DIR^1 + 0.00000000000000000130 \* ENTITY^1\*LON\_DMS^1 + -  
0.000000000000220640831 \* ENTITY^1\*LON\_DIR^1 + 0.00000159477553019607 \*  
ENTITY^1\*DD\_TEMP0^1 + -0.000000000000000069217 \* ENTITY^1\*STRUCHT^1 + -  
0.00000000000000000867 \* ENTITY^1\*STRUCADD^1 + -0.00000000000000007524 \*  
ENTITY^1\*STRUCCITY^1 + -0.000000000000000834047 \* ENTITY^1\*STRUCSTATE^1 + -  
0.000000000000000005204 \* ENTITY^1\*FAASTUDY^1 + 0.000000000000002148939 \*  
ENTITY^1\*FAACIRC^1 + 0.00000000000000005936 \* ENTITY^1\*LICID^1 + -0.0000000000000004513 \*  
ENTITY^1\*CONTNAME^1 + -0.000000000000000008462 \* ENTITY^1\*CONTADD^1 +  
0.000000000000000004538 \* ENTITY^1\*CONTPO^1 + -0.00000000000000003521 \*  
ENTITY^1\*CONTCITY^1 + 0.000000000000000909068 \* ENTITY^1\*CONTSTATE^1 + -  
0.0000000000000000012737 \* ENTITY^1\*CONTZIP^1 + 0.00000000000000004857 \* LAT\_DMS^2 +  
0.00133945165912740236 \* LAT\_DMS^1\*LAT\_DIR^1 + -0.00000000000000008327 \*  
LAT\_DMS^1\*LON\_DMS^1 + -0.00000015013417641518 \* LAT\_DMS^1\*LON\_DIR^1 + -  
0.00000314591630053412 \* LAT\_DMS^1\*DD\_TEMP0^1 + 0.000000000000000623088 \*  
LAT\_DMS^1\*STRUCHT^1 + 0.00000000000000004163 \* LAT\_DMS^1\*STRUCADD^1 +  
0.000000000000000001388 \* LAT\_DMS^1\*STRUCCITY^1 + 0.00000000000006052262 \*  
LAT\_DMS^1\*STRUCSTATE^1 + -0.00000000000000000694 \* LAT\_DMS^1\*FAASTUDY^1 + -  
0.000000000000005768074 \* LAT\_DMS^1\*FAACIRC^1 + -0.00000000000000001041 \*  
LAT\_DMS^1\*LICID^1 + -0.00000000000000005464 \* LAT\_DMS^1\*CONTNAME^1 +  
0.00000000000000005464 \* LAT\_DMS^1\*CONTADD^1 + 0.00000000000000053730 \*  
LAT\_DMS^1\*CONTPO^1 + 0.00000000000000003101 \* LAT\_DMS^1\*CONTCITY^1 +  
0.00000000000004955121 \* LAT\_DMS^1\*CONTSTATE^1 + -0.00000000000000064857 \*  
LAT\_DMS^1\*CONTZIP^1 + 0.00000494137455093665 \* LAT\_DIR^2 + 0.00045900966932943104 \*  
LAT\_DIR^1\*LON\_DMS^1 + 0.00008992179642592877 \* LAT\_DIR^1\*LON\_DIR^1 + -  
0.00025650878488109785 \* LAT\_DIR^1\*DD\_TEMP0^1 + -0.00142510691433814598 \*  
LAT\_DIR^1\*STRUCHT^1 + 0.00000007231462565691 \* LAT\_DIR^1\*STRUCADD^1 +  
0.00000047021504431317 \* LAT\_DIR^1\*STRUCCITY^1 + 0.00000775091966358013 \*  
LAT\_DIR^1\*STRUCSTATE^1 + -0.00001040952814803750 \* LAT\_DIR^1\*FAASTUDY^1 + -  
0.00276592612447065832 \* LAT\_DIR^1\*FAACIRC^1 + -0.00021703383781480947 \* LAT\_DIR^1\*LICID^1

+ -0.00002254391212212646 \* LAT\_DIR^1\*CONTNAME^1 + -0.00003020673019605963 \*  
LAT\_DIR^1\*CONTADD^1 + -0.00023941213367338678 \* LAT\_DIR^1\*CONTPO^1 +  
0.00087497927667741602 \* LAT\_DIR^1\*CONTCITY^1 + -0.00006490611076780766 \*  
LAT\_DIR^1\*CONTSTATE^1 + -0.00105399650130544699 \* LAT\_DIR^1\*CONTZIP^1 +  
0.00000000000000005031 \* LON\_DMS^2 + -0.00000007672531760764 \* LON\_DMS^1\*LON\_DIR^1 +  
0.00000103975777936632 \* LON\_DMS^1\*DD\_TEMP0^1 + -0.00000000000000276863 \*  
LON\_DMS^1\*STRUCHT^1 + 0.00000000000000001735 \* LON\_DMS^1\*STRUCADD^1 +  
0.00000000000000002277 \* LON\_DMS^1\*STRUCCITY^1 + -0.00000000000000508478 \*  
LON\_DMS^1\*STRUCSTATE^1 + 0.000000000000000011449 \* LON\_DMS^1\*FAASTUDY^1 + -  
0.000000000000000041246 \* LON\_DMS^1\*FAACIRC^1 + -0.00000000000000000716 \*  
LON\_DMS^1\*LICID^1 + 0.00000000000000003455 \* LON\_DMS^1\*CONTNAME^1 + -  
0.00000000000000001106 \* LON\_DMS^1\*CONTADD^1 + 0.00000000000000003491 \*  
LON\_DMS^1\*CONTPO^1 + -0.00000000000000000938 \* LON\_DMS^1\*CONTCITY^1 + -  
0.000000000000000009280 \* LON\_DMS^1\*CONTSTATE^1 + 0.000000000000000015325 \*  
LON\_DMS^1\*CONTZIP^1 + 0.00008992184291393695 \* LON\_DIR^2 + 0.00000402346811271785 \*  
LON\_DIR^1\*DD\_TEMP0^1 + -0.00000001412461566906 \* LON\_DIR^1\*STRUCHT^1 +  
0.00000000000536801433 \* LON\_DIR^1\*STRUCADD^1 + 0.00000000003327382329 \*  
LON\_DIR^1\*STRUCCITY^1 + -0.00000088596023166897 \* LON\_DIR^1\*STRUCSTATE^1 +  
0.00000000000268682069 \* LON\_DIR^1\*FAASTUDY^1 + 0.00000002029680183611 \*  
LON\_DIR^1\*FAACIRC^1 + 0.00000000008762143288 \* LON\_DIR^1\*LICID^1 + 0.00000000015084108709  
\* LON\_DIR^1\*CONTNAME^1 + -0.00000000000989803290 \* LON\_DIR^1\*CONTADD^1 +  
0.00000000029814906346 \* LON\_DIR^1\*CONTPO^1 + 0.00000000011788893004 \*  
LON\_DIR^1\*CONTCITY^1 + 0.00000001876985603139 \* LON\_DIR^1\*CONTSTATE^1 +  
0.00000000082913622252 \* LON\_DIR^1\*CONTZIP^1 + -0.00232195896975922588 \* DD\_TEMP0^2 +  
0.00073558396078029933 \* DD\_TEMP0^1\*STRUCHT^1 + -0.00000011703744374918 \*  
DD\_TEMP0^1\*STRUCADD^1 + 0.00000017077156531760 \* DD\_TEMP0^1\*STRUCCITY^1 + -  
0.00010951168159223391 \* DD\_TEMP0^1\*STRUCSTATE^1 + -0.00000010306884088310 \*  
DD\_TEMP0^1\*FAASTUDY^1 + 0.00004440092512574779 \* DD\_TEMP0^1\*FAACIRC^1 + -  
0.00000447539688753645 \* DD\_TEMP0^1\*LICID^1 + -0.00000565133893423254 \*  
DD\_TEMP0^1\*CONTNAME^1 + 0.00000148972438037532 \* DD\_TEMP0^1\*CONTADD^1 + -  
0.00000060004556416550 \* DD\_TEMP0^1\*CONTPO^1 + -0.00000351764365681543 \*  
DD\_TEMP0^1\*CONTCITY^1 + -0.00015340168968329371 \* DD\_TEMP0^1\*CONTSTATE^1 + -  
0.00003428676769268545 \* DD\_TEMP0^1\*CONTZIP^1 + -0.00000000000011450732 \* STRUCHT^2 +  
0.0000000000000000102805 \* STRUCHT^1\*STRUCADD^1 + 0.00000000000000123790 \*  
STRUCHT^1\*STRUCCITY^1 + -0.00000000000131541990 \* STRUCHT^1\*STRUCSTATE^1 + -  
0.000000000000000008647 \* STRUCHT^1\*FAASTUDY^1 + 0.00000000000074135766 \*  
STRUCHT^1\*FAACIRC^1 + 0.00000000000000138517 \* STRUCHT^1\*LICID^1 +  
0.00000000000000234734 \* STRUCHT^1\*CONTNAME^1 + 0.0000000000000366629 \*  
STRUCHT^1\*CONTADD^1 + 0.00000000000002367165 \* STRUCHT^1\*CONTPO^1 +  
0.00000000000000010095 \* STRUCHT^1\*CONTCITY^1 + 0.0000000000011675987 \*  
STRUCHT^1\*CONTSTATE^1 + 0.00000000000000190998 \* STRUCHT^1\*CONTZIP^1 +  
0.00000000000000011796 \* STRUCADD^2 + 0.0000000000000002776 \* STRUCADD^1\*STRUCCITY^1 +  
-0.000000000000000063001 \* STRUCADD^1\*STRUCSTATE^1 + 0.0000000000000000694 \*  
STRUCADD^1\*FAASTUDY^1 + -0.00000000000000285411 \* STRUCADD^1\*FAACIRC^1 + -

0.00000000000000002168 \* STRUCADD^1\*LICID^1 + -0.00000000000000006072 \*  
STRUCADD^1\*CONTNAME^1 + -0.00000000000000008717 \* STRUCADD^1\*CONTADD^1 +  
0.00000000000000006456 \* STRUCADD^1\*CONTPO^1 + -0.00000000000000009498 \*  
STRUCADD^1\*CONTCITY^1 + 0.000000000000000039115 \* STRUCADD^1\*CONTSTATE^1 + -  
0.000000000000000007112 \* STRUCADD^1\*CONTZIP^1 + -0.00000000000000005421 \* STRUCCITY^2 +  
0.0000000000000000158841 \* STRUCCITY^1\*STRUCSTATE^1 + -0.00000000000000001561 \*  
STRUCCITY^1\*FAASTUDY^1 + -0.0000000000000000180085 \* STRUCCITY^1\*FAACIRC^1 + -  
0.00000000000000004012 \* STRUCCITY^1\*LICID^1 + -0.00000000000000006367 \*  
STRUCCITY^1\*CONTNAME^1 + -0.00000000000000006283 \* STRUCCITY^1\*CONTADD^1 + -  
0.000000000000000002505 \* STRUCCITY^1\*CONTPO^1 + -0.000000000000000010946 \*  
STRUCCITY^1\*CONTCITY^1 + -0.0000000000000000141438 \* STRUCCITY^1\*CONTSTATE^1 + -  
0.000000000000000005338 \* STRUCCITY^1\*CONTZIP^1 + 0.000000000000564290815 \* STRUCSTATE^2 +  
0.000000000000000032001 \* STRUCSTATE^1\*FAASTUDY^1 + 0.000000000000998544536 \*  
STRUCSTATE^1\*FAACIRC^1 + 0.000000000000001199589 \* STRUCSTATE^1\*LICID^1 + -  
0.000000000000000257582 \* STRUCSTATE^1\*CONTNAME^1 + 0.00000000000000164373 \*  
STRUCSTATE^1\*CONTADD^1 + -0.000000000000002287243 \* STRUCSTATE^1\*CONTPO^1 + -  
0.000000000000002056345 \* STRUCSTATE^1\*CONTCITY^1 + 0.00000000000242636750 \*  
STRUCSTATE^1\*CONTSTATE^1 + 0.00000000000011803215 \* STRUCSTATE^1\*CONTZIP^1 +  
0.00000000000000007633 \* FAASTUDY^2 + 0.00000000000000146821 \* FAASTUDY^1\*FAACIRC^1 + -  
0.00000000000000001821 \* FAASTUDY^1\*LICID^1 + -0.00000000000000004380 \*  
FAASTUDY^1\*CONTNAME^1 + -0.00000000000000006418 \* FAASTUDY^1\*CONTADD^1 + -  
0.00000000000000000659 \* FAASTUDY^1\*CONTPO^1 + -0.00000000000000008457 \*  
FAASTUDY^1\*CONTCITY^1 + -0.000000000000000038018 \* FAASTUDY^1\*CONTSTATE^1 + -  
0.000000000000000010983 \* FAASTUDY^1\*CONTZIP^1 + 0.000000000005400268224 \* FAACIRC^2 +  
0.000000000000001065215 \* FAACIRC^1\*LICID^1 + -0.00000000000000771418 \*  
FAACIRC^1\*CONTNAME^1 + -0.000000000000001039916 \* FAACIRC^1\*CONTADD^1 + -  
0.000000000000009787167 \* FAACIRC^1\*CONTPO^1 + 0.000000000000003638557 \*  
FAACIRC^1\*CONTCITY^1 + 0.000000000000758441304 \* FAACIRC^1\*CONTSTATE^1 +  
0.00000000000002122853 \* FAACIRC^1\*CONTZIP^1 + 0.0000000000000006543 \* LICID^2 +  
0.00000000000000003125 \* LICID^1\*CONTNAME^1 + -0.00000000000000003372 \*  
LICID^1\*CONTADD^1 + 0.000000000000000013491 \* LICID^1\*CONTPO^1 + -0.00000000000000001430 \*  
LICID^1\*CONTCITY^1 + -0.000000000000000319856 \* LICID^1\*CONTSTATE^1 +  
0.000000000000000028135 \* LICID^1\*CONTZIP^1 + -0.00000000000000000039 \* CONTNAME^2 + -  
0.00000000000000000607 \* CONTNAME^1\*CONTADD^1 + 0.000000000000000014041 \*  
CONTNAME^1\*CONTPO^1 + -0.000000000000000001346 \* CONTNAME^1\*CONTCITY^1 +  
0.000000000000001399918 \* CONTNAME^1\*CONTSTATE^1 + 0.0000000000000007596 \*  
CONTNAME^1\*CONTZIP^1 + 0.00000000000000001545 \* CONTADD^2 + -0.00000000000000001464 \*  
CONTADD^1\*CONTPO^1 + -0.000000000000000011715 \* CONTADD^1\*CONTCITY^1 + -  
0.000000000000000316432 \* CONTADD^1\*CONTSTATE^1 + -0.00000000000000003377 \*  
CONTADD^1\*CONTZIP^1 + -0.00000000000000229465 \* CONTPO^2 + -0.00000000000000042035 \*  
CONTPO^1\*CONTCITY^1 + -0.000000000000001210469 \* CONTPO^1\*CONTSTATE^1 +  
0.00000000000000006743 \* CONTPO^1\*CONTZIP^1 + 0.00000000000000003384 \* CONTCITY^2 +  
0.000000000000009848626 \* CONTCITY^1\*CONTSTATE^1 + -0.0000000000000005689 \*

CONTCITY^1\*CONTZIP^1 + 0.000000000000217262903 \* CONTSTATE^2 + -0.00000000000001741368 \*  
CONTSTATE^1\*CONTZIP^1 + 0.00000000000000043718 \* CONTZIP^2

ENCODING WITHOUT DMS:

DD\_TEMP= 0.00010576230626213601 + -0.00000174095101137415 \* X + 0.50000130403377274213 \*  
Y + -0.00006511110488630435 \* FID + -0.00000316087842277951 \* REGNUM +  
0.00000440755907304179 \* FILENUM + 0.00000522239531959209 \* ISSUEDATE + -  
0.00000223396633363449 \* ENTITY + 0.00001054592131193315 \* LAT\_DMS +  
0.00000723888823740212 \* LAT\_DIR + -0.00023386335143328228 \* LON\_DMS +  
0.00004867207812449064 \* LON\_DIR + -0.00000443296812098102 \* DD\_TEMP0 + -  
0.00009467762825440859 \* STRUCHT + 0.00000050154855025786 \* STRUCADD +  
0.00000054682394215625 \* STRUCCITY + -0.00000029338273138416 \* STRUCSTATE + -  
0.00000174636596068962 \* FAASTUDY + -0.00000570040267122107 \* FAACIRC + -  
0.00001675999538907090 \* LICID + 0.00000131672343367331 \* CONTNAME + -  
0.00000148766673947339 \* CONTADD + -0.00000145259231411636 \* CONTPO +  
0.00022464540035893203 \* CONTCITY + 0.00000695760544986160 \* CONTSTATE + -  
0.00033408163777937295 \* CONTZIP + 0.00000000000000059674 \* index^2 +  
0.00006864412035253760 \* index^1\*X^1 + 0.000000000000316765728 \* index^1\*Y^1 +  
0.00000000000000006939 \* index^1\*FID^1 + 0.00000000000000005898 \* index^1\*REGNUM^1 + -  
0.000000000000000011102 \* index^1\*FILENUM^1 + 0.000000000000000061366 \* index^1\*ISSUEDATE^1 +  
+ 0.000000000000000007633 \* index^1\*ENTITY^1 + 0.000000000000000026368 \* index^1\*LAT\_DMS^1 +  
-0.00017551137836102786 \* index^1\*LAT\_DIR^1 + 0.000000000000000031225 \* index^1\*LON\_DMS^1 +  
+ 0.00000000105944581893 \* index^1\*LON\_DIR^1 + -0.00006864413752147434 \*  
index^1\*DD\_TEMP0^1 + 0.000000000000001918284 \* index^1\*STRUCHT^1 + 0.00000000000000001605  
\* index^1\*STRUCADD^1 + 0.000000000000000034001 \* index^1\*STRUCCITY^1 + -  
0.000000000000007507696 \* index^1\*STRUCSTATE^1 + 0.00000000000000002515 \*  
index^1\*FAASTUDY^1 + 0.00000000000012783470 \* index^1\*FAACIRC^1 + 0.00000000000000007329  
\* index^1\*LICID^1 + 0.000000000000000044235 \* index^1\*CONTNAME^1 + -0.00000000000000000694  
\* index^1\*CONTADD^1 + 0.000000000000000026839 \* index^1\*CONTPO^1 + 0.000000000000000015656  
\* index^1\*CONTCITY^1 + -0.000000000000001644235 \* index^1\*CONTSTATE^1 +  
0.00000000000000102696 \* index^1\*CONTZIP^1 + -0.00047354360387344543 \* X^2 +  
0.00004534485574031599 \* X^1\*Y^1 + -0.00007423459553249815 \* X^1\*FID^1 + -  
0.00000159447871112392 \* X^1\*REGNUM^1 + -0.00000066315100018271 \* X^1\*FILENUM^1 + -  
0.00000714945556567689 \* X^1\*ISSUEDATE^1 + -0.00001556784074416448 \* X^1\*ENTITY^1 + -  
0.00000018587636457738 \* X^1\*LAT\_DMS^1 + 0.00000231886325348656 \* X^1\*LAT\_DIR^1 + -  
0.00001918426821592109 \* X^1\*LON\_DMS^1 + -0.00000246611014691395 \* X^1\*LON\_DIR^1 + -  
0.00000079276145427020 \* X^1\*DD\_TEMP0^1 + 0.00014866894967023979 \* X^1\*STRUCHT^1 + -  
0.00000049827874430482 \* X^1\*STRUCADD^1 + -0.00000282730216788391 \* X^1\*STRUCCITY^1 + -  
0.00002292352209385020 \* X^1\*STRUCSTATE^1 + -0.00000054972982783970 \* X^1\*FAASTUDY^1 +  
0.00000836215019043474 \* X^1\*FAACIRC^1 + 0.00003665822018225841 \* X^1\*LICID^1 +  
0.00003642371899628211 \* X^1\*CONTNAME^1 + -0.00001255416396715745 \* X^1\*CONTADD^1 +

0.00001085334788082865 \* X^1\*CONTPO^1 + 0.00003356907883732859 \* X^1\*CONTCITY^1 + -  
0.00002680908955299351 \* X^1\*CONTSTATE^1 + 0.00024656119727870364 \* X^1\*CONTZIP^1 +  
0.00000001251236735875 \* Y^2 + -0.00000000000549063542 \* Y^1\*FID^1 +  
0.00000000000022671341 \* Y^1\*REGNUM^1 + -0.0000000000009706796 \* Y^1\*FILENUM^1 + -  
0.00000000000510647314 \* Y^1\*ISSUEDATE^1 + -0.00000000000331134716 \* Y^1\*ENTITY^1 + -  
0.00000000000437808480 \* Y^1\*LAT\_DMS^1 + 0.50000274574337888467 \* Y^1\*LAT\_DIR^1 + -  
0.00000000000279535422 \* Y^1\*LON\_DMS^1 + 0.00000483828298438299 \* Y^1\*LON\_DIR^1 + -  
0.00004535055271666296 \* Y^1\*DD\_TEMP0^1 + 0.00000000008789835909 \* Y^1\*STRUCHT^1 + -  
0.00000000000013777202 \* Y^1\*STRUCADD^1 + -0.0000000000080953631 \* Y^1\*STRUCCITY^1 +  
0.00000000099584666881 \* Y^1\*STRUCSTATE^1 + -0.0000000000045721241 \* Y^1\*FAASTUDY^1 +  
0.00000000142046559607 \* Y^1\*FAACIRC^1 + 0.00000000000380806604 \* Y^1\*LICID^1 +  
0.00000000000578271896 \* Y^1\*CONTNAME^1 + -0.00000000000187735176 \* Y^1\*CONTADD^1 + -  
0.00000000001385363982 \* Y^1\*CONTPO^1 + 0.00000000000269818949 \* Y^1\*CONTCITY^1 + -  
0.000000000205248493752 \* Y^1\*CONTSTATE^1 + 0.00000000004682335635 \* Y^1\*CONTZIP^1 + -  
0.00000000000000072164 \* FID^2 + -0.00000000000000013184 \* FID^1\*REGNUM^1 +  
0.0000000000000002776 \* FID^1\*FILENUM^1 + -0.00000000000000032461 \* FID^1\*ISSUEDATE^1 + -  
0.0000000000000001214 \* FID^1\*ENTITY^1 + 0.0000000000000002082 \* FID^1\*LAT\_DMS^1 +  
0.00006511053443755139 \* FID^1\*LAT\_DIR^1 + -0.00000000000000043715 \* FID^1\*LON\_DMS^1 + -  
0.000000000201508975500 \* FID^1\*LON\_DIR^1 + 0.00007423461361159702 \* FID^1\*DD\_TEMP0^1 + -  
0.00000000000002936831 \* FID^1\*STRUCHT^1 + -0.00000000000000020296 \* FID^1\*STRUCADD^1 +  
0.0000000000000009714 \* FID^1\*STRUCCITY^1 + -0.00000000000005239133 \* FID^1\*STRUCSTATE^1  
+ -0.00000000000000023419 \* FID^1\*FAASTUDY^1 + 0.00000000000006464151 \* FID^1\*FAACIRC^1 +  
0.00000000000000036342 \* FID^1\*LICID^1 + 0.00000000000000017954 \* FID^1\*CONTNAME^1 +  
0.00000000000000010105 \* FID^1\*CONTADD^1 + -0.00000000000000087864 \* FID^1\*CONTPO^1 + -  
0.00000000000000015092 \* FID^1\*CONTCITY^1 + -0.0000000000017003096 \* FID^1\*CONTSTATE^1 +  
0.000000000000000222999 \* FID^1\*CONTZIP^1 + -0.0000000000000002776 \* REGNUM^2 + -  
0.00000000000000016653 \* REGNUM^1\*FILENUM^1 + 0.0000000000000008153 \*  
REGNUM^1\*ISSUEDATE^1 + -0.0000000000000008327 \* REGNUM^1\*ENTITY^1 +  
0.0000000000000002776 \* REGNUM^1\*LAT\_DMS^1 + 0.00000316091945676186 \*  
REGNUM^1\*LAT\_DIR^1 + 0.00000000000000000000 \* REGNUM^1\*LON\_DMS^1 + -  
0.000000000004156447970 \* REGNUM^1\*LON\_DIR^1 + 0.00000159447902129931 \*  
REGNUM^1\*DD\_TEMP0^1 + -0.000000000000000317389 \* REGNUM^1\*STRUCHT^1 + -  
0.0000000000000002776 \* REGNUM^1\*STRUCADD^1 + -0.0000000000000007980 \*  
REGNUM^1\*STRUCCITY^1 + -0.000000000000000324559 \* REGNUM^1\*STRUCSTATE^1 +  
0.00000000000000013878 \* REGNUM^1\*FAASTUDY^1 + 0.000000000000000728377 \*  
REGNUM^1\*FAACIRC^1 + -0.00000000000000013704 \* REGNUM^1\*LICID^1 + -  
0.0000000000000004684 \* REGNUM^1\*CONTNAME^1 + 0.0000000000000001041 \*  
REGNUM^1\*CONTADD^1 + 0.00000000000000023679 \* REGNUM^1\*CONTPO^1 +  
0.00000000000000014572 \* REGNUM^1\*CONTCITY^1 + -0.000000000000000304455 \*  
REGNUM^1\*CONTSTATE^1 + -0.0000000000000003816 \* REGNUM^1\*CONTZIP^1 + -  
0.0000000000000002776 \* FILENUM^2 + 0.0000000000000005768 \* FILENUM^1\*ISSUEDATE^1 + -  
0.0000000000000008674 \* FILENUM^1\*ENTITY^1 + -0.0000000000000005551 \*  
FILENUM^1\*LAT\_DMS^1 + -0.00000440755121025107 \* FILENUM^1\*LAT\_DIR^1 +  
0.00000000000000000000 \* FILENUM^1\*LON\_DMS^1 + -0.00000000001871399786 \*



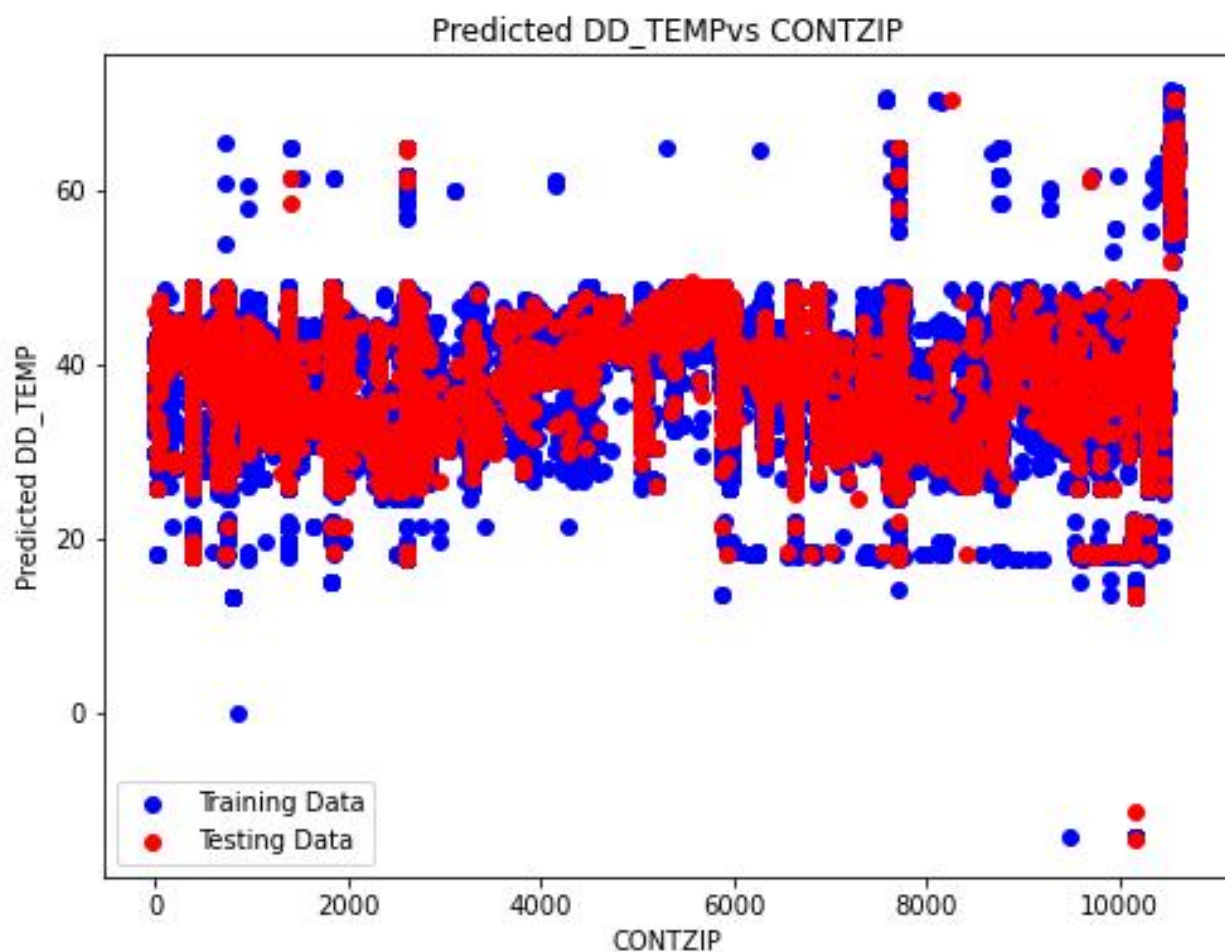
FILENUM^1\*LON\_DIR^1 + 0.00000066315116472401 \* FILENUM^1\*DD\_TEMP0^1 + -  
0.0000000000000000185605 \* FILENUM^1\*STRUCHT^1 + 0.00000000000000005551 \*  
FILENUM^1\*STRUCADD^1 + -0.00000000000000007286 \* FILENUM^1\*STRUCCITY^1 + -  
0.00000000000000002013460 \* FILENUM^1\*STRUCSTATE^1 + -0.00000000000000004163 \*  
FILENUM^1\*FAASTUDY^1 + 0.0000000000000000632000 \* FILENUM^1\*FAACIRC^1 +  
0.000000000000000008500 \* FILENUM^1\*LICID^1 + -0.00000000000000003643 \*  
FILENUM^1\*CONTNAME^1 + -0.00000000000000008327 \* FILENUM^1\*CONTADD^1 +  
0.000000000000000014450 \* FILENUM^1\*CONTPO^1 + -0.00000000000000009541 \*  
FILENUM^1\*CONTCITY^1 + -0.0000000000000000408701 \* FILENUM^1\*CONTSTATE^1 + -  
0.000000000000000000607 \* FILENUM^1\*CONTZIP^1 + -0.000000000000000028542 \* ISSUEDATE^2 + -  
0.0000000000000000050380 \* ISSUEDATE^1\*ENTITY^1 + 0.000000000000000096949 \*  
ISSUEDATE^1\*LAT\_DMS^1 + -0.00000522265658655712 \* ISSUEDATE^1\*LAT\_DIR^1 +  
0.000000000000000002914 \* ISSUEDATE^1\*LON\_DMS^1 + -0.00000000013418338845 \*  
ISSUEDATE^1\*LON\_DIR^1 + 0.00000714945766576693 \* ISSUEDATE^1\*DD\_TEMP0^1 +  
0.00000000000000005196728 \* ISSUEDATE^1\*STRUCHT^1 + -0.00000000000000009498 \*  
ISSUEDATE^1\*STRUCADD^1 + -0.000000000000000013334 \* ISSUEDATE^1\*STRUCCITY^1 +  
0.00000000000000008548451 \* ISSUEDATE^1\*STRUCSTATE^1 + 0.00000000000000005248 \*  
ISSUEDATE^1\*FAASTUDY^1 + -0.000000000000028441671 \* ISSUEDATE^1\*FAACIRC^1 +  
0.000000000000000039557 \* ISSUEDATE^1\*LICID^1 + 0.000000000000000080895 \*  
ISSUEDATE^1\*CONTNAME^1 + 0.000000000000000060141 \* ISSUEDATE^1\*CONTADD^1 +  
0.0000000000000000655791 \* ISSUEDATE^1\*CONTPO^1 + -0.000000000000000233300 \*  
ISSUEDATE^1\*CONTCITY^1 + 0.000000000000014128980 \* ISSUEDATE^1\*CONTSTATE^1 +  
0.000000000000000277901 \* ISSUEDATE^1\*CONTZIP^1 + 0.00000000000000008110 \* ENTITY^2 +  
0.0000000000000000034001 \* ENTITY^1\*LAT\_DMS^1 + 0.00000223393752293879 \*  
ENTITY^1\*LAT\_DIR^1 + -0.00000000000000008023 \* ENTITY^1\*LON\_DMS^1 + -  
0.00000000040003238532 \* ENTITY^1\*LON\_DIR^1 + 0.00001556784423160812 \*  
ENTITY^1\*DD\_TEMP0^1 + 0.00000000000000608565 \* ENTITY^1\*STRUCHT^1 + -  
0.00000000000000006765 \* ENTITY^1\*STRUCADD^1 + -0.00000000000000014550 \*  
ENTITY^1\*STRUCCITY^1 + -0.000000000000005133362 \* ENTITY^1\*STRUCSTATE^1 + -  
0.000000000000000005898 \* ENTITY^1\*FAASTUDY^1 + 0.00000000000007289915 \*  
ENTITY^1\*FAACIRC^1 + 0.00000000000000026682 \* ENTITY^1\*LICID^1 + 0.00000000000000003838 \*  
ENTITY^1\*CONTNAME^1 + 0.00000000000000019049 \* ENTITY^1\*CONTADD^1 + -  
0.000000000000000020170 \* ENTITY^1\*CONTPO^1 + 0.00000000000000021595 \*  
ENTITY^1\*CONTCITY^1 + 0.000000000000003007101 \* ENTITY^1\*CONTSTATE^1 +  
0.00000000000000006424 \* ENTITY^1\*CONTZIP^1 + 0.00000000000000015266 \* LAT\_DMS^2 + -  
0.00001057275165975765 \* LAT\_DMS^1\*LAT\_DIR^1 + 0.00000000000000019429 \*  
LAT\_DMS^1\*LON\_DMS^1 + -0.00000002696887039275 \* LAT\_DMS^1\*LON\_DIR^1 +  
0.00000018587743723886 \* LAT\_DMS^1\*DD\_TEMP0^1 + -0.00000000000001402083 \*  
LAT\_DMS^1\*STRUCHT^1 + -0.00000000000000005551 \* LAT\_DMS^1\*STRUCADD^1 +  
0.000000000000000014398 \* LAT\_DMS^1\*STRUCCITY^1 + -0.00000000000018484561 \*  
LAT\_DMS^1\*STRUCSTATE^1 + 0.00000000000000005551 \* LAT\_DMS^1\*FAASTUDY^1 + -  
0.00000000000030104196 \* LAT\_DMS^1\*FAACIRC^1 + -0.00000000000000025934 \*  
LAT\_DMS^1\*LICID^1 + -0.00000000000000050220 \* LAT\_DMS^1\*CONTNAME^1 +  
0.000000000000000032092 \* LAT\_DMS^1\*CONTADD^1 + 0.00000000000000281451 \*

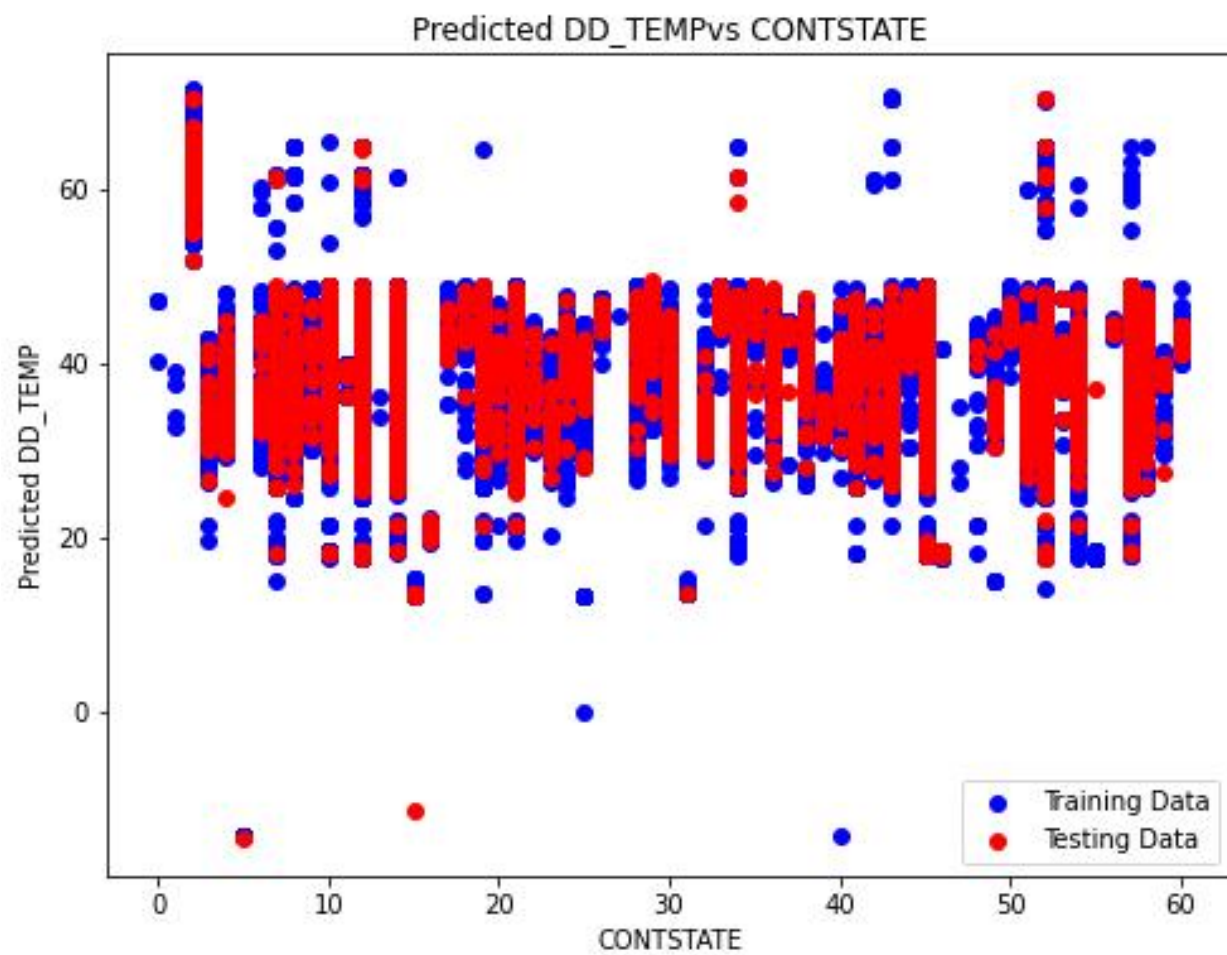
LAT\_DMS^1\*CONTPO^1 + 0.00000000000000006549 \* LAT\_DMS^1\*CONTCITY^1 +  
0.00000000000035385606 \* LAT\_DMS^1\*CONTSTATE^1 + -0.00000000000000546134 \*  
LAT\_DMS^1\*CONTZIP^1 + -0.00000012724415322133 \* LAT\_DIR^2 + 0.00023388185670245438 \*  
LAT\_DIR^1\*LON\_DMS^1 + 0.00004638107339939518 \* LAT\_DIR^1\*LON\_DIR^1 +  
0.00000035638887647786 \* LAT\_DIR^1\*DD\_TEMP0^1 + 0.00009467720615143546 \*  
LAT\_DIR^1\*STRUCHT^1 + -0.00000050155425021323 \* LAT\_DIR^1\*STRUCADD^1 + -  
0.00000054682106866862 \* LAT\_DIR^1\*STRUCCITY^1 + 0.00000021138171054890 \*  
LAT\_DIR^1\*STRUCSTATE^1 + 0.00000174636251649942 \* LAT\_DIR^1\*FAASTUDY^1 +  
0.00000564130828803707 \* LAT\_DIR^1\*FAACIRC^1 + 0.00001676029881689953 \* LAT\_DIR^1\*LICID^1  
+ -0.00000131642609509163 \* LAT\_DIR^1\*CONTNAME^1 + 0.00000148755732955542 \*  
LAT\_DIR^1\*CONTADD^1 + 0.00000145292708282536 \* LAT\_DIR^1\*CONTPO^1 + -  
0.00022464498346261243 \* LAT\_DIR^1\*CONTCITY^1 + -0.00000690000241796867 \*  
LAT\_DIR^1\*CONTSTATE^1 + 0.00033408322247044619 \* LAT\_DIR^1\*CONTZIP^1 + -  
0.000000000000000062277 \* LON\_DMS^2 + 0.00000001821047927867 \* LON\_DMS^1\*LON\_DIR^1 +  
0.00001918427118026466 \* LON\_DMS^1\*DD\_TEMP0^1 + 0.00000000000000375161 \*  
LON\_DMS^1\*STRUCHT^1 + 0.00000000000000001388 \* LON\_DMS^1\*STRUCADD^1 + -  
0.00000000000000002212 \* LON\_DMS^1\*STRUCCITY^1 + -0.00000000000001765971 \*  
LON\_DMS^1\*STRUCSTATE^1 + 0.00000000000000000000 \* LON\_DMS^1\*FAASTUDY^1 +  
0.00000000000001753145 \* LON\_DMS^1\*FAACIRC^1 + 0.0000000000000007026 \*  
LON\_DMS^1\*LICID^1 + 0.00000000000000015656 \* LON\_DMS^1\*CONTNAME^1 + -  
0.00000000000000005334 \* LON\_DMS^1\*CONTADD^1 + -0.0000000000000005603 \*  
LON\_DMS^1\*CONTPO^1 + 0.00000000000000025056 \* LON\_DMS^1\*CONTCITY^1 +  
0.00000000000001723009 \* LON\_DMS^1\*CONTSTATE^1 + 0.0000000000000076065 \*  
LON\_DMS^1\*CONTZIP^1 + -0.00000012515230997563 \* LON\_DIR^2 + -0.00000132039906229322 \*  
LON\_DIR^1\*DD\_TEMP0^1 + 0.00000000524745812092 \* LON\_DIR^1\*STRUCHT^1 + -  
0.00000000001079355659 \* LON\_DIR^1\*STRUCADD^1 + -0.00000000007767771833 \*  
LON\_DIR^1\*STRUCCITY^1 + -0.00000001669208505289 \* LON\_DIR^1\*STRUCSTATE^1 + -  
0.00000000001414732031 \* LON\_DIR^1\*FAASTUDY^1 + -0.00000003198730638366 \*  
LON\_DIR^1\*FAACIRC^1 + 0.00000000103918018367 \* LON\_DIR^1\*LICID^1 + 0.00000000109628557079  
\* LON\_DIR^1\*CONTNAME^1 + -0.0000000036113721325 \* LON\_DIR^1\*CONTADD^1 +  
0.00000000031110045890 \* LON\_DIR^1\*CONTPO^1 + 0.00000000111721027615 \*  
LON\_DIR^1\*CONTCITY^1 + 0.00000004307331219250 \* LON\_DIR^1\*CONTSTATE^1 +  
0.00000000678564056121 \* LON\_DIR^1\*CONTZIP^1 + 0.00047433591833243987 \* DD\_TEMP0^2 + -  
0.00014866899330102630 \* DD\_TEMP0^1\*STRUCHT^1 + 0.00000049827880532496 \*  
DD\_TEMP0^1\*STRUCADD^1 + 0.00000282730288937030 \* DD\_TEMP0^1\*STRUCCITY^1 +  
0.00002292316866353692 \* DD\_TEMP0^1\*STRUCSTATE^1 + 0.00000054972994623536 \*  
DD\_TEMP0^1\*FAASTUDY^1 + -0.00000836176482101934 \* DD\_TEMP0^1\*FAACIRC^1 + -  
0.00003665822875463256 \* DD\_TEMP0^1\*LICID^1 + -0.00003642372790861711 \*  
DD\_TEMP0^1\*CONTNAME^1 + 0.00001255416701220747 \* DD\_TEMP0^1\*CONTADD^1 + -  
0.00001085335254628254 \* DD\_TEMP0^1\*CONTPO^1 + -0.00003356908761722463 \*  
DD\_TEMP0^1\*CONTCITY^1 + 0.00002680848737377332 \* DD\_TEMP0^1\*CONTSTATE^1 + -  
0.00024656125185020959 \* DD\_TEMP0^1\*CONTZIP^1 + 0.0000000000029239553 \* STRUCHT^2 +  
0.000000000000000066870 \* STRUCHT^1\*STRUCADD^1 + 0.0000000000000460429 \*  
STRUCHT^1\*STRUCCITY^1 + 0.00000000000184333127 \* STRUCHT^1\*STRUCSTATE^1 +

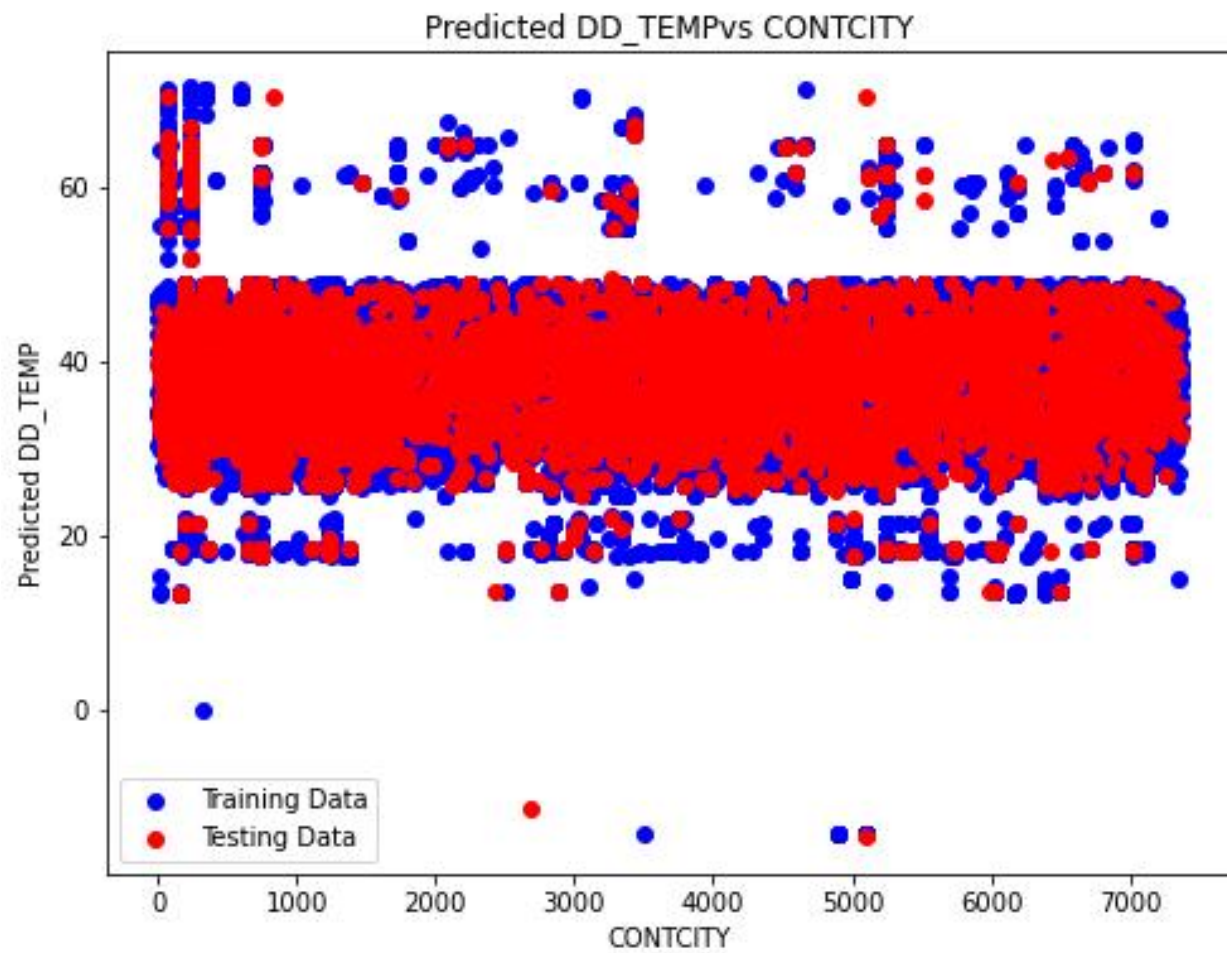
0.0000000000000000163061 \* STRUCHT^1\*FAASTUDY^1 + 0.000000000000660070169 \*  
STRUCHT^1\*FAACIRC^1 + 0.000000000000001477792 \* STRUCHT^1\*LICID^1 +  
0.00000000000000001350478 \* STRUCHT^1\*CONTNAME^1 + 0.000000000000000846564 \*  
STRUCHT^1\*CONTADD^1 + 0.0000000000000014700593 \* STRUCHT^1\*CONTPO^1 +  
0.00000000000000001084881 \* STRUCHT^1\*CONTCITY^1 + -0.000000000000253635422 \*  
STRUCHT^1\*CONTSTATE^1 + 0.000000000000003414932 \* STRUCHT^1\*CONTZIP^1 + -  
0.0000000000000000012490 \* STRUCADD^2 + -0.000000000000000010408 \* STRUCADD^1\*STRUCCITY^1  
+ 0.0000000000000000059483 \* STRUCADD^1\*STRUCSTATE^1 + 0.00000000000000004163 \*  
STRUCADD^1\*FAASTUDY^1 + -0.0000000000000000657538 \* STRUCADD^1\*FAACIRC^1 +  
0.0000000000000000005898 \* STRUCADD^1\*LICID^1 + -0.000000000000000010061 \*  
STRUCADD^1\*CONTNAME^1 + -0.000000000000000008327 \* STRUCADD^1\*CONTADD^1 + -  
0.0000000000000000001855 \* STRUCADD^1\*CONTPO^1 + -0.000000000000000008717 \*  
STRUCADD^1\*CONTCITY^1 + -0.0000000000000000475838 \* STRUCADD^1\*CONTSTATE^1 +  
0.0000000000000000002342 \* STRUCADD^1\*CONTZIP^1 + -0.000000000000000010300 \* STRUCCITY^2 + -  
0.00000000000000000817757 \* STRUCCITY^1\*STRUCSTATE^1 + -0.000000000000000011276 \*  
STRUCCITY^1\*FAASTUDY^1 + -0.000000000000003658368 \* STRUCCITY^1\*FAACIRC^1 + -  
0.0000000000000000003567 \* STRUCCITY^1\*LICID^1 + -0.00000000000000009069 \*  
STRUCCITY^1\*CONTNAME^1 + 0.000000000000000000163 \* STRUCCITY^1\*CONTADD^1 +  
0.00000000000000000029694 \* STRUCCITY^1\*CONTPO^1 + -0.000000000000000017157 \*  
STRUCCITY^1\*CONTCITY^1 + 0.0000000000000000569471 \* STRUCCITY^1\*CONTSTATE^1 +  
0.0000000000000000000932 \* STRUCCITY^1\*CONTZIP^1 + 0.00000000005987727088 \* STRUCSTATE^2 +  
0.0000000000000000110263 \* STRUCSTATE^1\*FAASTUDY^1 + 0.00000000006992085076 \*  
STRUCSTATE^1\*FAACIRC^1 + 0.000000000000009226288 \* STRUCSTATE^1\*LICID^1 + -  
0.00000000000000005192722 \* STRUCSTATE^1\*CONTNAME^1 + 0.00000000000000915708 \*  
STRUCSTATE^1\*CONTADD^1 + -0.000000000000004762631 \* STRUCSTATE^1\*CONTPO^1 + -  
0.0000000000000013282681 \* STRUCSTATE^1\*CONTCITY^1 + 0.00000000001237680814 \*  
STRUCSTATE^1\*CONTSTATE^1 + 0.00000000000078978785 \* STRUCSTATE^1\*CONTZIP^1 +  
0.00000000000000004163 \* FAASTUDY^2 + 0.00000000000000198331 \* FAASTUDY^1\*FAACIRC^1 + -  
0.000000000000000009281 \* FAASTUDY^1\*LICID^1 + -0.00000000000000004597 \*  
FAASTUDY^1\*CONTNAME^1 + -0.00000000000000002082 \* FAASTUDY^1\*CONTADD^1 + -  
0.000000000000000000535 \* FAASTUDY^1\*CONTPO^1 + -0.00000000000000002949 \*  
FAASTUDY^1\*CONTCITY^1 + -0.00000000000000770247 \* FAASTUDY^1\*CONTSTATE^1 + -  
0.00000000000000004684 \* FAASTUDY^1\*CONTZIP^1 + 0.00000000021881985360 \* FAACIRC^2 +  
0.00000000000010063057 \* FAACIRC^1\*LICID^1 + -0.00000000000000428773 \*  
FAACIRC^1\*CONTNAME^1 + -0.000000000000003672254 \* FAACIRC^1\*CONTADD^1 + -  
0.000000000000111818169 \* FAACIRC^1\*CONTPO^1 + 0.00000000000043546090 \*  
FAACIRC^1\*CONTCITY^1 + 0.00000000004785866957 \* FAACIRC^1\*CONTSTATE^1 +  
0.00000000000015161313 \* FAACIRC^1\*CONTZIP^1 + 0.0000000000000047184 \* LICID^2 + -  
0.000000000000000012436 \* LICID^1\*CONTNAME^1 + -0.0000000000000006451 \*  
LICID^1\*CONTADD^1 + -0.000000000000000018795 \* LICID^1\*CONTPO^1 + 0.00000000000000004025 \*  
LICID^1\*CONTCITY^1 + 0.000000000000003419803 \* LICID^1\*CONTSTATE^1 +  
0.00000000000000134712 \* LICID^1\*CONTZIP^1 + -0.0000000000000010266 \* CONTNAME^2 +  
0.000000000000000011953 \* CONTNAME^1\*CONTADD^1 + 0.00000000000000145730 \*  
CONTNAME^1\*CONTPO^1 + -0.00000000000000054256 \* CONTNAME^1\*CONTCITY^1 +

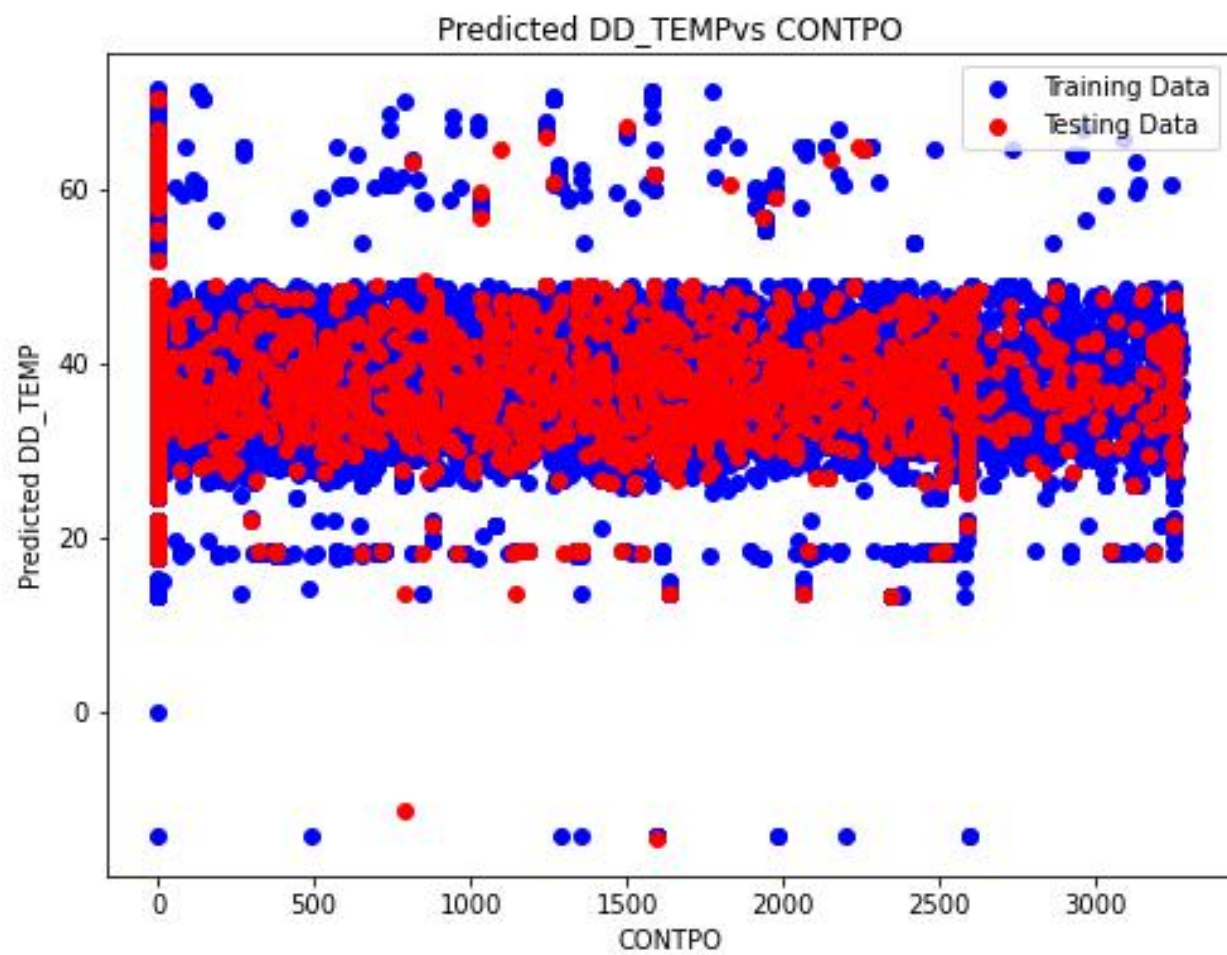
$0.00000000000013528052 * \text{CONTNAME}^1 * \text{CONTSTATE}^1 + 0.0000000000000048477 * \text{CONTNAME}^1 * \text{CONTZIP}^1 + 0.0000000000000020090 * \text{CONTADD}^2 + -0.0000000000000000382 * \text{CONTADD}^1 * \text{CONTPO}^1 + -0.00000000000000055625 * \text{CONTADD}^1 * \text{CONTCITY}^1 + -0.000000000000003190033 * \text{CONTADD}^1 * \text{CONTSTATE}^1 + -0.00000000000000025285 * \text{CONTADD}^1 * \text{CONTZIP}^1 + -0.000000000000001243002 * \text{CONTPO}^2 + -0.000000000000000322062 * \text{CONTPO}^1 * \text{CONTCITY}^1 + -0.000000000000003709503 * \text{CONTPO}^1 * \text{CONTSTATE}^1 + 0.000000000000000227687 * \text{CONTPO}^1 * \text{CONTZIP}^1 + 0.00000000000000099026 * \text{CONTCITY}^2 + 0.000000000000066389578 * \text{CONTCITY}^1 * \text{CONTSTATE}^1 + -0.0000000000000032523 * \text{CONTCITY}^1 * \text{CONTZIP}^1 + 0.00000000000526906979 * \text{CONTSTATE}^2 + -0.00000000000015545706 * \text{CONTSTATE}^1 * \text{CONTZIP}^1 + 0.00000000000000346911 * \text{CONTZIP}^2$

ENCODING ONLY CATEGORICAL VARIABLES:

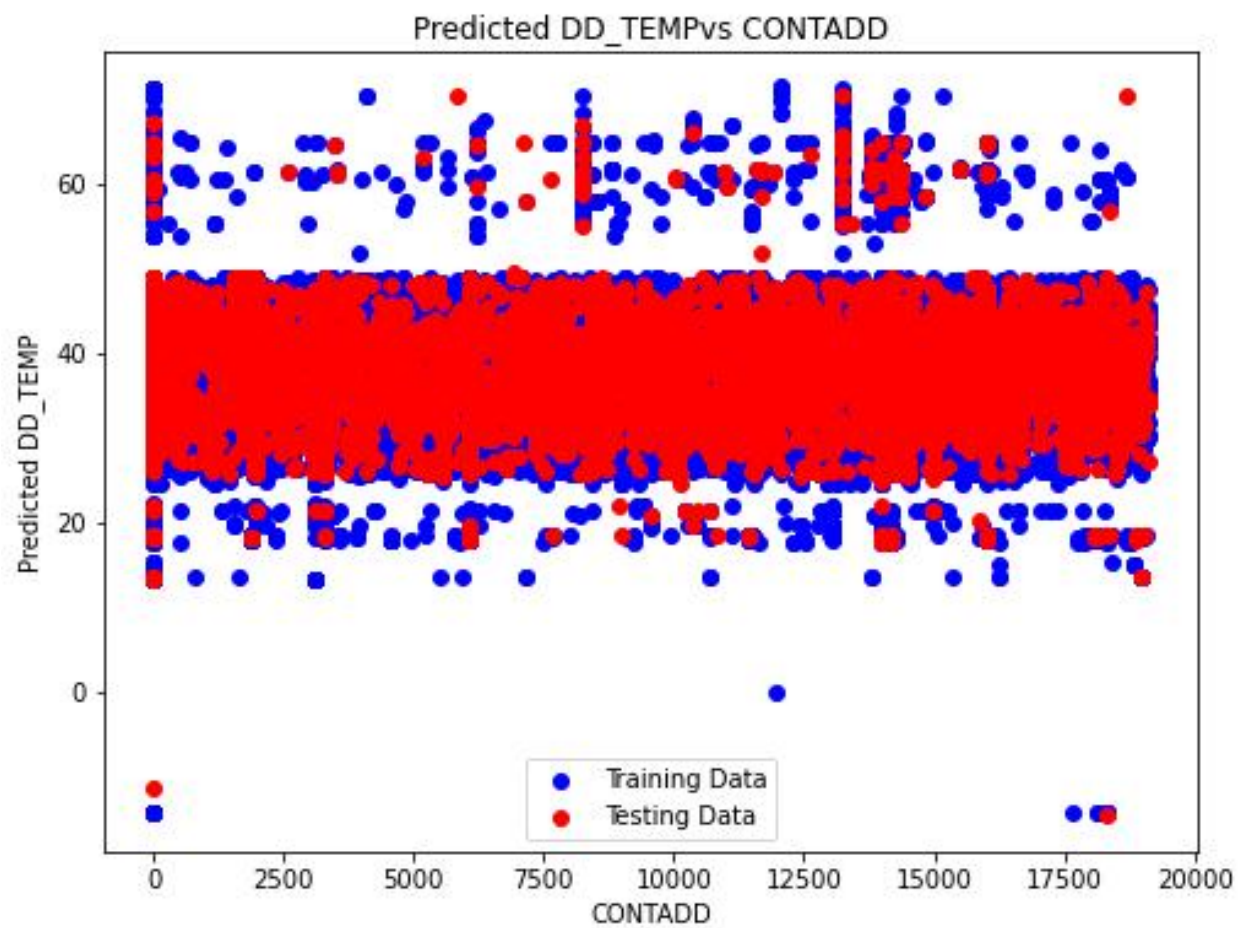


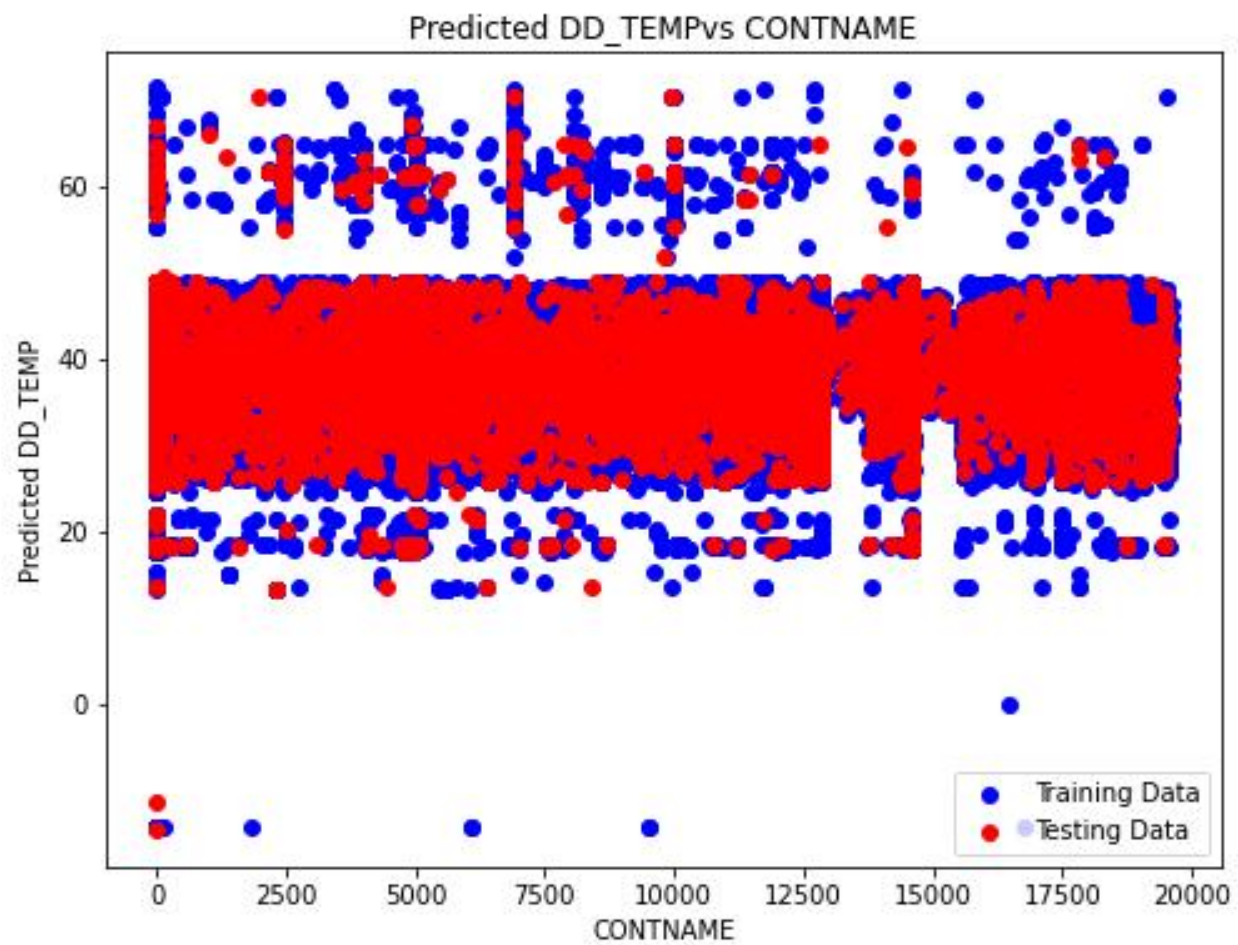


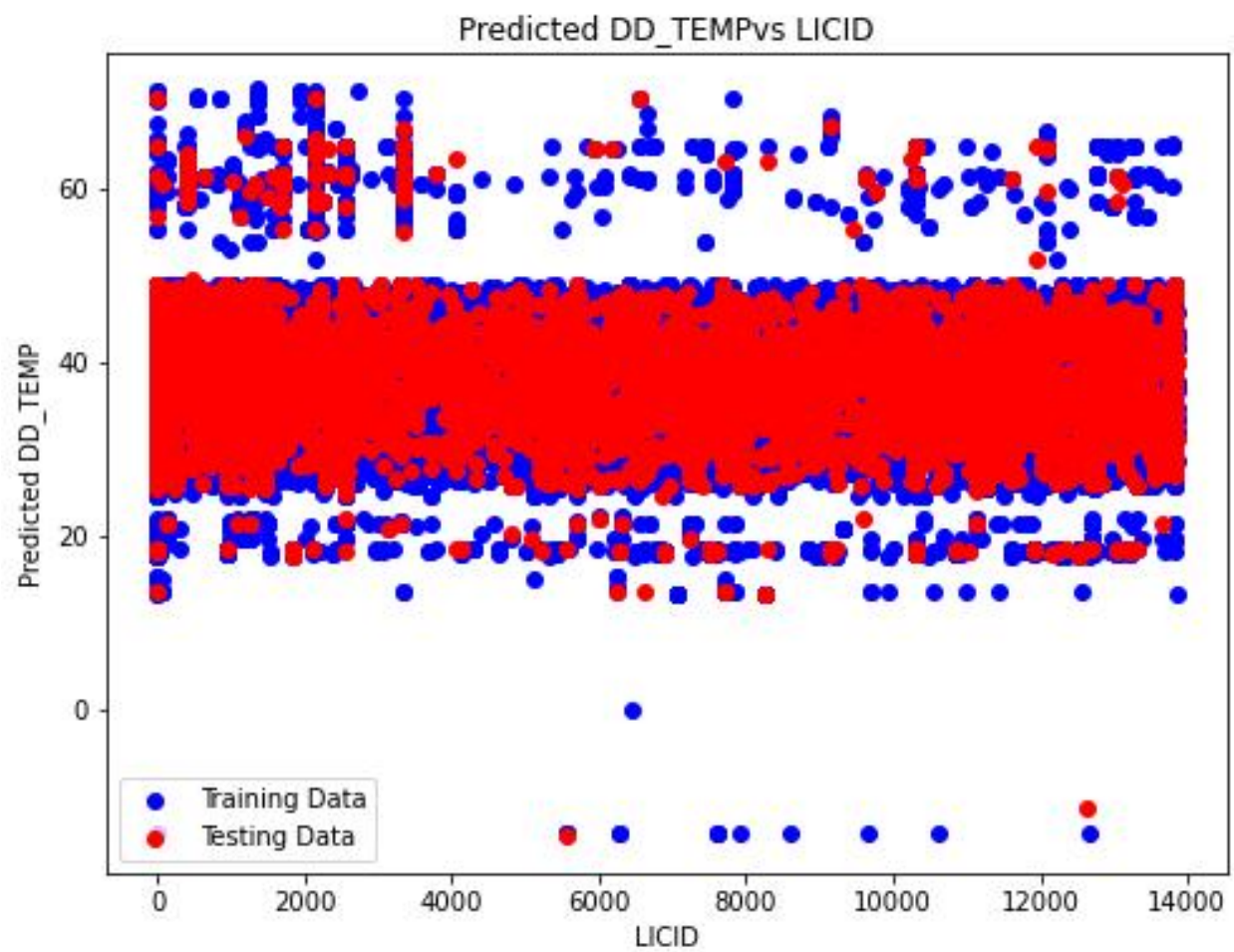


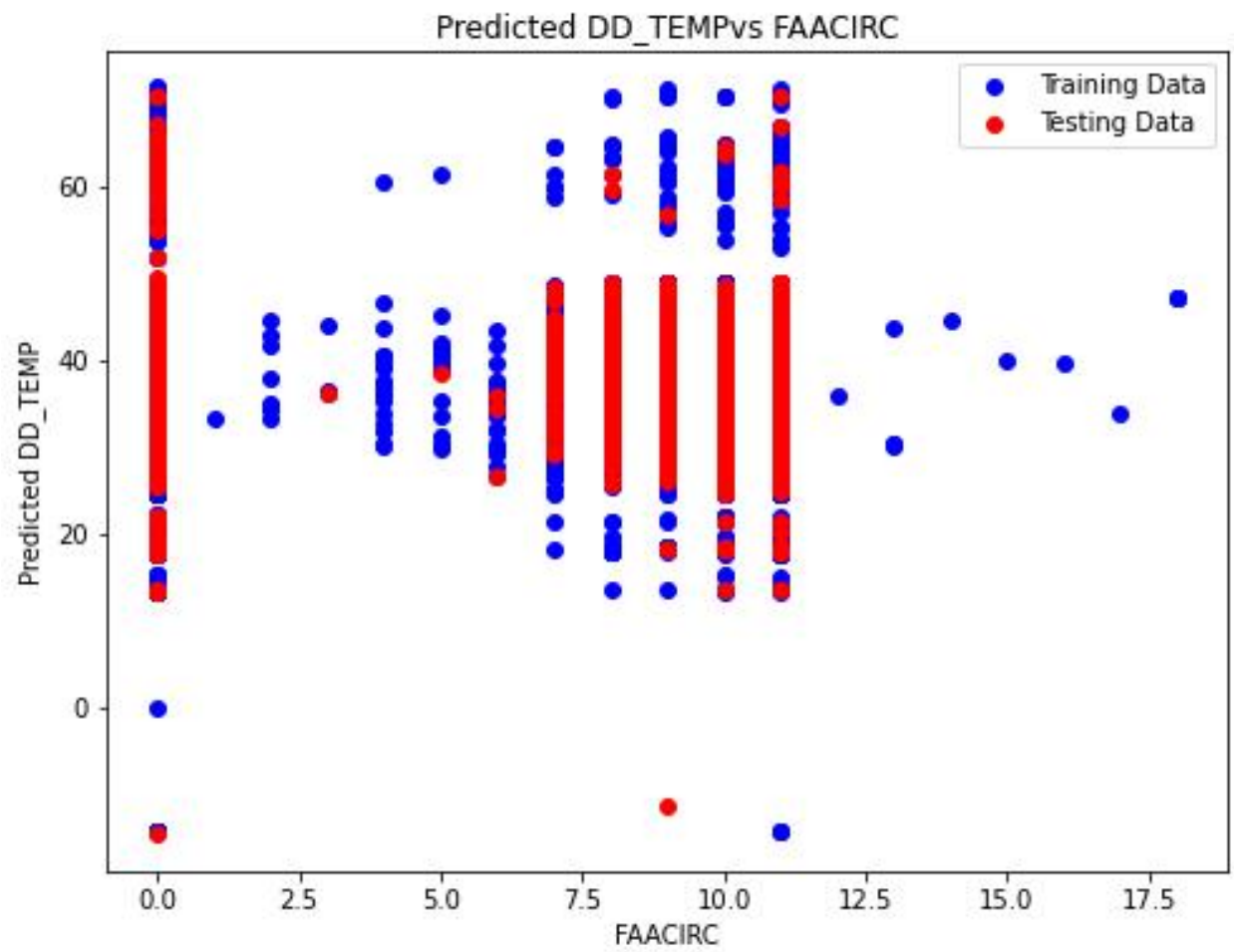


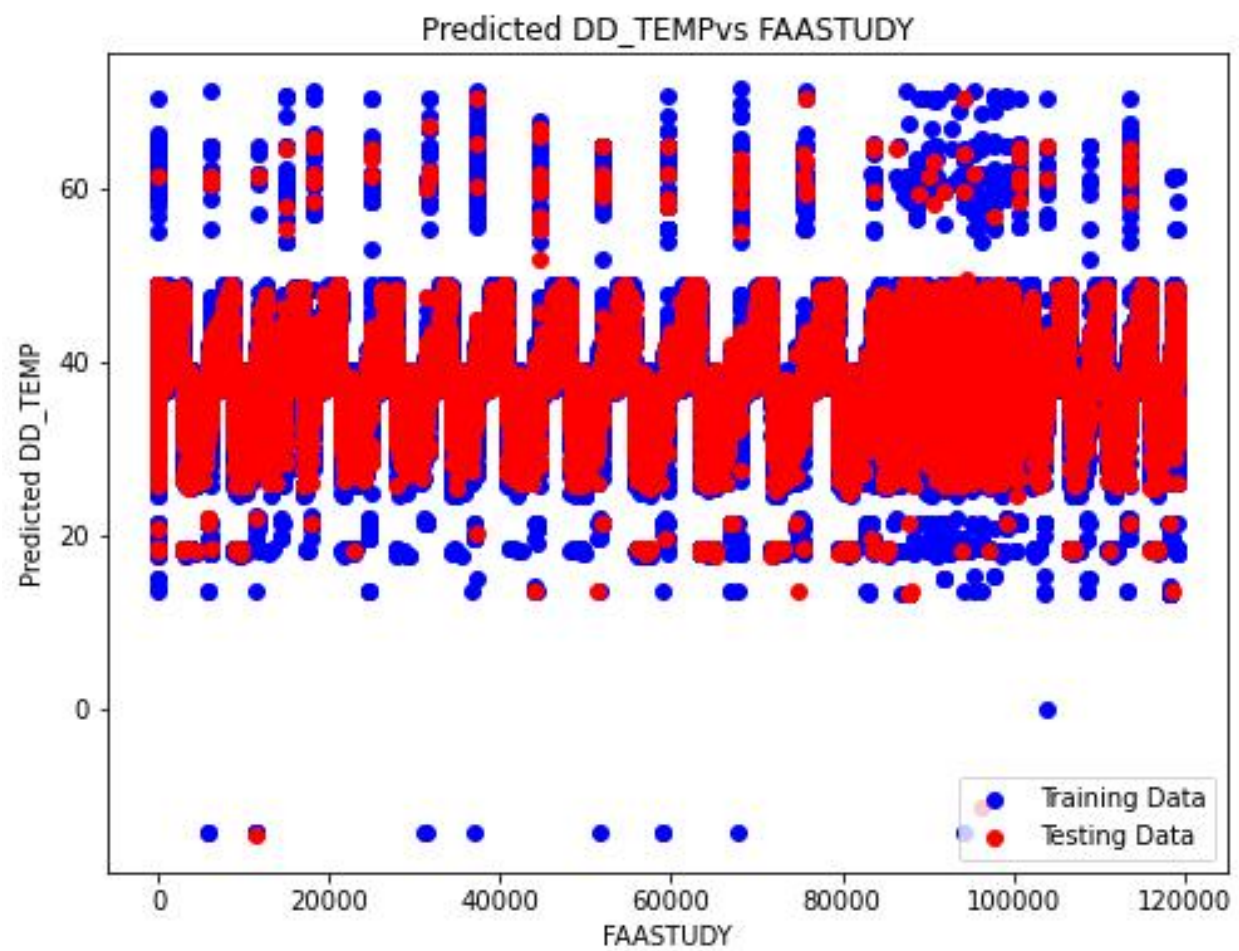


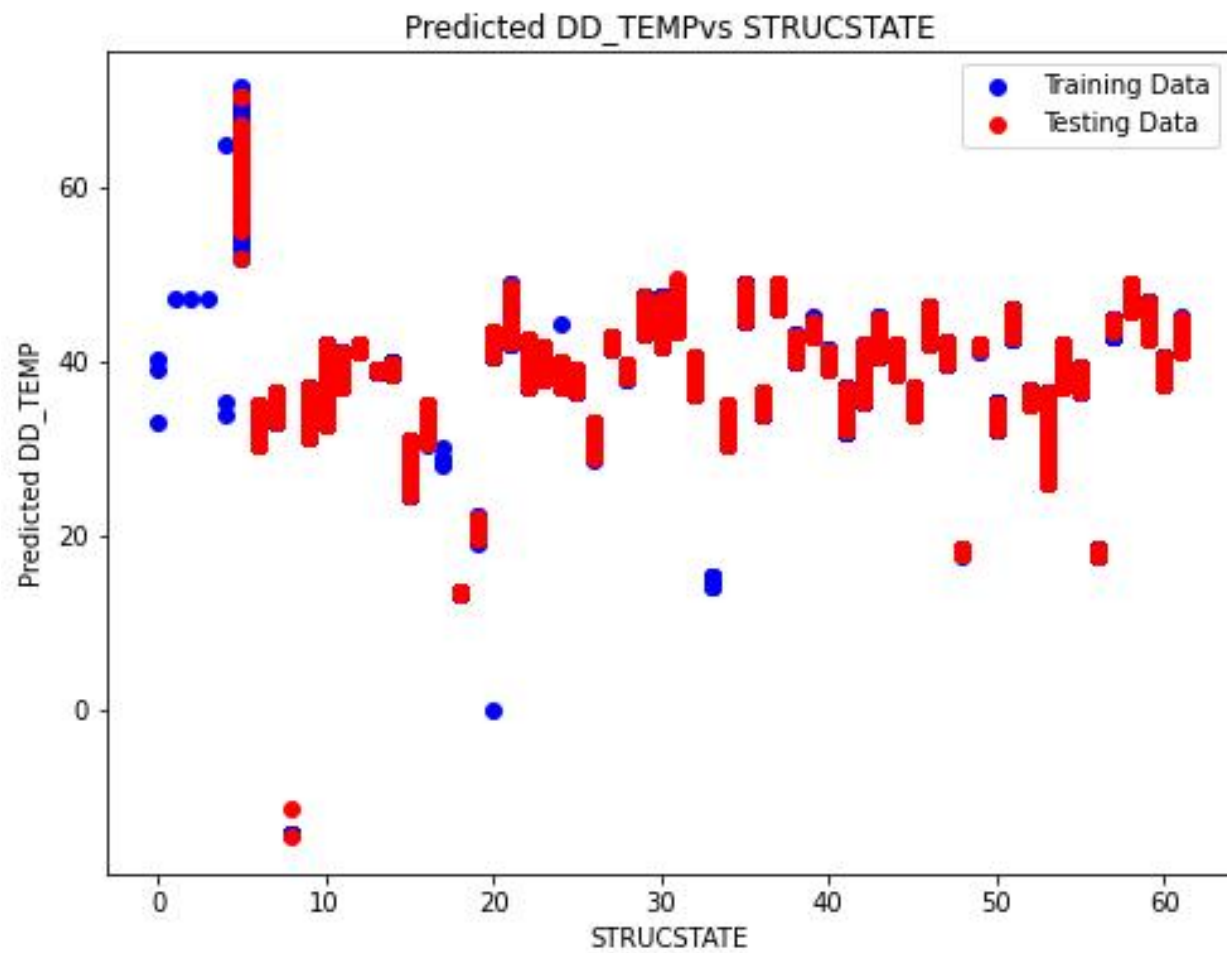




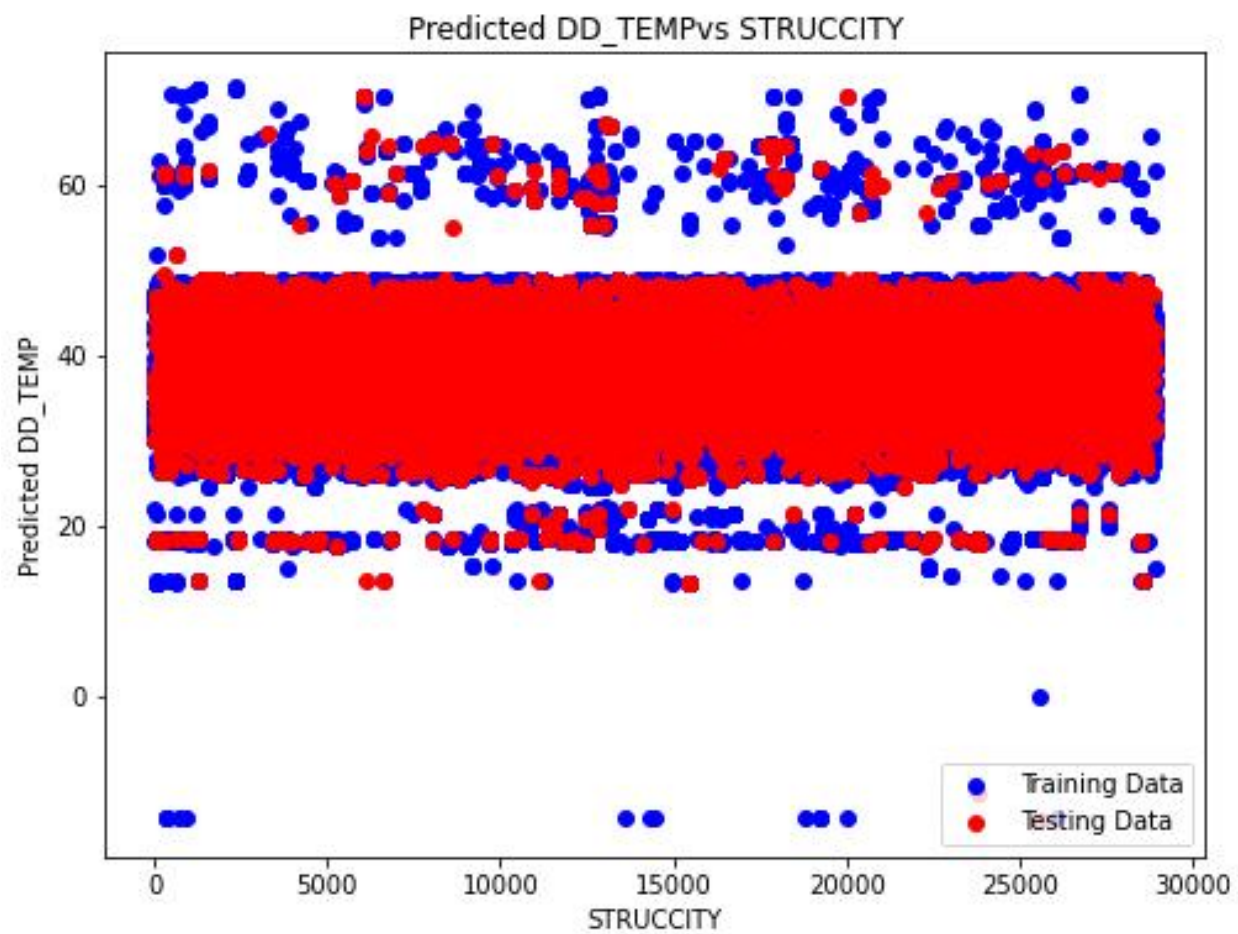


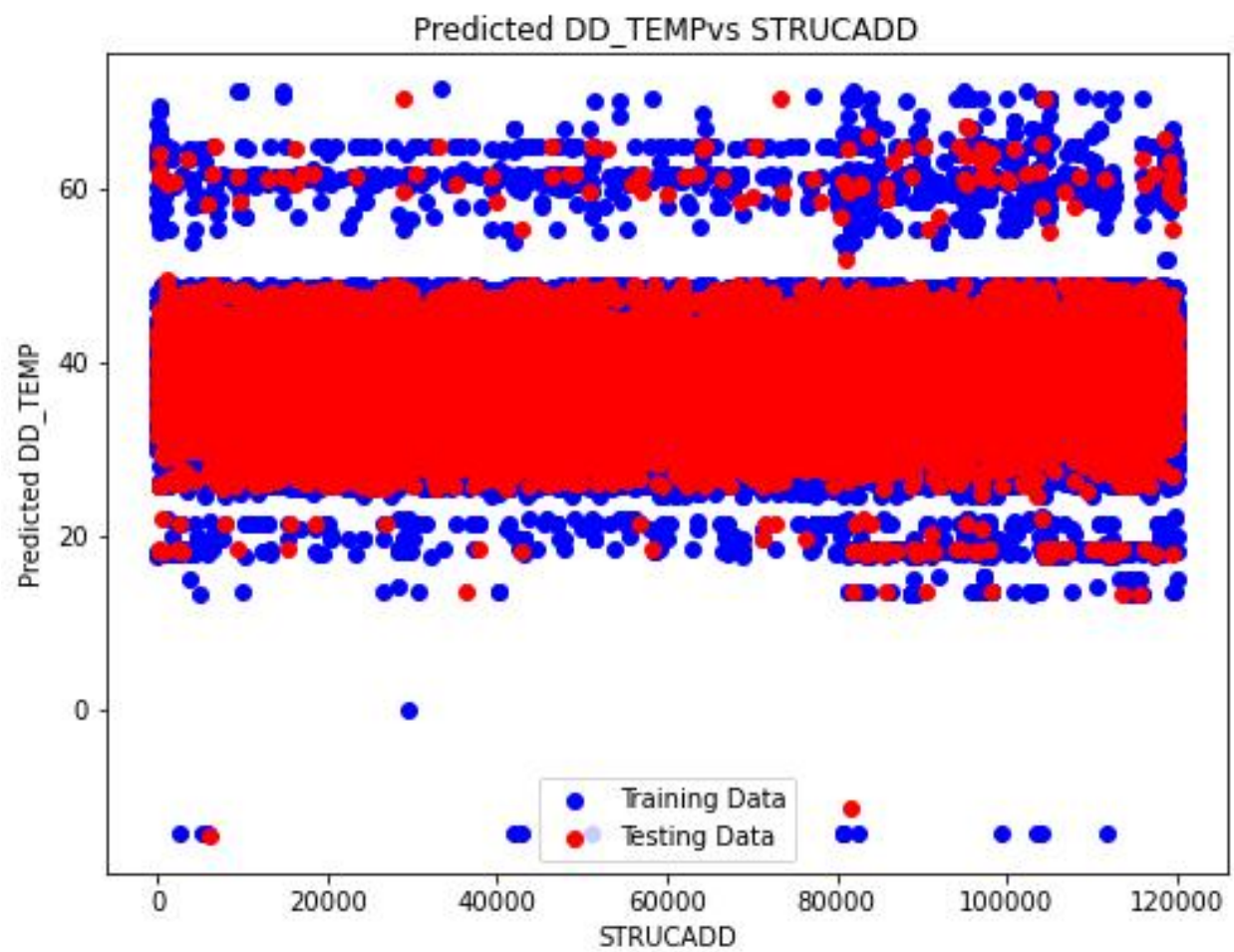




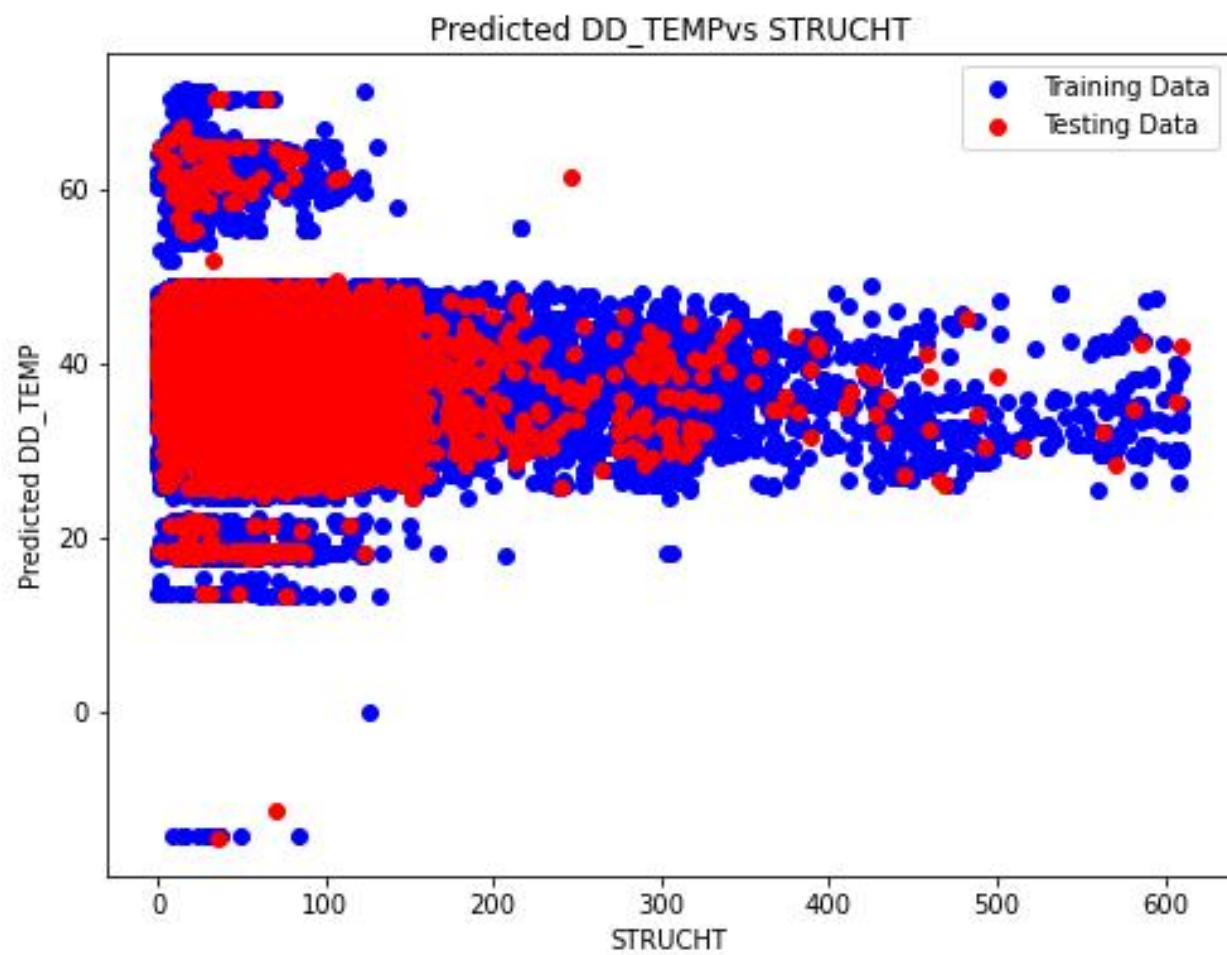


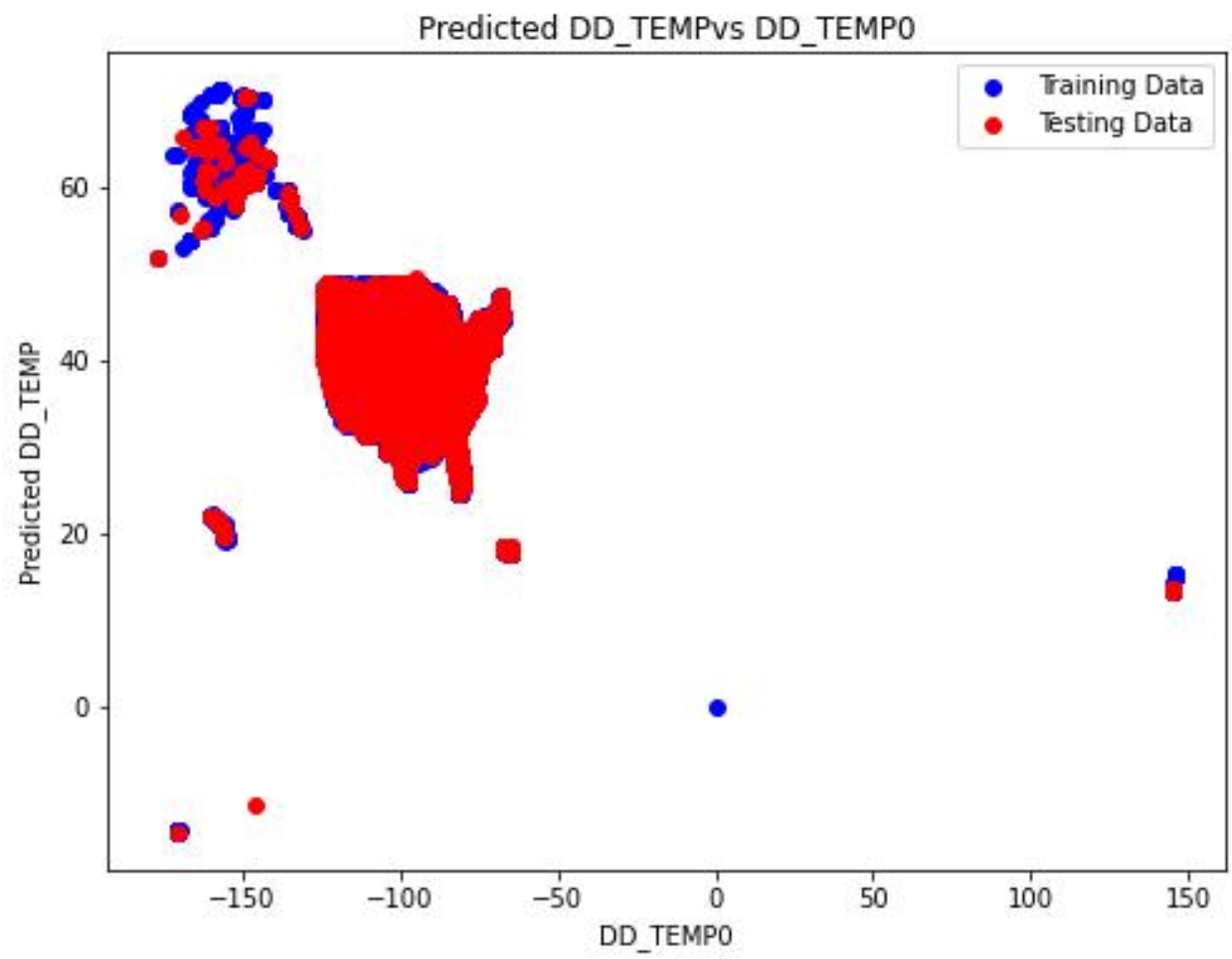


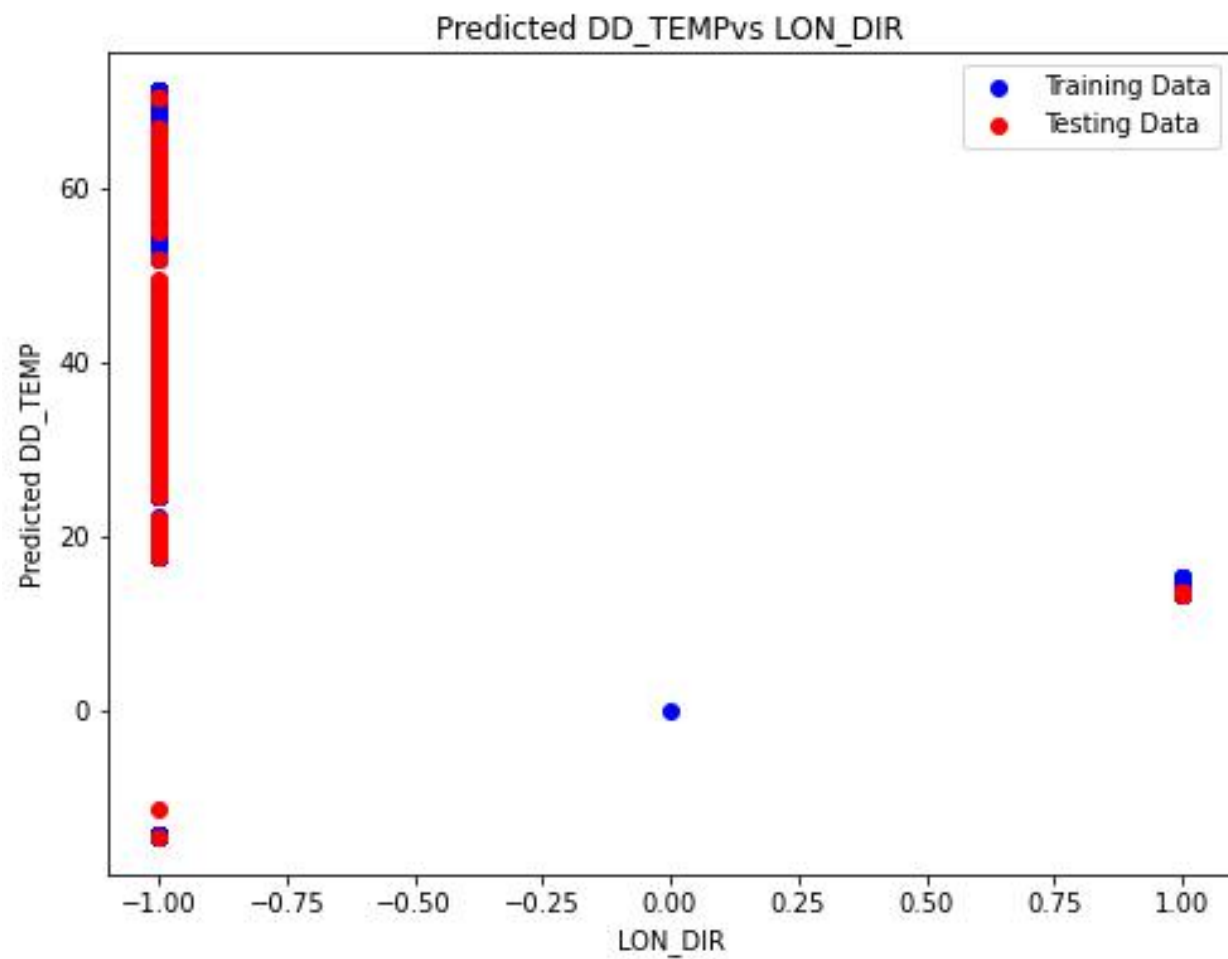


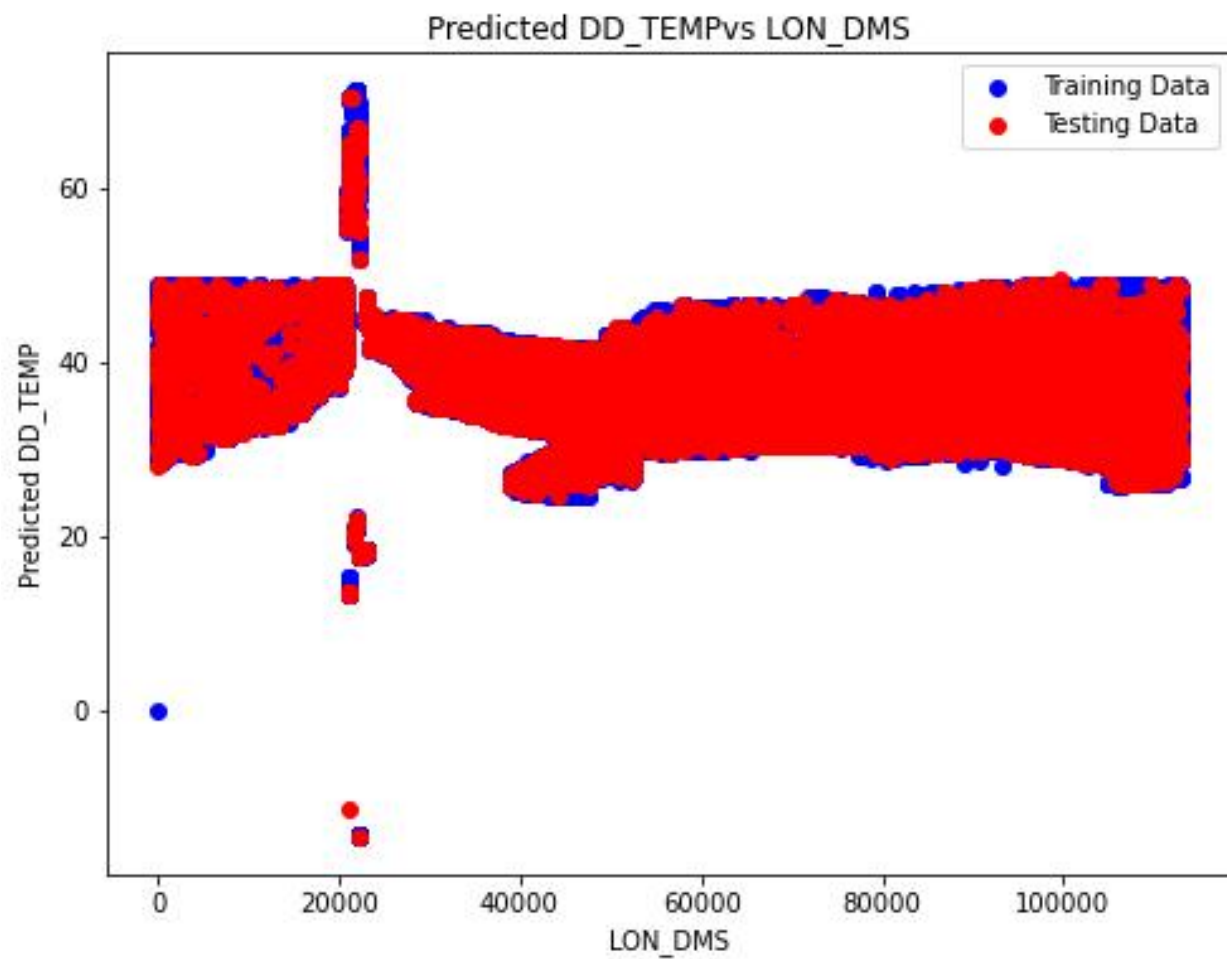


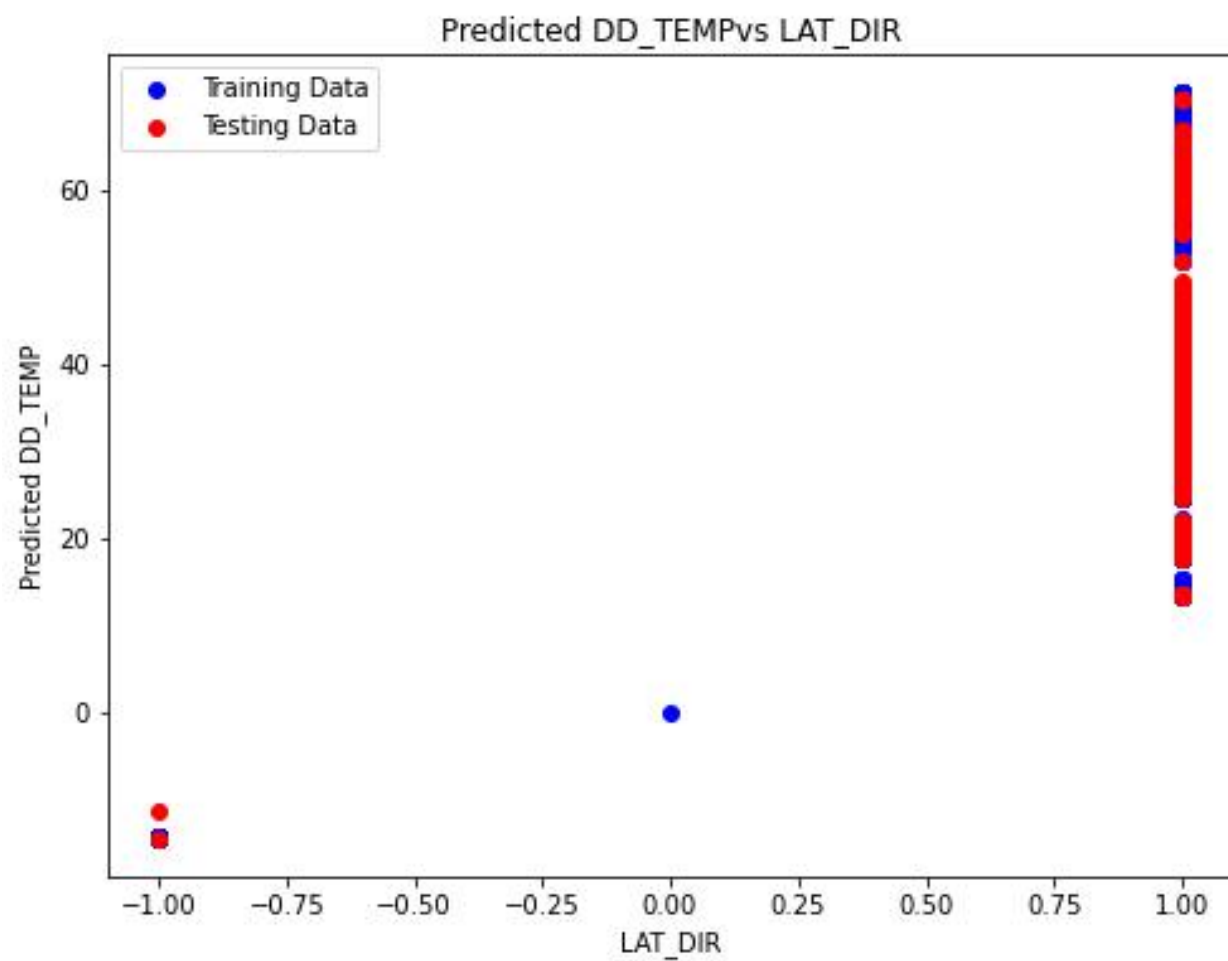


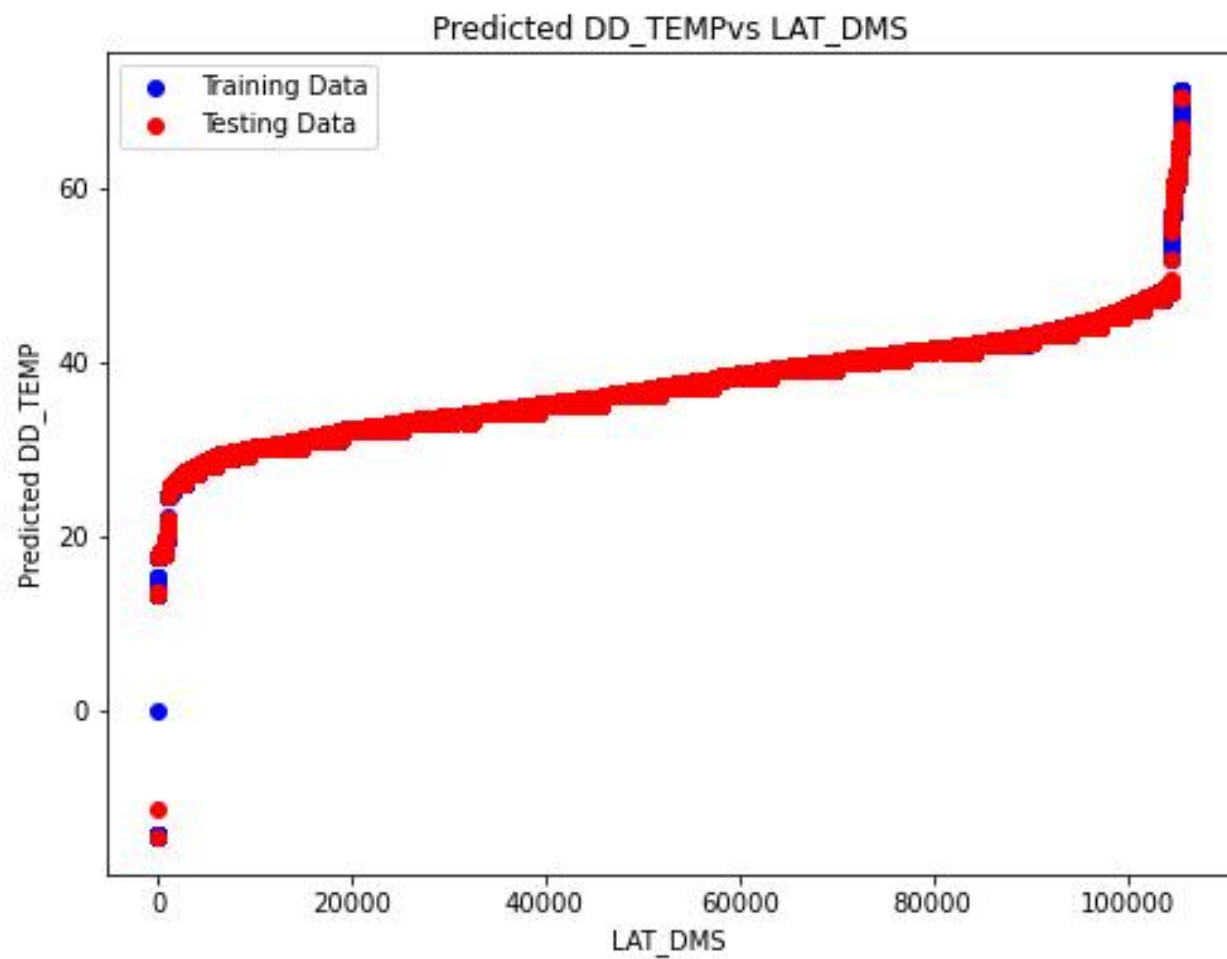


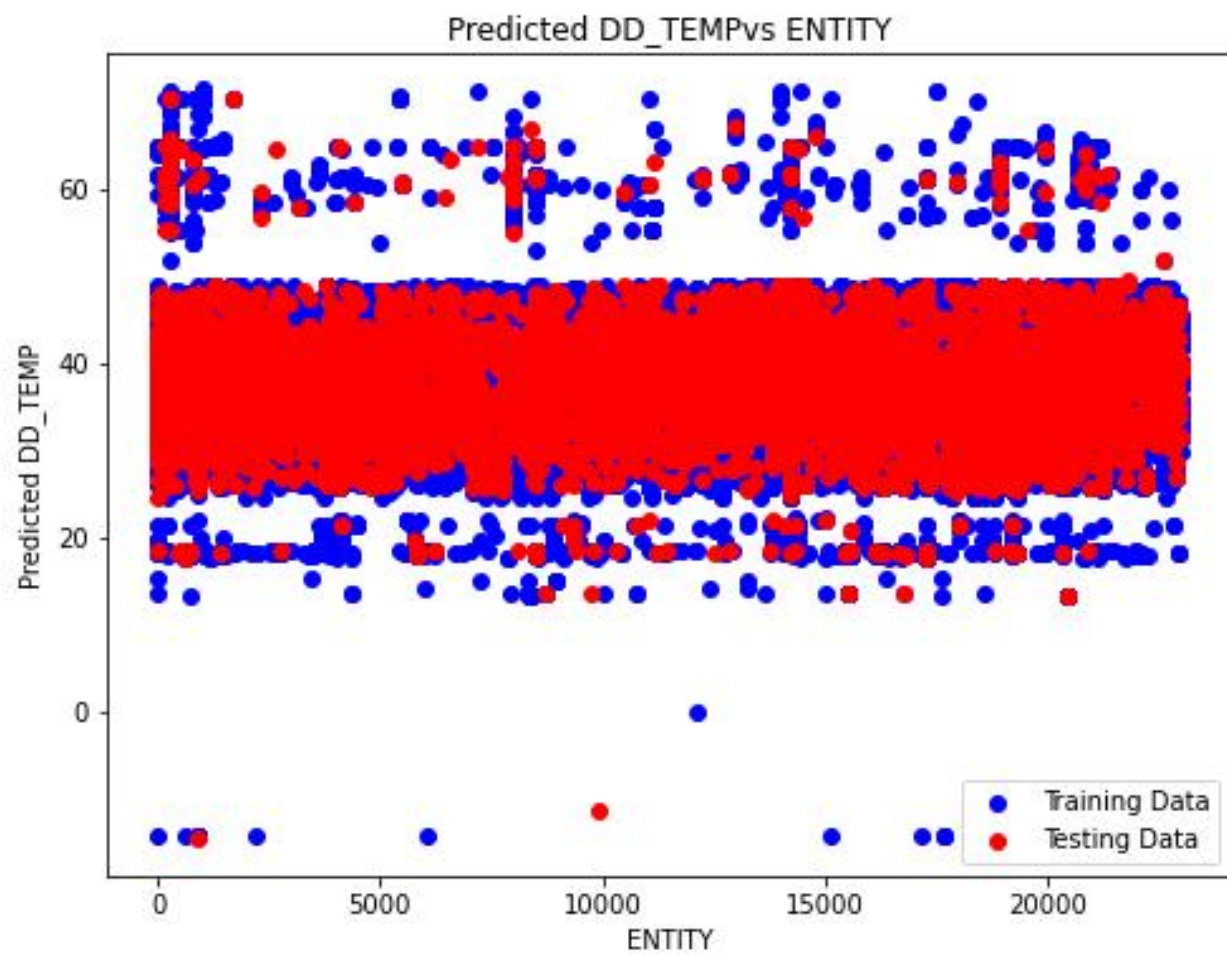


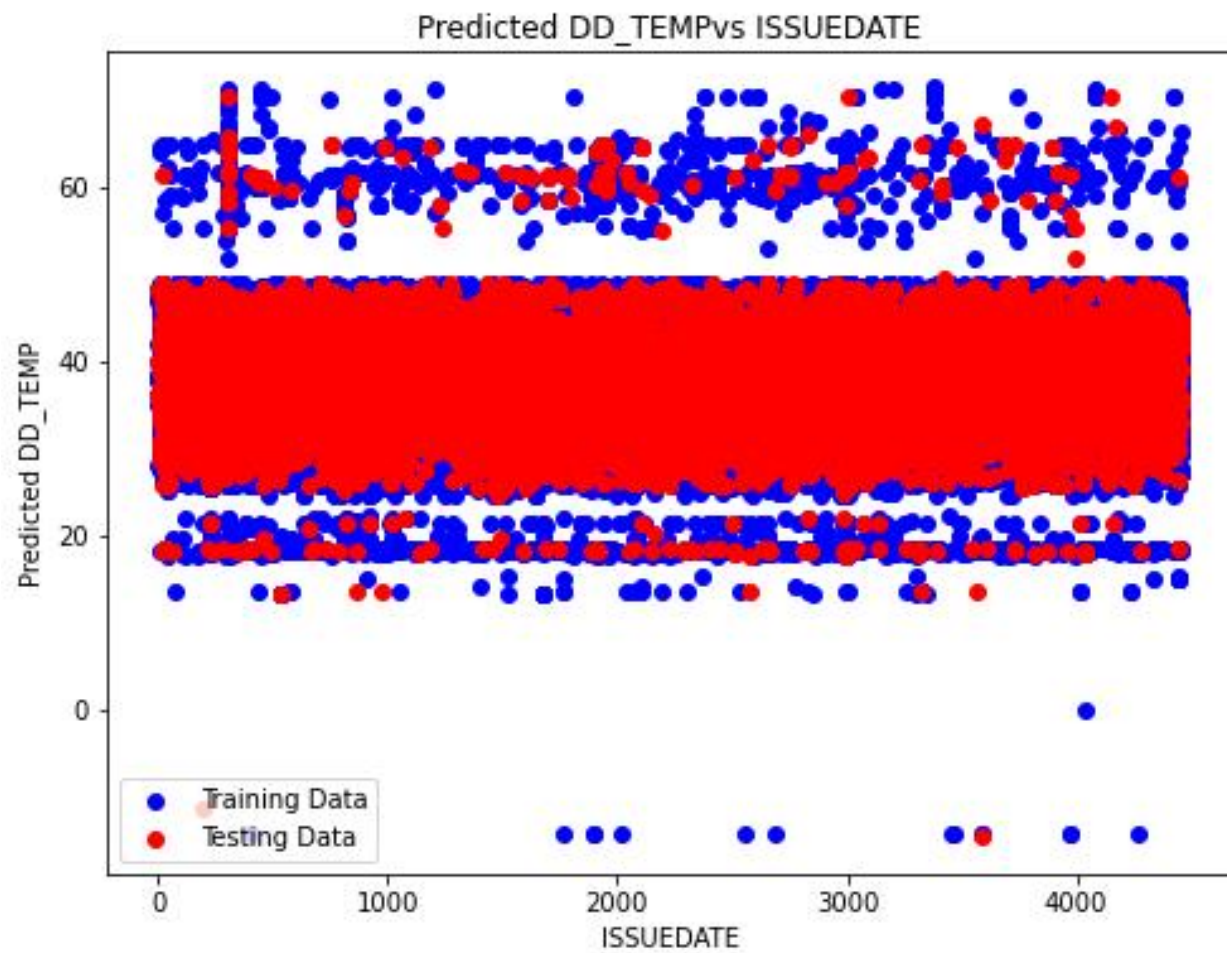




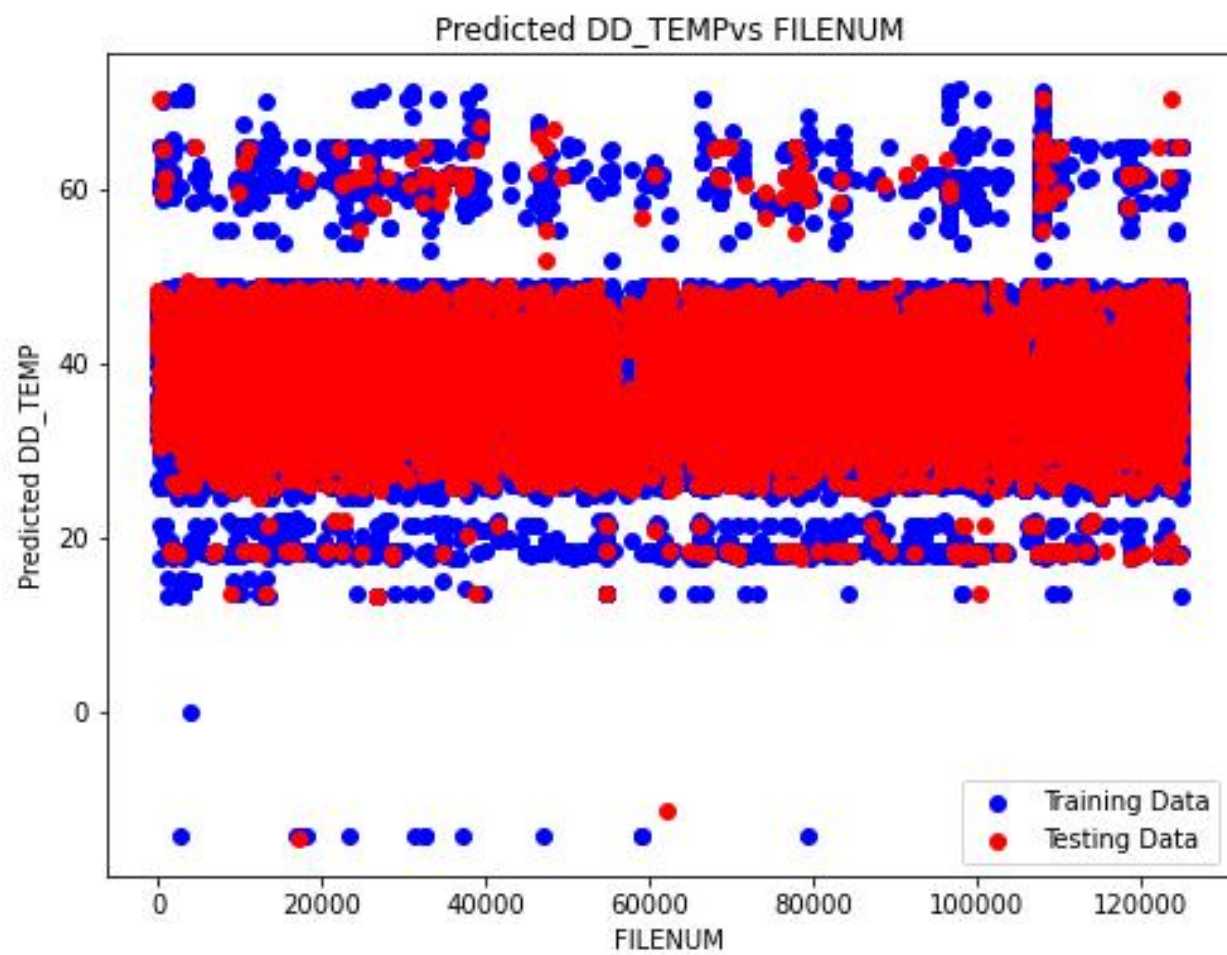


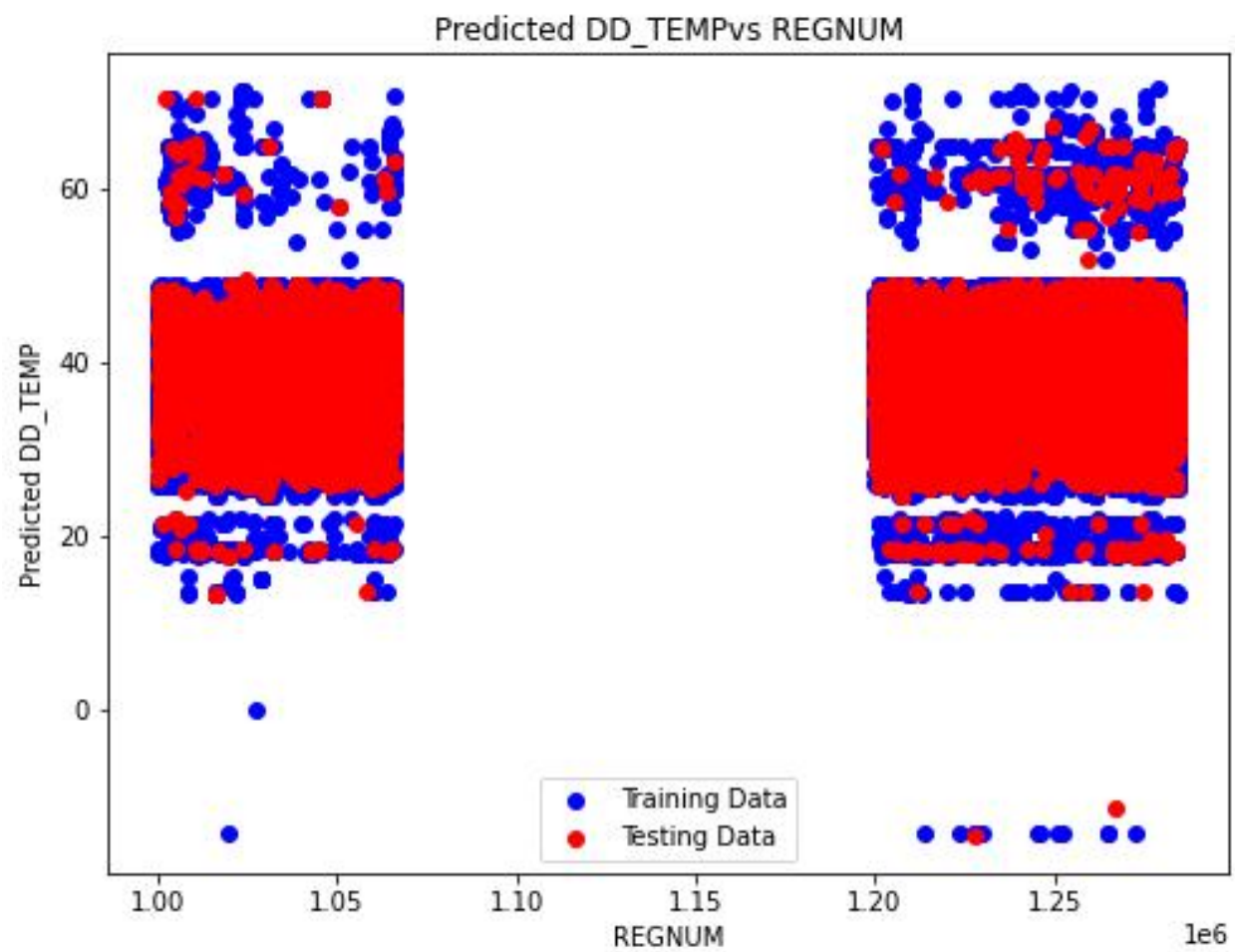


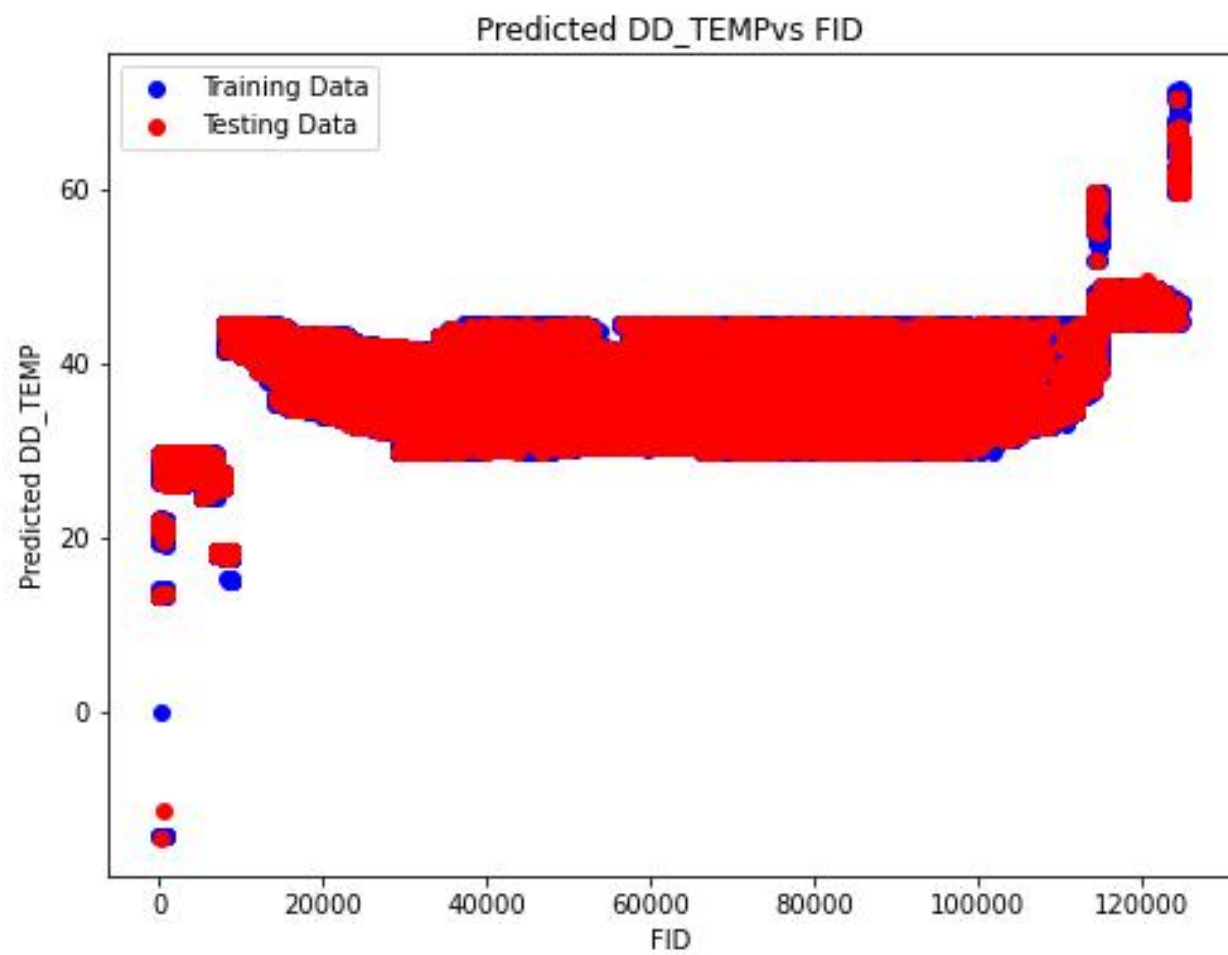


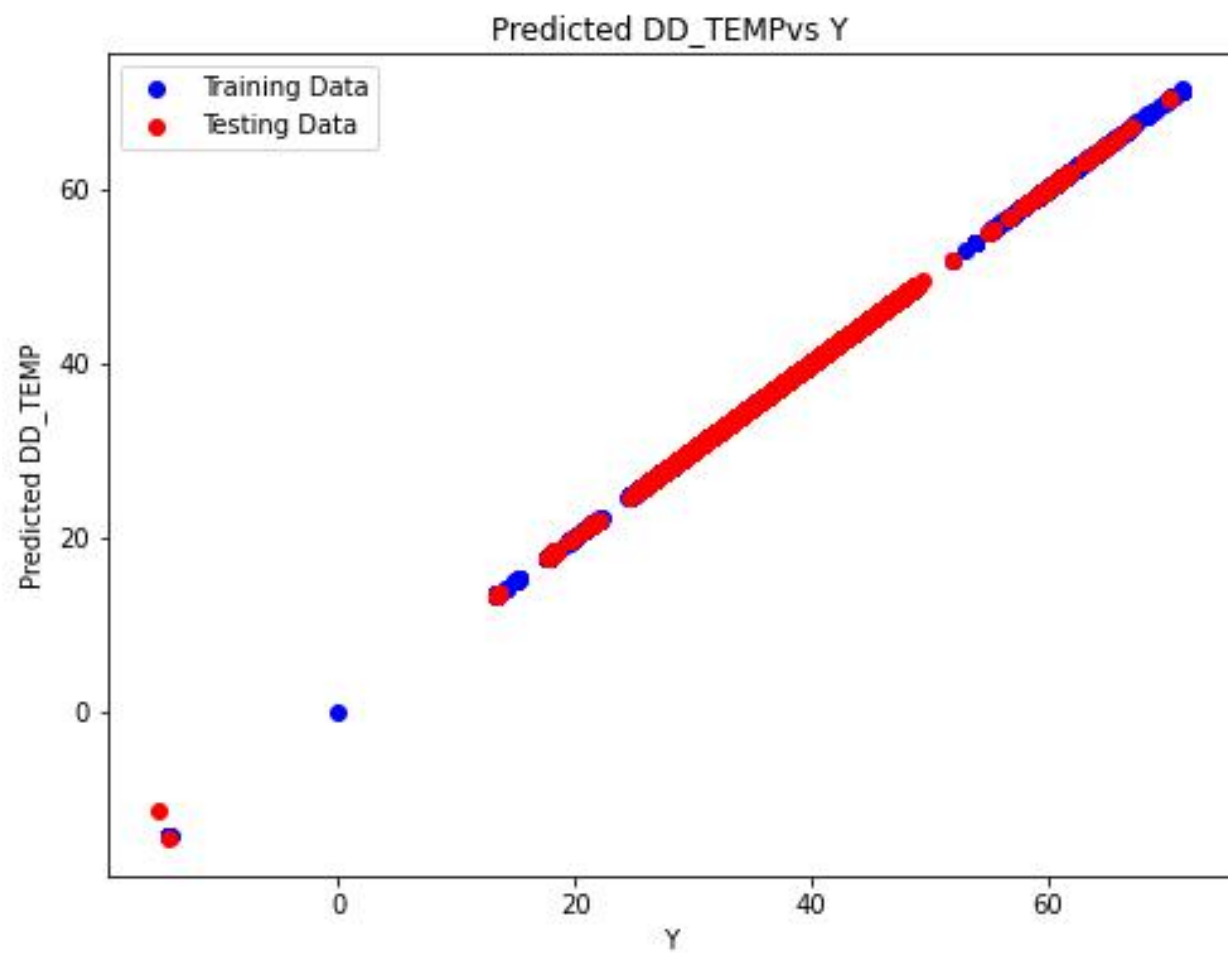


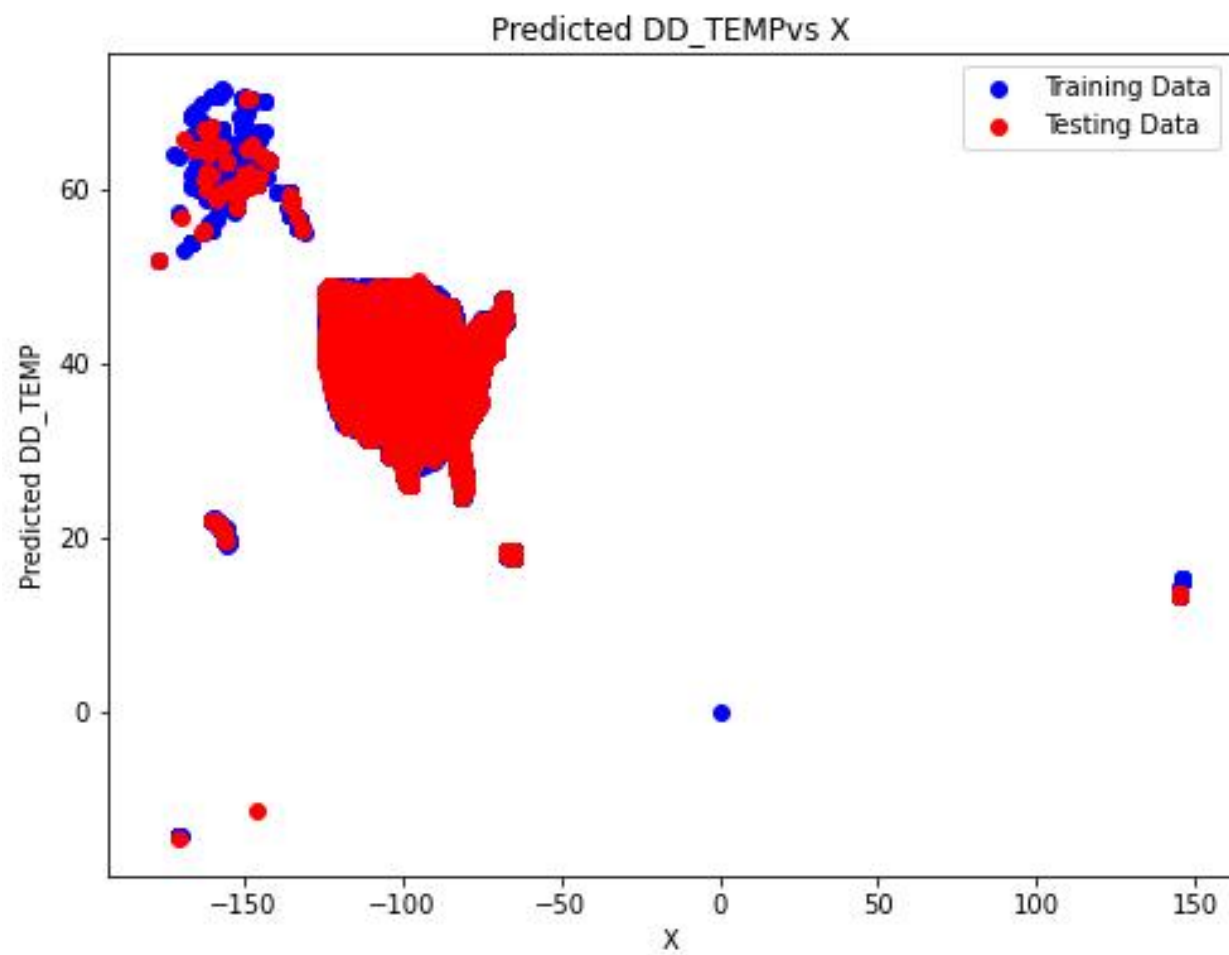


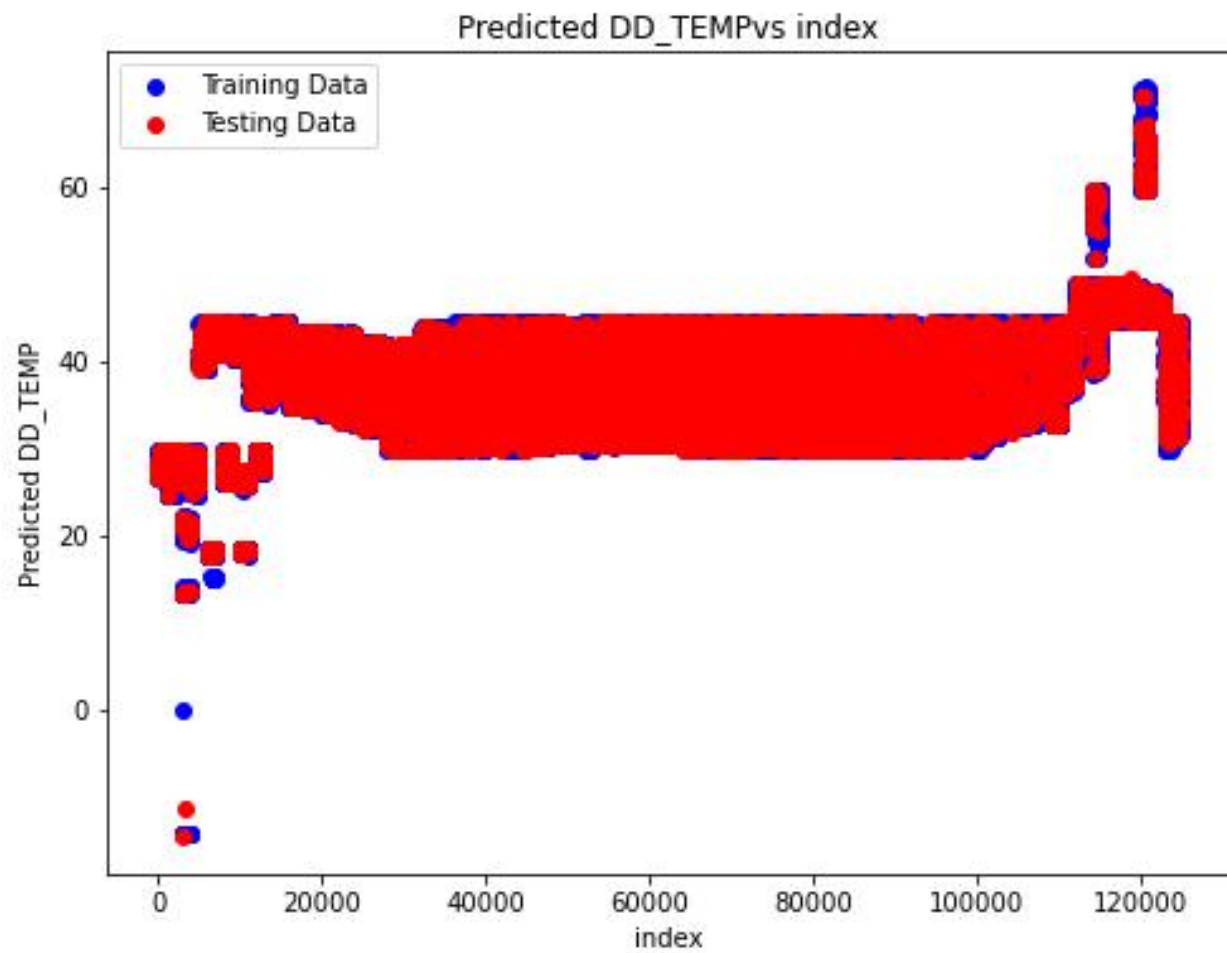






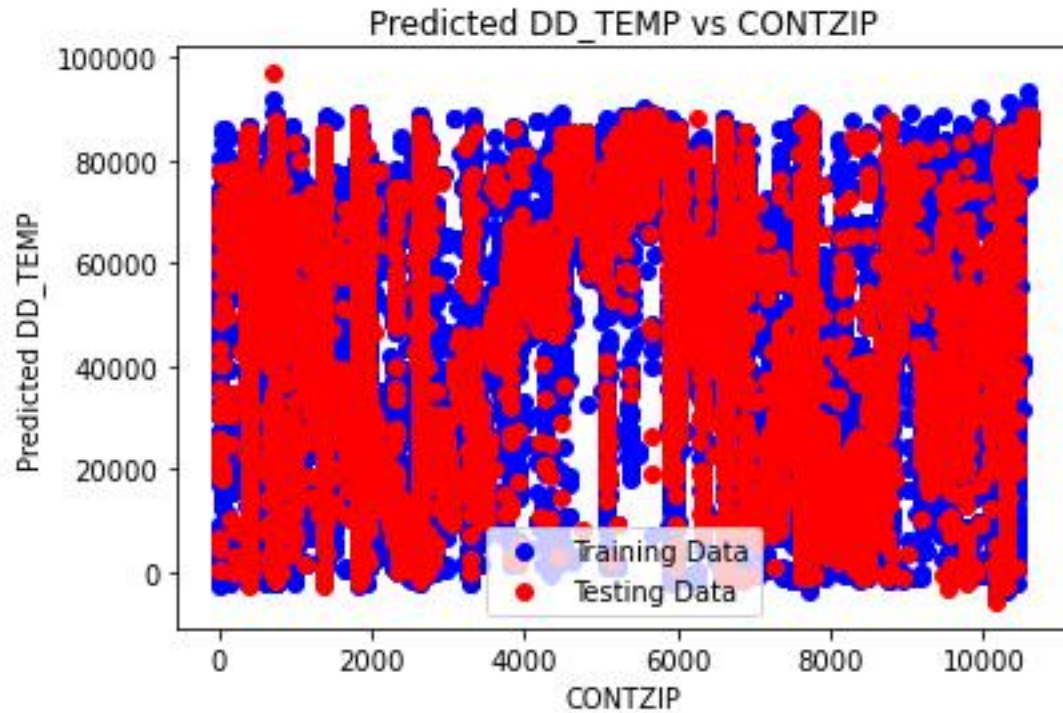






ENCODING EVERY VARIABLES :

GRAPH:



The x-axis, labeled "CONTZIP," likely represents a continuous independent variable. On the other hand, the y-axis, labeled "Predicted DD\_TEMP,"

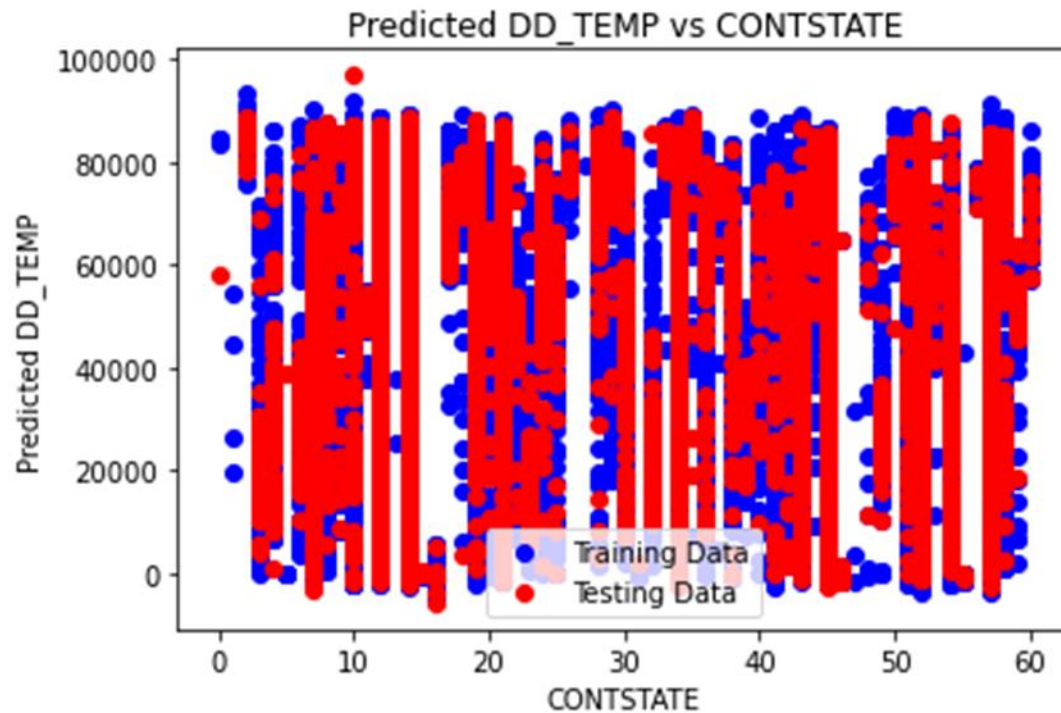
The plot consists of two lines:

1. The blue line illustrates (DD\_TEMP) for the training data.
2. The red line represents (DD\_TEMP) for the testing data.

Given that the plot displays the difference between predicted and actual values, rather than the predicted values themselves, a conclusive assessment of the model's performance is challenging. Ideally, both the blue and red lines would converge around zero, indicating that the model's predictions align closely with the actual values.

However, the plot reveals a trend where the model tends to produce positive predictions for lower values of CONTZIP and negative predictions for higher values of CONTZIP. This pattern suggests a potential bias in the model, where it underestimates DD\_TEMP for lower CONTZIP values and overestimates it for higher CONTZIP values.

To gain a comprehensive understanding of the model's performance, additional visualizations such as scatter plots comparing predicted versus actual values for both training and testing data would be beneficial. These additional insights would provide a clearer assessment of the model's accuracy and any potential biases present in its predictions.



The x-axis, labeled "CONTSTATE," likely denotes a categorical independent variable. Conversely, the y-axis, labeled "Predicted DD\_TEMP,"

The graph features two components:

1. The red line represents the (DD\_TEMP) for the testing data.
2. Although labeled as "Training Data," there is no visible blue line depicting the (DD\_TEMP) for the training data.

As the plot illustrates the disparity between predicted and actual values, rather than the predicted values themselves, determining the model's performance definitively poses a challenge. Ideally, the red line would center around zero, indicating that the model's predictions align closely with the actual values.

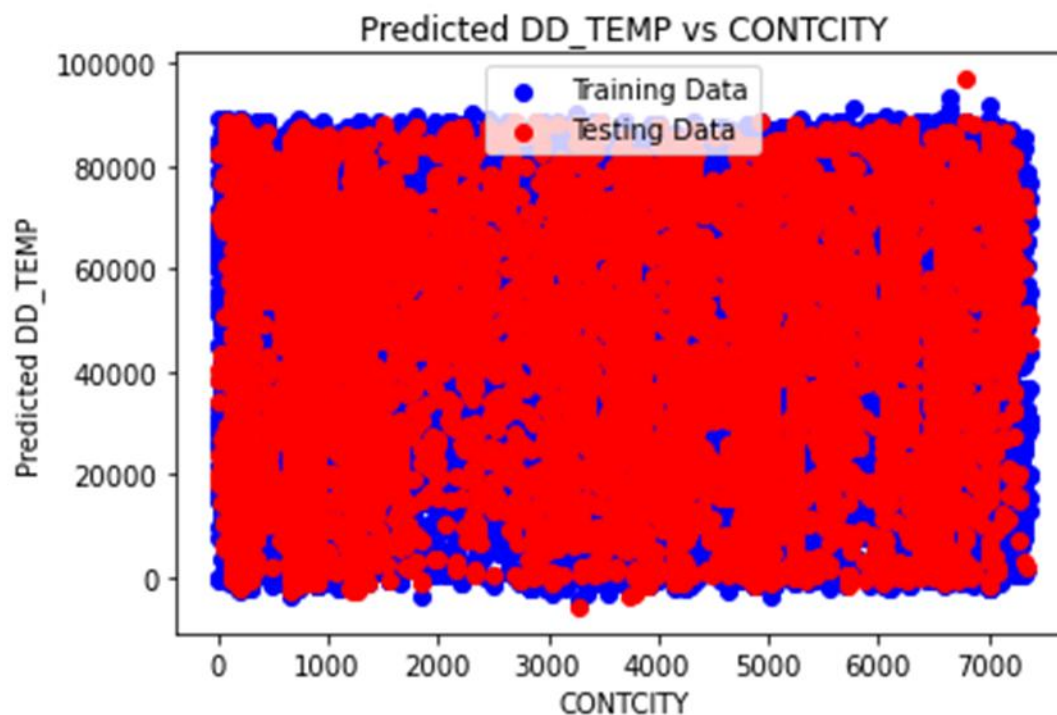


However, the plot suggests a trend where the model's predictions for the testing data tend to be positive for lower values of CONTSTATE and negative for higher values of CONTSTATE. This trend implies a potential bias in the model, where it underestimates DD\_TEMP for lower CONTSTATE values and overestimates it for higher CONTSTATE values.

To comprehensively evaluate the model's performance, the following would be beneficial:

- Visualizing the blue line representing the predicted (DD\_TEMP) for the training data.
- Examining a scatter plot comparing predicted versus actual values for both training and testing data.

These additional visualizations would offer deeper insights into the model's accuracy and any potential biases inherent in its predictions.



The x-axis, labeled "CONTCITY," is indicative of a categorical independent variable, likely denoting different cities. Conversely, the y-axis, labeled "Predicted DD\_TEMP,"

The plot comprises two distinct regions:

1. The red area illustrates the predicted (DD\_TEMP) for the testing data.

2. Although labeled "Training Data," there is no discernible blue area representing the (DD\_TEMP) for the training data.

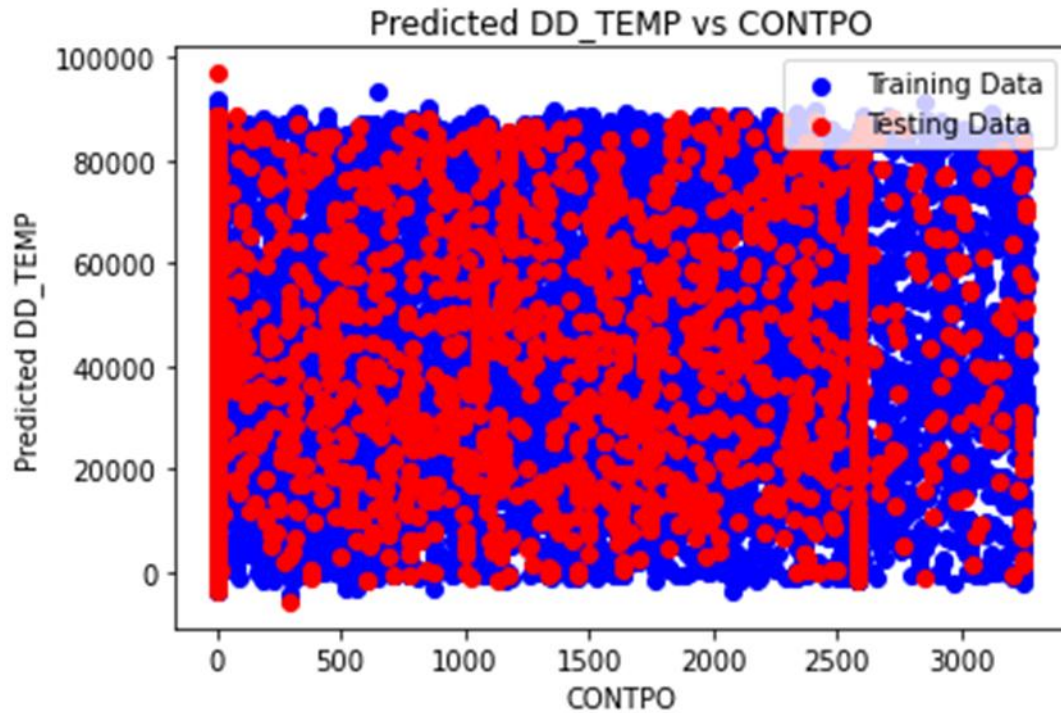
As the plot showcases the deviation between predicted and actual values, rather than the predicted values themselves, definitively assessing the model's performance poses a challenge. Ideally, the red area would be centered around zero, indicating a close alignment between the model's predictions and the actual values.

However, it is apparent from the plot that the model's predictions for the testing data tend to exhibit a positive trend for lower values of CONTCITY and a negative trend for higher values of CONTCITY. This trend suggests a potential bias in the model, wherein it tends to underestimate DD\_TEMP for cities with lower CONTCITY values and overestimate DD\_TEMP for cities with higher CONTCITY values.

To comprehensively evaluate the model's performance, the following steps would be beneficial:

- Visualization of the blue line representing the predicted (DD\_TEMP) for the training data.
- Examination of a scatter plot comparing predicted versus actual values for both training and testing data.

These additional visualizations would provide deeper insights into the accuracy of the model and any inherent biases in its predictions.



The x-axis, labeled "CONTPO," is likely indicative of some continuous independent variable. Conversely, the y-axis, labeled "Predicted DD\_TEMP,"

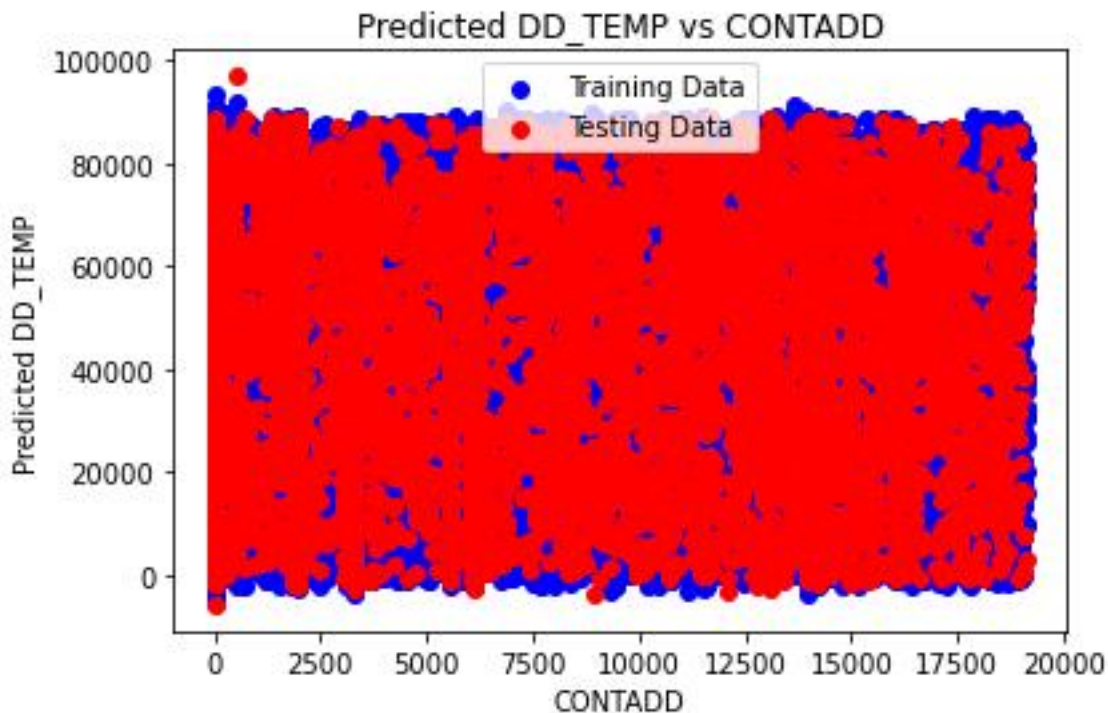
Two lines are visible on the plot:

1. The red line represents the predicted (DD\_TEMP) for the testing data.
2. The blue line represents the predicted (DD\_TEMP) for the training data.

As the plot showcases the deviation between predicted and actual values, rather than the predicted values themselves, definitively assessing the model's performance poses a challenge. Ideally, both the blue and red lines would be centered around zero, indicating a close alignment between the model's predictions and the actual values.

However, it is apparent from the plot that the model's predictions for both the training and testing data tend to exhibit a positive trend for lower values of CONTPO and a negative trend for higher values of CONTPO. This trend suggests a potential bias in the model, wherein it tends to underestimate DD\_TEMP for lower values of CONTPO and overestimate DD\_TEMP for higher values of CONTPO.

To comprehensively evaluate the model's performance, additional visualizations such as scatter plots comparing predicted versus actual values for both training and testing data would be beneficial. These visualizations would provide deeper insights into the accuracy of the model and any inherent biases in its predictions.



The x-axis, labeled "CONTADD," presumably denotes some continuous independent variable, potentially indicating a count or quantity of something. On the other hand, the y-axis labeled "Predicted DD\_TEMP" represents the (DD\_TEMP) as inferred by the model.

Two lines are discernible on the plot:

1. The blue line signifies the predicted (DD\_TEMP) for the training data.
2. The red line indicates the predicted (DD\_TEMP) for the testing data.

Both lines exhibit a similar trend, suggesting that the model anticipates a higher predicted (DD\_TEMP) for lower values of CONTADD and a lower predicted difference for higher values of CONTADD.

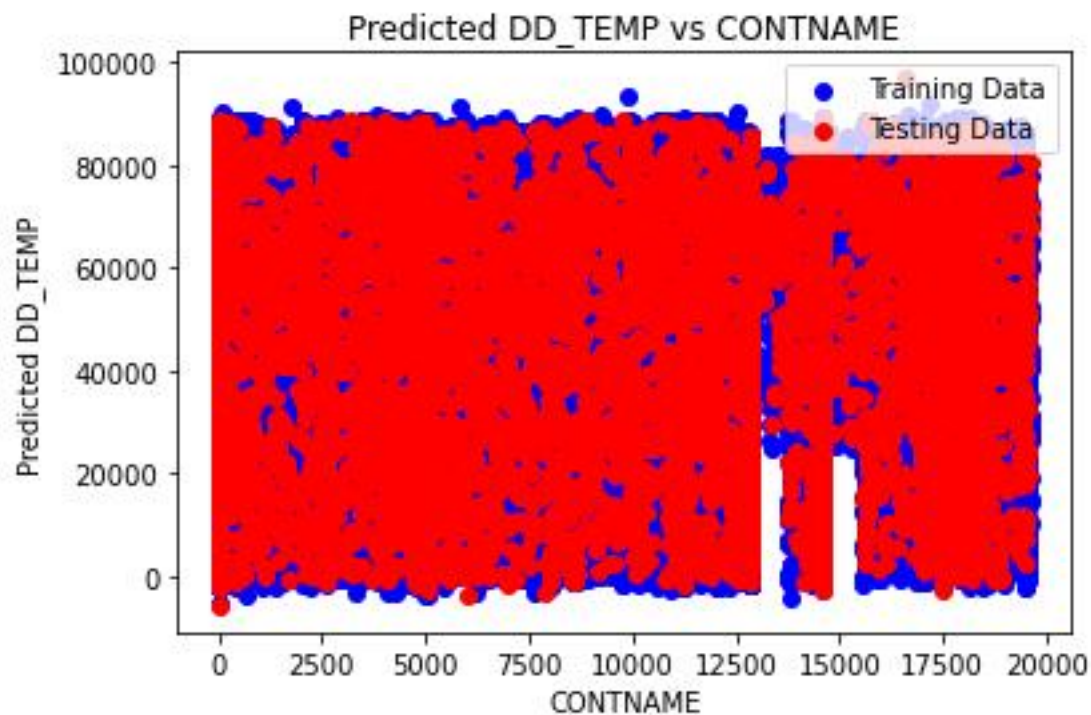
However, assessing the model's performance conclusively from this plot is challenging. Ideally, both the blue and red lines would be centered around zero, indicative of the model's predictions aligning closely with the actual values.

In this plot, data points are concentrated in the upper left and lower right portions, and neither line is centered around zero. This implies a potential bias in the model, wherein it tends to overestimate positive values of predicted (DD\_TEMP) and underestimate negative values.

To gain a more comprehensive understanding of the model's performance, additional visualizations are warranted, including:

- \* A scatter plot comparing predicted values versus actual values for both training and testing data. This would elucidate the degree of alignment between the model's predictions and the actual values.

- \* A plot depicting the absolute error of the model's predictions for both training and testing data. This would provide insights into the magnitude of differences between predicted values and actual values.



The x-axis, labeled "CONTNAME," presumably denotes some categorical independent variable, potentially representing names. Conversely, the y-axis labeled "Predicted DD\_TEMP" represents the predicted (DD\_TEMP) as inferred by the model.

Two lines are discernible on the plot:

1. The blue line signifies the predicted (DD\_TEMP) for the training data.
2. The red line indicates the predicted (DD\_TEMP) for the testing data.

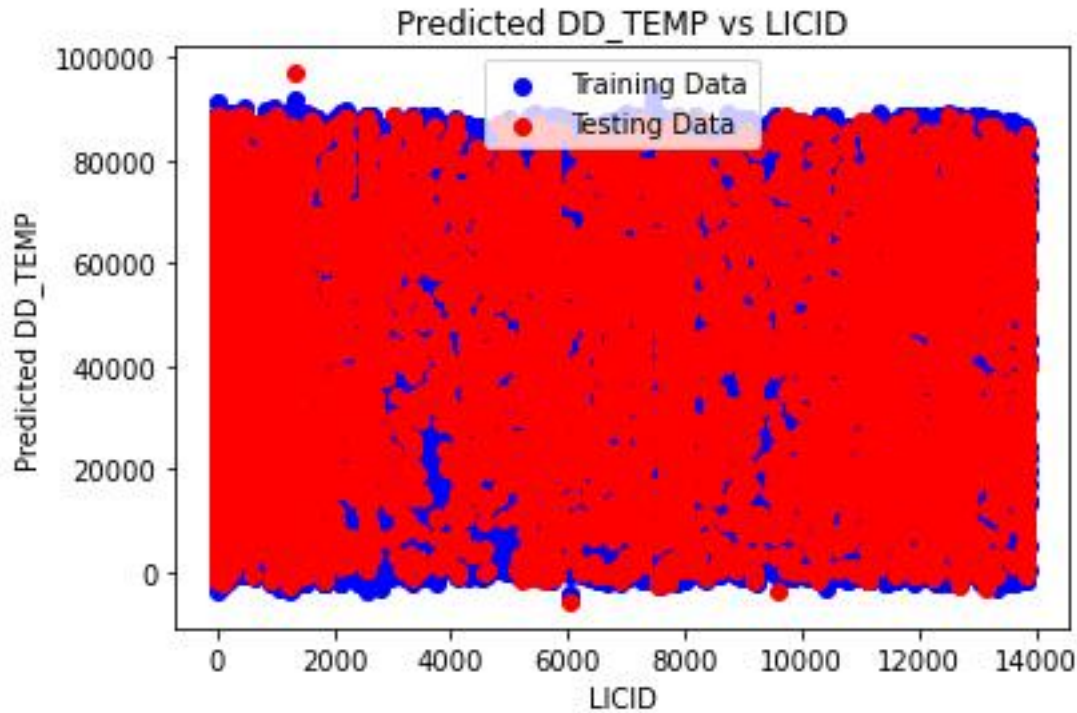
Both lines exhibit a similar trend, indicating that the model predicts a (DD\_TEMP) for lower alphabetical values of CONTNAME and a lower difference for higher alphabetical values of CONTNAME.

However, assessing the model's performance conclusively from this plot is challenging. Ideally, both the blue and red lines would be centered around zero, indicative of the model's predictions aligning closely with the actual values.

In this plot, neither line is centered around zero. The data points suggest a potential bias in the model, wherein it tends to overestimate positive values of the predicted (DD\_TEMP) and underestimate negative values, particularly for certain alphabetical values of CONTNAME.

To gain a more comprehensive understanding of the model's performance, additional visualizations are warranted, including:

- \* A scatter plot comparing predicted values versus actual values for both training and testing data. This would elucidate the degree of alignment between the model's predictions and the actual values.
- \* A plot depicting the absolute error of the model's predictions for both training and testing data. This would provide insights into the magnitude of differences between predicted values and actual values.



The plot provided compares predicted values from a model to actual values for antenna structure elevation, likely measured in meters.

The x-axis labeled "LICID" presumably represents a unique identifier for each antenna structure. On the other hand, the y-axis labeled "Predicted DD\_TEMP" signifies the predicted difference in elevation (DD\_TEMP) between the actual elevation and the model's prediction, based on the model.

Two lines are depicted on the plot:

1. The blue line represents the predicted difference in elevation (DD\_TEMP) for the training data.
2. The red line represents the predicted difference in elevation (DD\_TEMP) for the testing data.

While the plot illustrates the difference between predicted and actual values, rather than the predicted values themselves, assessing the model's performance definitively is challenging. Ideally, both the blue and red lines would be centered around zero, indicating that the model's predictions are generally accurate.

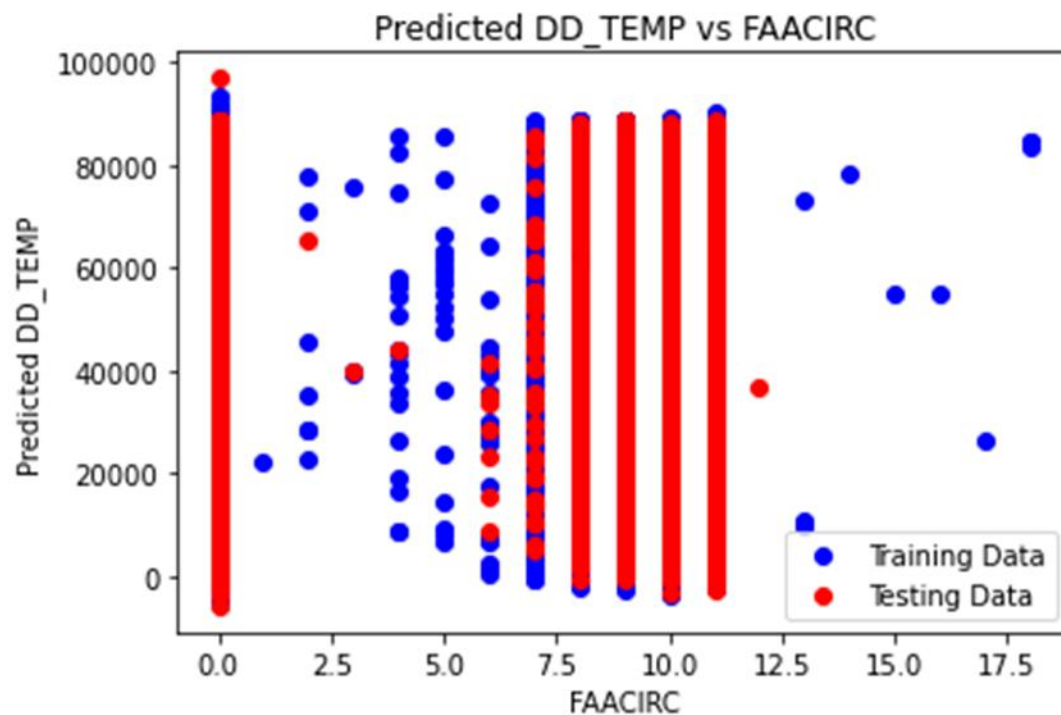


However, from the plot, it is observable that the model's predictions tend to be positive for lower values of LICID and negative for higher values of LICID, for both the training and testing data. This implies a potential bias in the model towards underestimating the elevation of antenna structures with lower LICID values and overestimating the elevation of those with higher LICID values.

To comprehensively evaluate the model's performance, additional visualizations would be beneficial, including:

- \* A scatter plot comparing predicted elevation to actual elevation for both the training and testing data. This would provide insights into the alignment between the model's predictions and the actual values.

- \* A plot showcasing the absolute error of the model's predictions for both the training and testing data. This would elucidate the magnitude of differences between the predicted values and the actual values.



The plot provided compares predicted values from a model to actual values for antenna structure elevation, likely measured in meters.

The x-axis labeled "FAACIRC" presumably represents a continuous variable related to the antenna structure. On the other hand, the y-axis labeled "Predicted DD\_TEMP" signifies the predicted difference in elevation (DD\_TEMP) between the actual elevation and the model's prediction, based on the model.



Two lines are depicted on the plot:

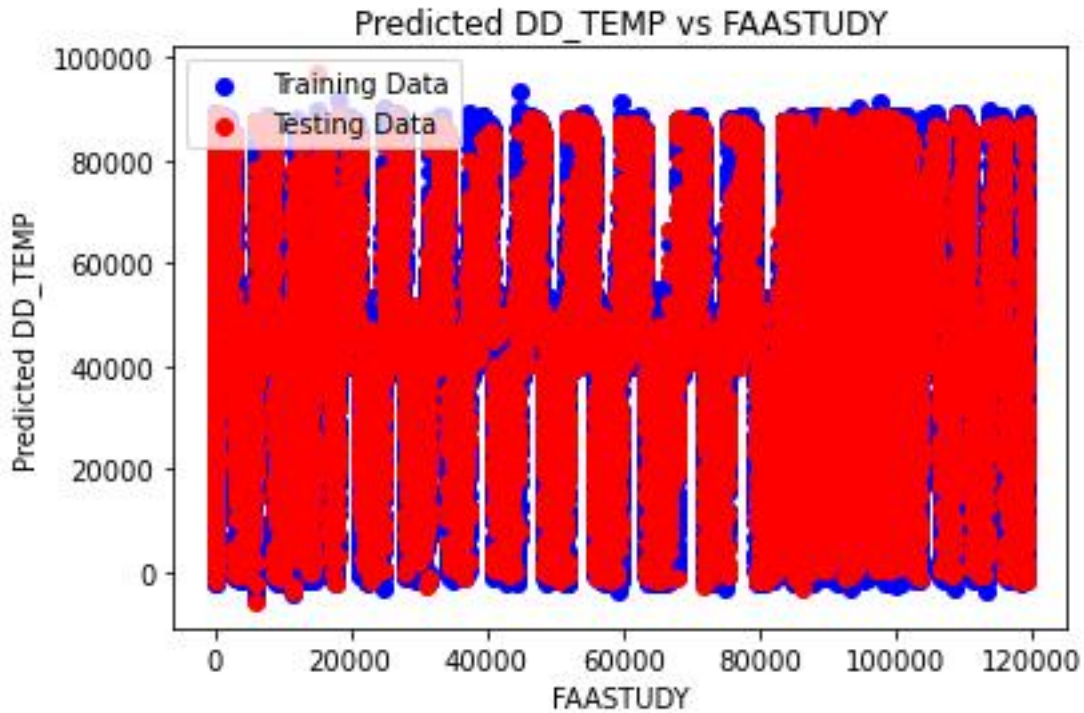
1. The red line represents the predicted difference in elevation (DD\_TEMP) for the testing data.
2. Although not visible, there should be a blue line representing the predicted difference in elevation (DD\_TEMP) for the training data, as indicated by the blue text.

While the plot illustrates the difference between predicted and actual values, rather than the predicted values themselves, definitively assessing the model's performance is challenging. Ideally, the red line would be centered around zero, indicating that the model's predictions are generally accurate.

However, it appears from the plot that the model's predictions for the testing data tend to be positive for lower values of FAACIRC and negative for higher values of FAACIRC. This suggests a potential bias in the model towards underestimating the elevation of antenna structures with lower FAACIRC values and overestimating the elevation of structures with higher FAACIRC values.

To comprehensively evaluate the model's performance, additional visualizations would be beneficial, including:

- \* A plot showcasing the predicted difference in elevation (DD\_TEMP) for the training data. This would provide insights into the model's performance during the training phase.
- \* A scatter plot comparing predicted elevation to actual elevation for both the training and testing data. This would elucidate how closely the model's predictions align with the actual values.
- \* A plot depicting the absolute error of the model's predictions for both the training and testing data. This would highlight the magnitude of differences between the predicted values and the actual values.



The provided plot illustrates a comparison between predicted values from a model and actual values for antenna structure elevation, presumably measured in meters. The x-axis is labeled "FAASTUDY," indicating a categorical variable likely associated with a study conducted by the Federal Aviation Administration (FAA). On the y-axis, "Predicted DD\_TEMP" denotes the predicted difference in elevation (DD\_TEMP) between the actual elevation and the model's prediction, based on the model.

Two areas are depicted on the plot:

- The red area illustrates the predicted difference in elevation (DD\_TEMP) for the testing data.
- Although not visible, there should be a blue area representing the predicted difference in elevation (DD\_TEMP) for the training data, as indicated by the blue text.

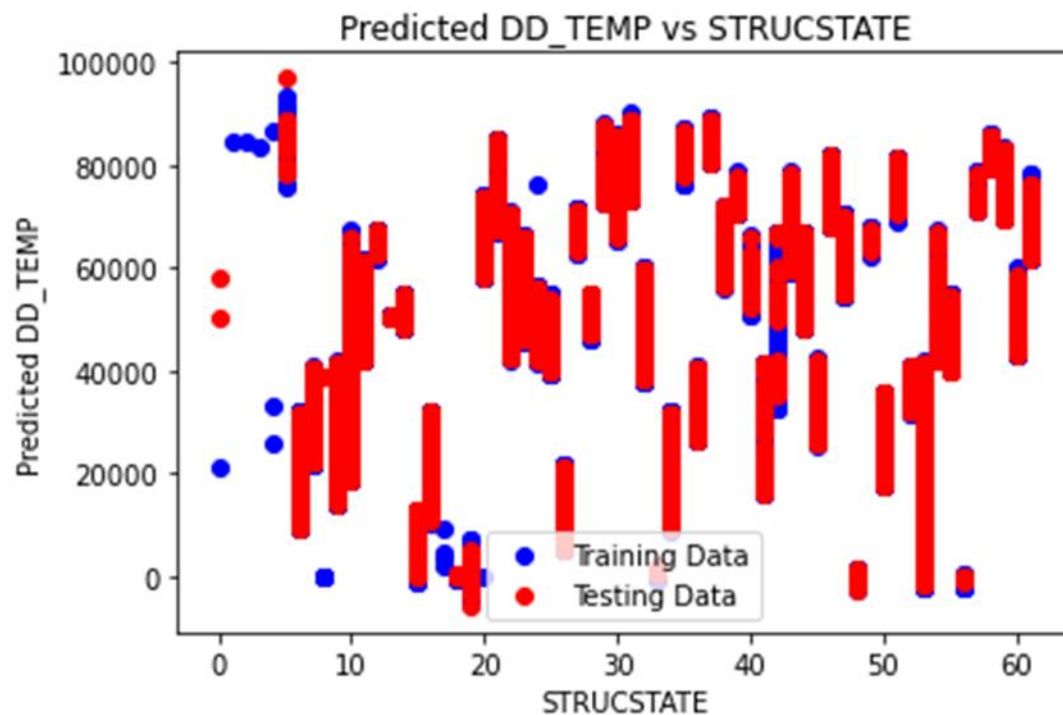
As the plot shows the difference between predicted and actual values, rather than the predicted values themselves, definitively assessing the model's performance is challenging. Ideally, the red area would be centered around zero, indicating that the model's predictions align closely with the actual values.

However, from the plot, it's evident that the model's predictions for the testing data lean towards positive values for lower categories of FAASTUDY and negative values for higher categories of FAASTUDY.

This suggests a potential bias in the model towards underestimating the elevation of antenna structures in lower FAASTUDY categories and overestimating the elevation in higher categories.

To comprehensively evaluate the model's performance, additional visualizations would be beneficial, including:

- The blue line representing the predicted difference in elevation (DD\_TEMP) for the training data, providing insights into the model's performance during the training phase.
- A scatter plot comparing predicted elevation to actual elevation for both the training and testing data, elucidating the alignment between the model's predictions and the actual values.
- A plot illustrating the absolute error of the model's predictions for both the training and testing data, offering insights into the magnitude of differences between the predicted values and the actual values.



The provided plot illustrates a comparison between predicted values from a model and actual values for antenna structure elevation, presumably measured in meters. The x-axis is labeled "STRUCSTATE," representing a categorical variable likely associated with the state in which the antenna structure is located. On the y-axis, "Predicted DD\_TEMP" denotes the predicted difference in elevation (DD\_TEMP) between the actual elevation and the model's prediction, based on the model.

Two lines are depicted on the plot:

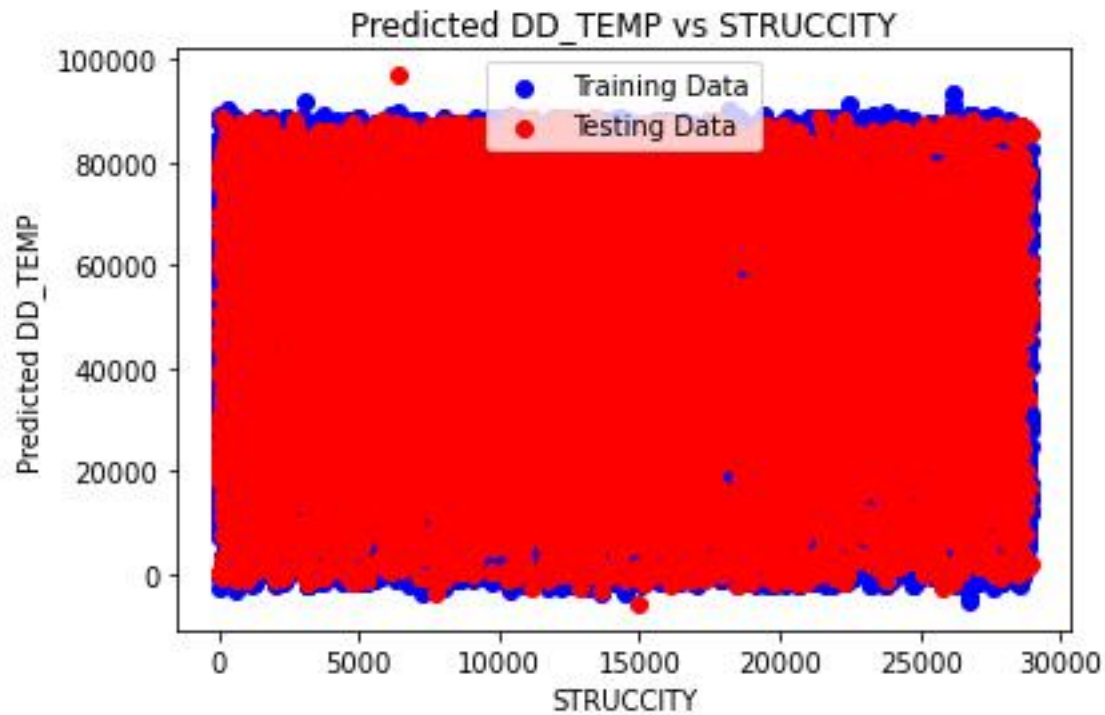
- The red line represents the predicted difference in elevation (DD\_TEMP) for the testing data.
- The blue line represents the predicted difference in elevation (DD\_TEMP) for the training data.

Both lines exhibit a similar trend, indicating that the model predicts a positive difference in temperature (DD\_TEMP) for lower values of STRUCSTATE and a negative difference for higher values. However, it's challenging to conclusively assess the model's performance solely based on this plot. Ideally, both the blue and red lines would center around zero, indicating that the model's predictions align closely with the actual values.

Nevertheless, the concentration of data points in the upper left and lower right portions of the graph, coupled with the lack of centering around zero for both lines, suggests potential bias in the model. Specifically, the model may tend to overestimate positive values of the predicted difference in temperature (DD\_TEMP) and underestimate negative values.

To comprehensively evaluate the model's performance, additional visualizations would be beneficial, including:

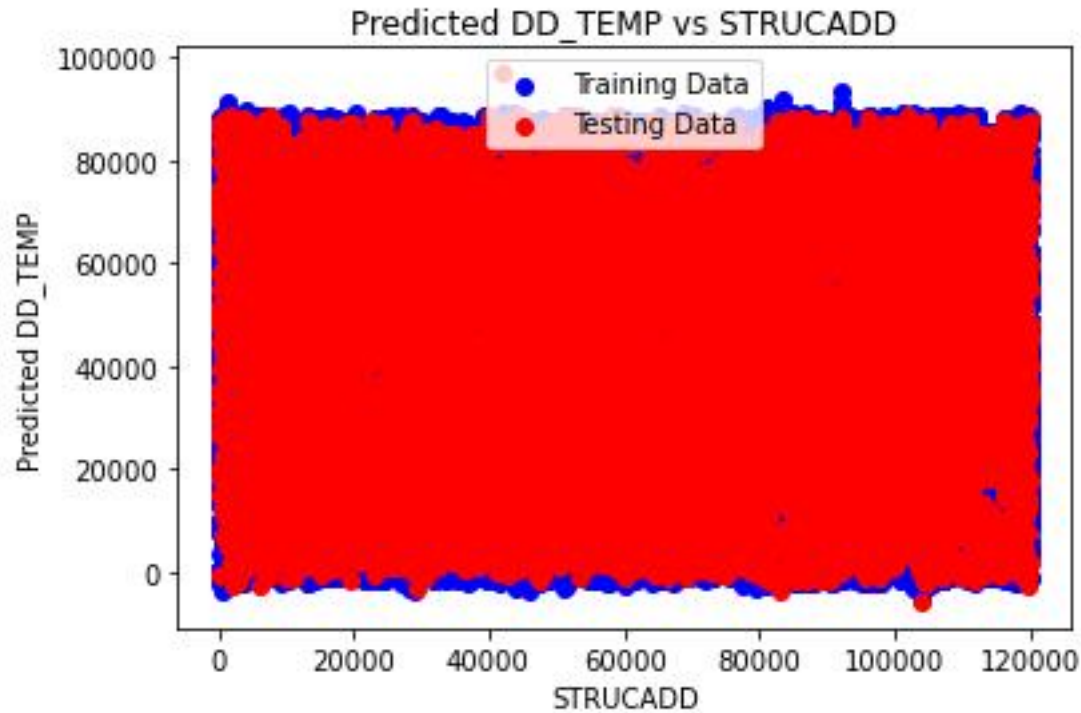
- A scatter plot comparing predicted elevation to actual elevation for both the training and testing data, providing insights into the alignment between the model's predictions and the actual values.
- A plot illustrating the absolute error of the model's predictions for both the training and testing data, offering insights into the magnitude of differences between the predicted values and the actual values.



The provided plot depicts the relationship between predicted DD\_TEMP, likely indicating elevation, and struckcity. The blue line corresponds to the training data, while the red line represents the testing data.

In principle, if the model has generalized well, the training and testing data should exhibit similar trends. In this plot, both the training and testing data show similar trends, indicating potential good generalization of the model. However, there are noticeable discrepancies between the two datasets, particularly evident at lower struckcity values. Assessing the significance of these differences solely based on this plot is challenging.

Further analysis is necessary to determine the significance of the disparities observed between the training and testing datasets. Additional evaluation metrics and visualizations, such as statistical tests or comparison of error distributions, would provide deeper insights into the model's performance and generalization ability.

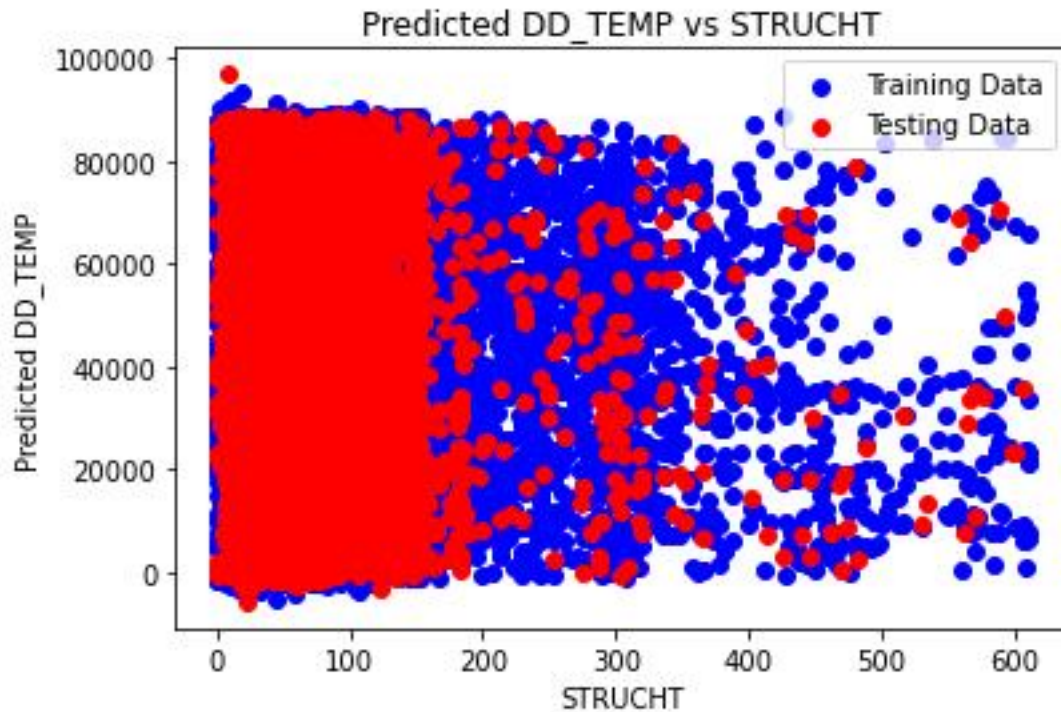


The provided plot illustrates the relationship between the difference in predicted DD\_TEMP and STRUCADD values. STRUCADD likely denotes a measurement, potentially representing elevation. The red line signifies the predicted DD\_TEMP, while the blue line represents the training data.

Key observations from the plot include:

- The x-axis indicates STRUCADD values, presumably ranging from 0 to 120,000.
- The y-axis displays the disparity between predicted DD\_TEMP and STRUCADD values, with a range appearing to span from -20,000 to 100,000.
- The training data (blue line) exhibits a positive correlation between predicted DD\_TEMP and STRUCADD. This implies that as the STRUCADD value increases, the predicted DD\_TEMP value tends to increase as well.
- The testing data (red line) generally aligns with the trend observed in the training data, albeit with some deviations. Notably, at lower STRUCADD values, the predicted DD\_TEMP values for the testing data tend to be lower compared to the training data.
- A cluster of points around the 60,000 mark on the x-axis demonstrates particularly high disparities between predicted DD\_TEMP and STRUCADD values for both the training and testing data.

Overall, the plot suggests that the model can predict DD\_TEMP from STRUCADD values to a certain degree. However, deviations between predicted and actual values, especially evident in the testing data, imply potential areas for model refinement.



The image's text labels delineate the following:

- The x-axis denotes the variable "STRUCHT."
- The y-axis represents the predicted values of "DD\_TEMP."
- The red region illustrates the predicted "DD\_TEMP" values corresponding to the testing data.
- The blue region depicts the predicted "DD\_TEMP" values corresponding to the training data.

General Trends:

The plot indicates a positive correlation between predicted "DD\_TEMP" and "STRUCHT" for both the training and testing datasets. This correlation suggests that as "STRUCHT" values increase, the predicted "DD\_TEMP" values also tend to increase.

A more pronounced linear trend is discernible in the training data (blue) compared to the testing data (red). This discrepancy implies that the model might have overfitted the training data, potentially hindering its ability to generalize effectively to unseen data.

#### Specific Observations:

Predicted "DD\_TEMP" values span a range from approximately 20,000 to 80,000.

"STRUCHT" values vary between 0 and around 600.

Greater dispersion is evident in the testing data (red) compared to the training data (blue), suggesting less consistency in the model's predictions for unseen data.

A concentration of data points appears around the 200 mark on the x-axis, where predicted "DD\_TEMP" values deviate from the overall trend for both training and testing data.

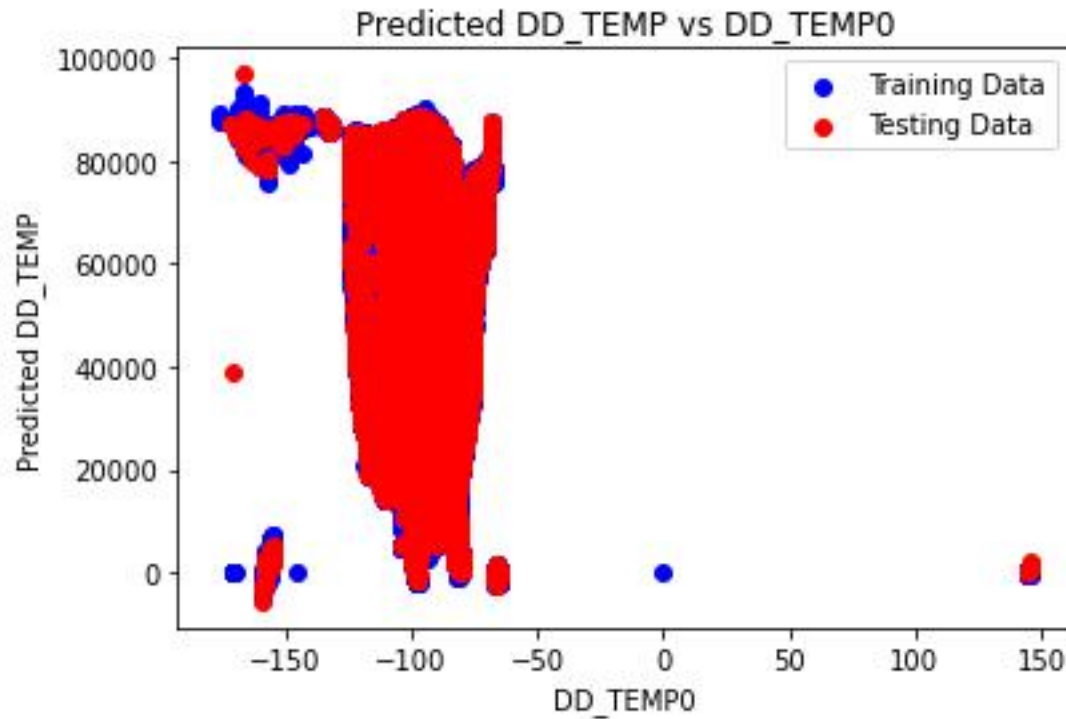
#### Possible Interpretations:

The model might inadequately capture the underlying relationship between "STRUCHT" and "DD\_TEMP," particularly concerning unseen data.

High data scatter could impede accurate prediction of "DD\_TEMP" values from "STRUCHT" values.

Potential outliers within the dataset may exert undue influence on the model's predictions.





The image's text labels specify the following:

- The x-axis denotes "DD\_TEMPO."
- The y-axis represents predicted "DD\_TEMP."
- The red line illustrates the predicted "DD\_TEMP" values corresponding to the testing data.
- The blue line represents the predicted "DD\_TEMP" values for the training data.

General Trends:

The plot indicates a positive correlation between predicted "DD\_TEMP" and "DD\_TEMPO" for both the training and testing datasets. This correlation implies that as "DD\_TEMPO" values increase, the predicted "DD\_TEMP" values also tend to increase.

Consistency in trends between the training and testing data suggests that the model has successfully generalized to unseen data.

Specific Observations:

Predicted "DD\_TEMP" values range from approximately -20,000 to 120,000.

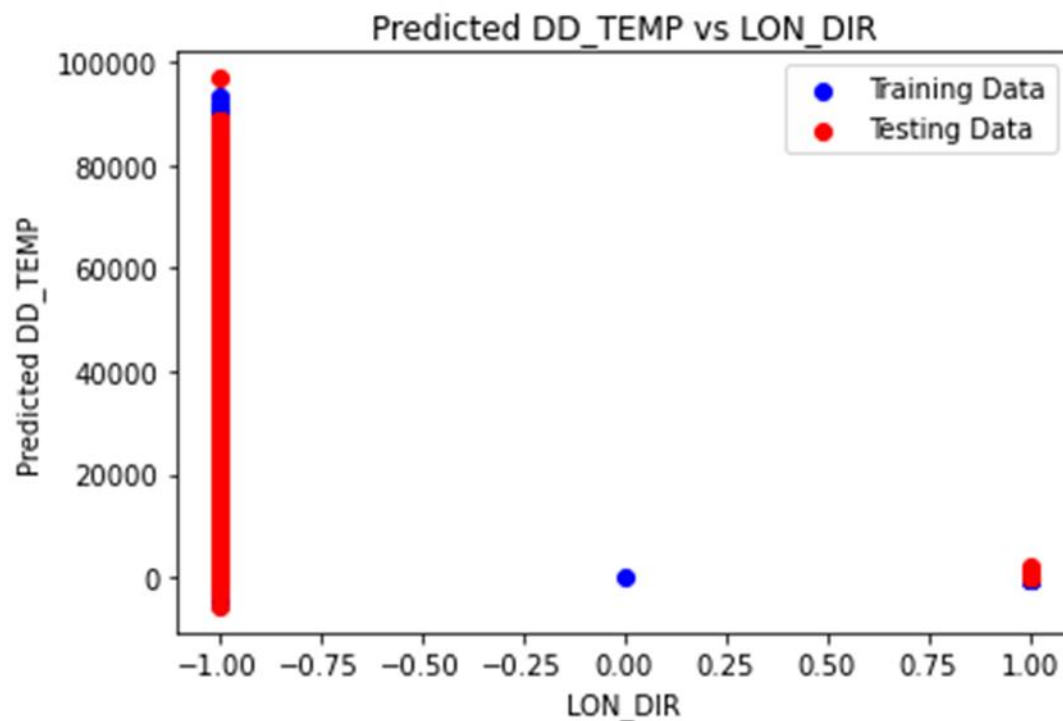
"DD\_TEMPO" values span from -150 to 150.

Data points are evenly distributed for both training (blue) and testing (red) datasets.

Possible Interpretations:

The model appears adept at capturing the relationship between "DD\_TEMPO" and "DD\_TEMP" across both training and testing datasets.

A linear relationship between the two variables is conceivable, although the scale on the y-axis may obscure finer details.



The text labels in the image delineate the following:

- The x-axis represents "LON\_DIR."
- The y-axis denotes predicted "DD\_TEMP."
- The red line illustrates predicted "DD\_TEMP" values for the testing data.
- The blue line represents predicted "DD\_TEMP" values for the training data.

### General Trends:

The plot does not exhibit a discernible correlation between predicted "DD\_TEMP" and "LON\_DIR" for either the training or testing datasets. A scattered distribution of points is evident across the x-axis for both the red and blue lines.

### Specific Observations:

Predicted "DD\_TEMP" values range from approximately -20,000 to 100,000.

"LON\_DIR" values span from -1 to 1.

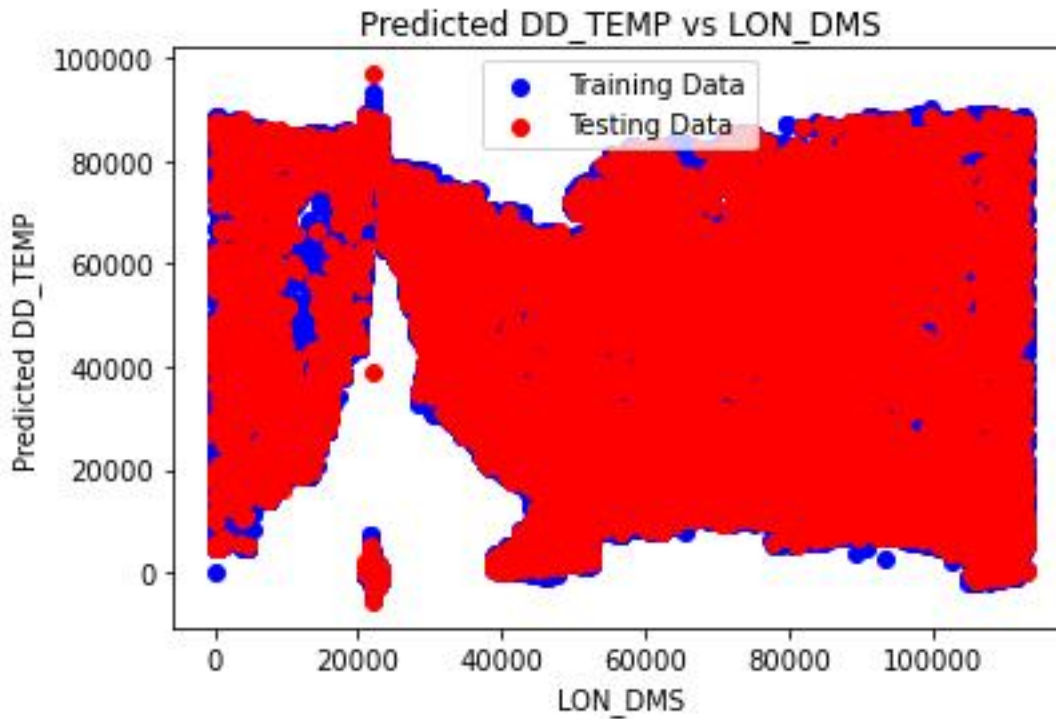
No discernible pattern is apparent in the distribution of data points for either the training (blue) or testing (red) datasets.

### Possible Interpretations:

The model may struggle to capture a meaningful relationship between "LON\_DIR" and "DD\_TEMP."

"LON\_DIR" might not wield significant predictive power in determining "DD\_TEMP."

The presence of noise or outliers in the dataset could potentially disrupt the model's predictive accuracy.



The image's text labels specify the following:

- The x-axis represents "LON\_DMS."
- The y-axis indicates the difference between predicted "DD\_TEMP" and "LON\_DMS."
- The red line illustrates the difference between predicted "DD\_TEMP" and "LON\_DMS" for the testing data.
- The blue line represents the difference between predicted "DD\_TEMP" and "LON\_DMS" for the training data.

General Trends:

Overall, the plot indicates that predicted "DD\_TEMP" values tend to be higher than the corresponding "LON\_DMS" values, and "LON\_DMS" values tend to be lower than the training data for most data points.

A weak positive correlation is observed between the predicted difference and "LON\_DMS" for both the training and testing data. This implies that as "LON\_DMS" values increase, the difference between predicted "DD\_TEMP" and "LON\_DMS" tends to increase as well.

However, significant scatter is evident in the data for both training and testing datasets, particularly at higher "LON\_DMS" values.

#### Specific Observations:

The difference between predicted "DD\_TEMP" and "LON\_DMS" ranges from approximately -80,000 to 100,000.

"LON\_DMS" values span from 0 to 100,000.

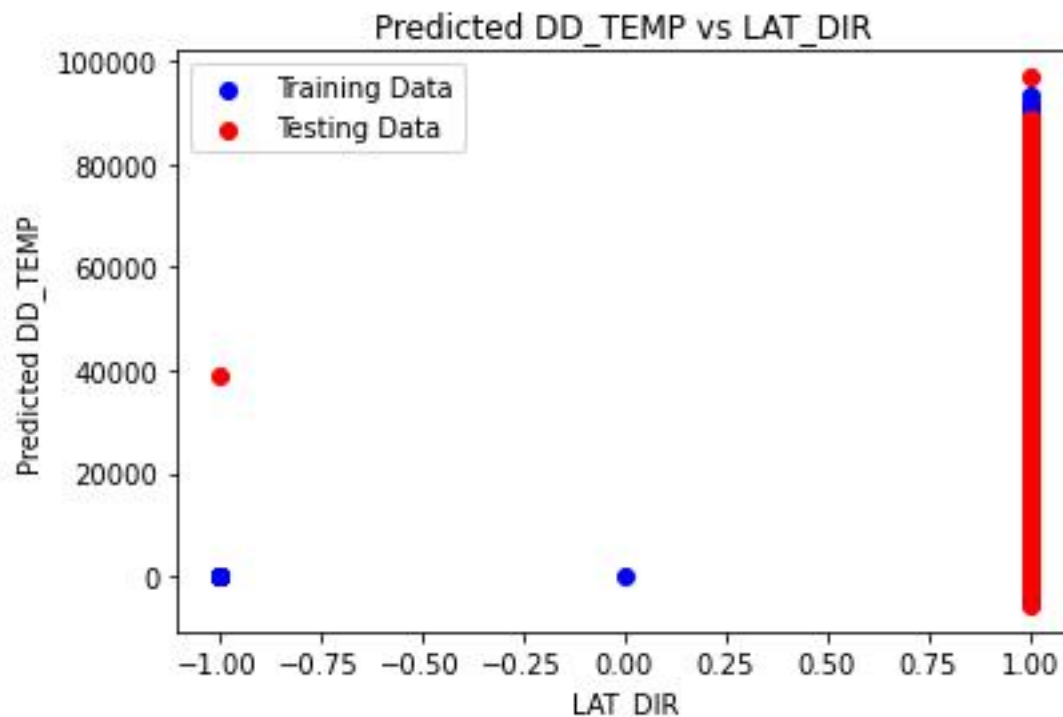
A cluster of points is noticeable around the 60,000 mark on the x-axis, where the difference between predicted "DD\_TEMP" and "LON\_DMS" is notably high for both training and testing data.

#### Possible Interpretations:

The model may exhibit a systematic tendency to overestimate "DD\_TEMP" in comparison to "LON\_DMS."

"LON\_DMS" might not exert strong predictive influence on "DD\_TEMP" independently.

The presence of noise or outliers in the dataset could potentially impact the model's predictive performance.



The image's text labels provide the following information:

- The x-axis represents "LAT\_DIR."
- The y-axis indicates predicted "DD\_TEMP."
- The red line illustrates predicted "DD\_TEMP" values for the testing data.
- The blue line represents predicted "DD\_TEMP" values for the training data.

#### General Trends:

Overall, the plot indicates a weak positive correlation between predicted "DD\_TEMP" and "LAT\_DIR" for both the training and testing data. This suggests that as "LAT\_DIR" values increase, the predicted values of "DD\_TEMP" also tend to increase. However, significant scatter is observed in the data for both training and testing datasets.

A stronger linear trend is apparent in the training data (blue) compared to the testing data (red), indicating potential overfitting of the model to the training data and less effective generalization to unseen data.

#### Specific Observations:

Predicted "DD\_TEMP" values range from approximately 20,000 to 80,000.

"LAT\_DIR" values span from -1 to 1.

Greater scatter is observed in the testing data (red) compared to the training data (blue), suggesting less consistency in the model's predictions for unseen data.

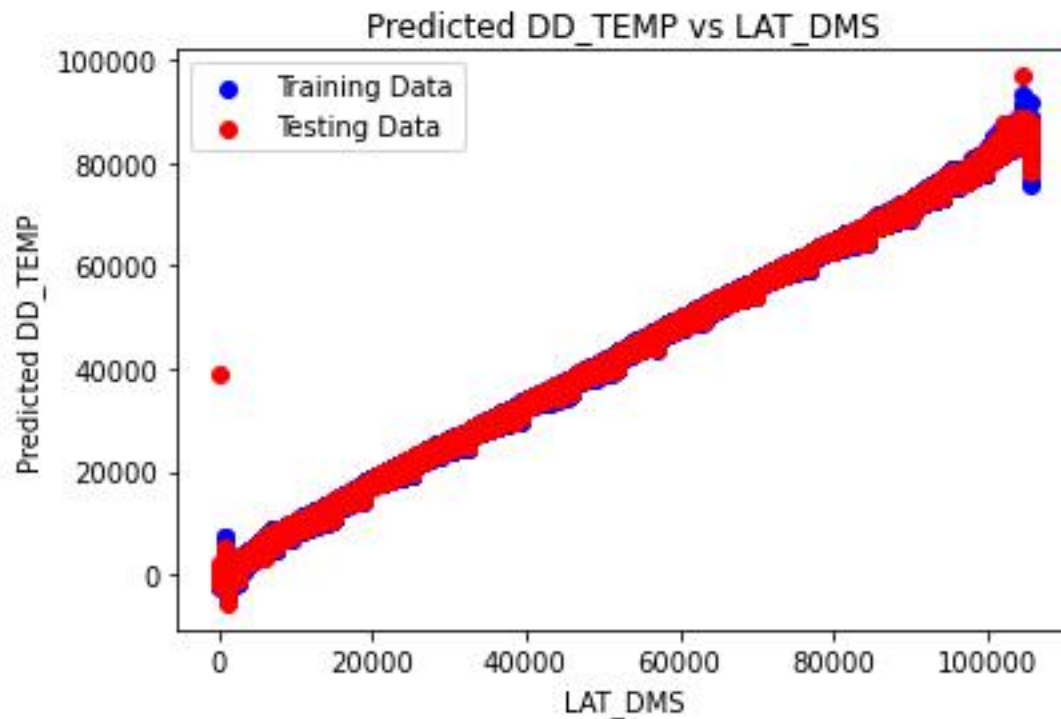
A cluster of points is noticeable around the 0 mark on the x-axis, where predicted "DD\_TEMP" values deviate from the overall trend for both training and testing data.

#### Possible Interpretations:

The model may not fully capture the underlying relationship between "LAT\_DIR" and "DD\_TEMP," particularly for unseen data.

High data scatter may hinder accurate prediction of "DD\_TEMP" values from "LAT\_DIR" values.

The presence of outliers in the dataset could potentially influence the model's predictions.



The provided plot illustrates the disparity between predicted elevation ("DD\_TEMP") values, both from training and testing data, and the latitude expressed in decimal degrees, minutes, and seconds (LAT\_DMS).

In the plot, training data is denoted by the color blue, while testing data is represented in red. The x-axis corresponds to LAT\_DMS, while the y-axis displays the predicted DD\_TEMP, ranging from 0 to 100,000 units.

Observations:

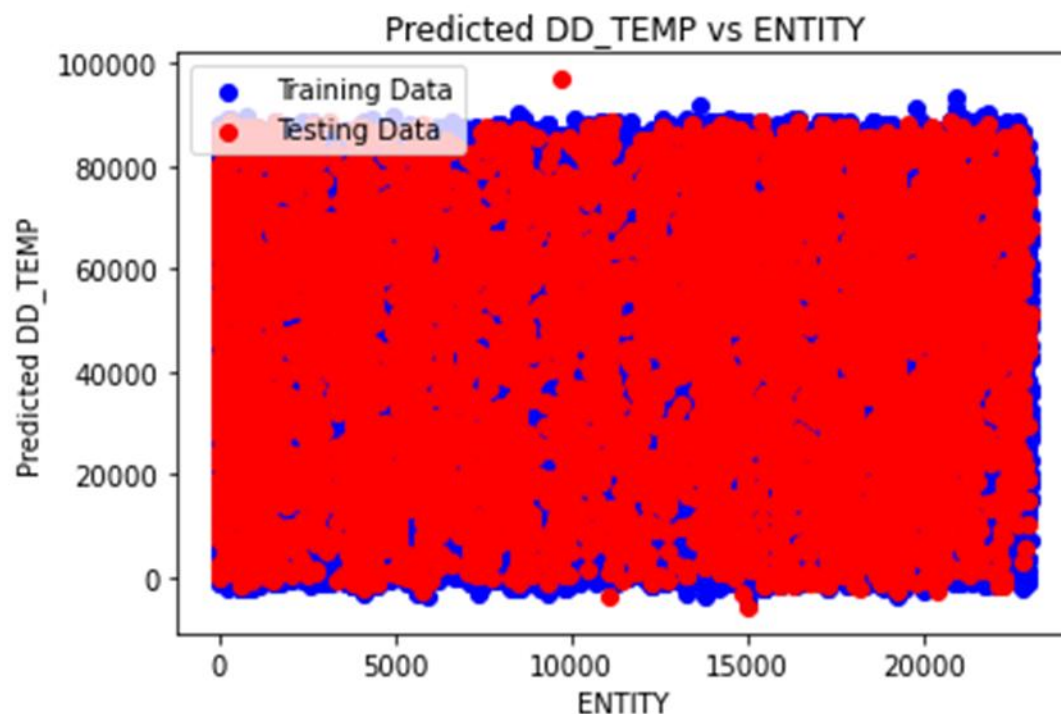
- It shows a linear function.

- Generally, predicted DD\_TEMP values derived from the training data tend to exceed those from the testing data. This indicates a tendency of the model to overestimate DD\_TEMP.

- Substantial variability is evident in both training and testing datasets, with predicted DD\_TEMP fluctuating by up to 100,000 units for a given LAT\_DMS value.

It's noteworthy that the efficacy of the model heavily relies on the quality and representativeness of the training data. If the training dataset fails to accurately mirror real-world conditions, the model's accuracy will consequently be compromised. In this context, it is plausible that the training data lacks diversity in LAT\_DMS values, which could elucidate the model's inadequacy in accurately predicting DD\_TEMP for certain LAT\_DMS values.

This insight underscores the critical importance of comprehensive and diverse training data to ensure the model's robustness and accuracy across various scenarios.



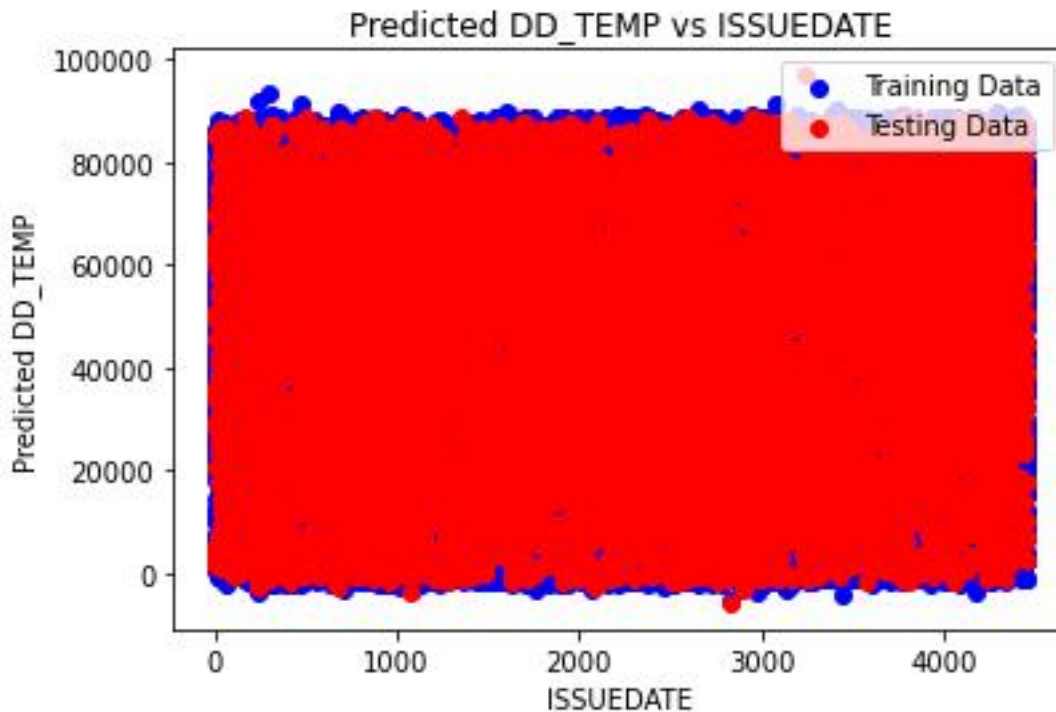
The provided plot illustrates a comparison between predicted and actual temperature (presumably representing elevation data). The x-axis is labeled as "ENTITY," likely serving as an identifier for each data point, while the y-axis is denoted as "Predicted DD\_TEMP," likely signifying the predicted change in elevation in degrees.

The data is segregated into two sets: training data, depicted in blue, and testing data, indicated in red. The training data displays a generally positive correlation, albeit with some scatter, implying that as the value of "ENTITY" increases, the predicted change also increases. In contrast, the testing data exhibits a weaker positive correlation with greater scatter compared to the training data.

Overall, the model's predictions suggest that as the value of "ENTITY" increases, the elevation is expected to rise. However, the model's predictive accuracy is not flawless, and there is more variability



observed in real-world data (testing data) than in the data used for model training (training data). This discrepancy implies potential limitations in the model's generalizability to real-world scenarios.



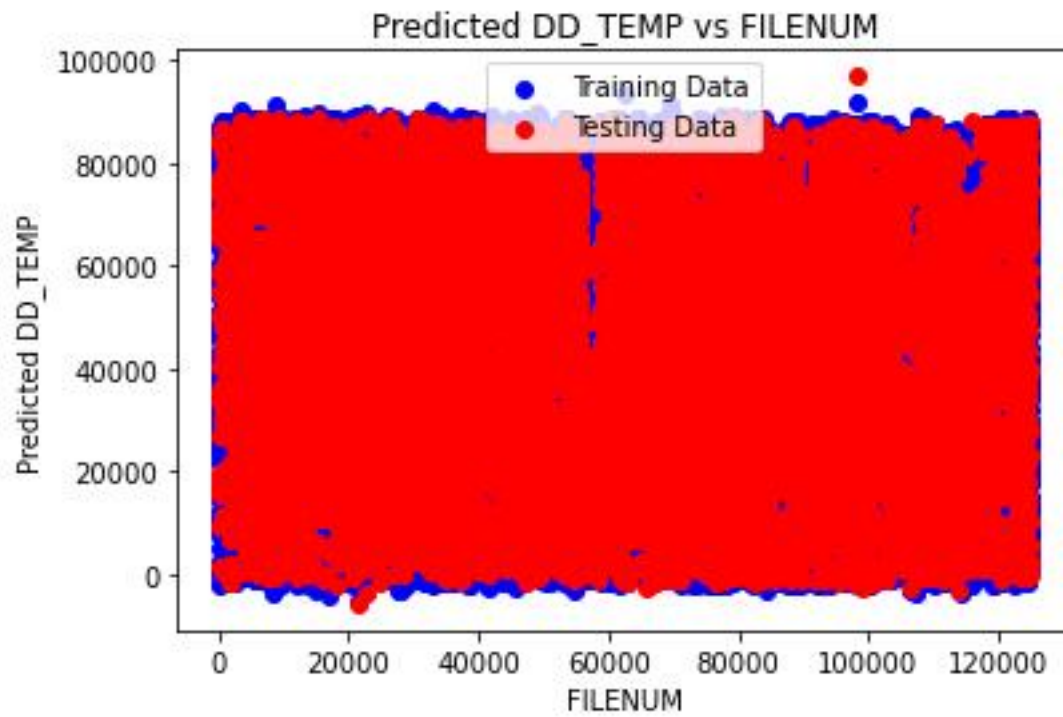
The plot illustrates the disparity between predicted and actual elevation values, with the training data depicted in blue and the testing data in red, over issuance date (ISSUEDATE).

Potential interpretations:

**Model Performance:** The model may be underestimating elevation if the y-axis denotes positive differences between predicted and actual elevation. In this scenario, the blue and red lines would trend below the x-axis, indicating that predicted values are consistently lower than actual values for most ISSUEDATE.

**Calibration Issue:** A consistent offset between predicted and actual elevations, regardless of being positive or negative, may indicate a bias in either the model or the data.

Error Type: If negative elevation values are present in the data (though this might be unlikely), the interpretation would need adjustment based on whether the y-axis represents absolute differences or signed differences between predicted and actual elevation.



The provided plot illustrates the predicted difference between training and testing data for DD\_TEMP (presumably representing elevation), with the x-axis labeled as FILENUM, likely signifying a unique identifier for each data point.

Interpretation:

General Trend: The predicted DD\_TEMP (red line) consistently appears lower than the measured DD\_TEMP (blue line) across most FILENUM values, indicating a bias in the model toward underestimating elevation.

Data Distribution: Both the training and testing data exhibit similar patterns, although slight variations may exist between the two datasets.

Possible Reasons for Underestimation:

Training Data Bias: It's conceivable that the training data used to construct the model contained more low-elevation values compared to high-elevation values, potentially leading to underestimation of elevation in new data.

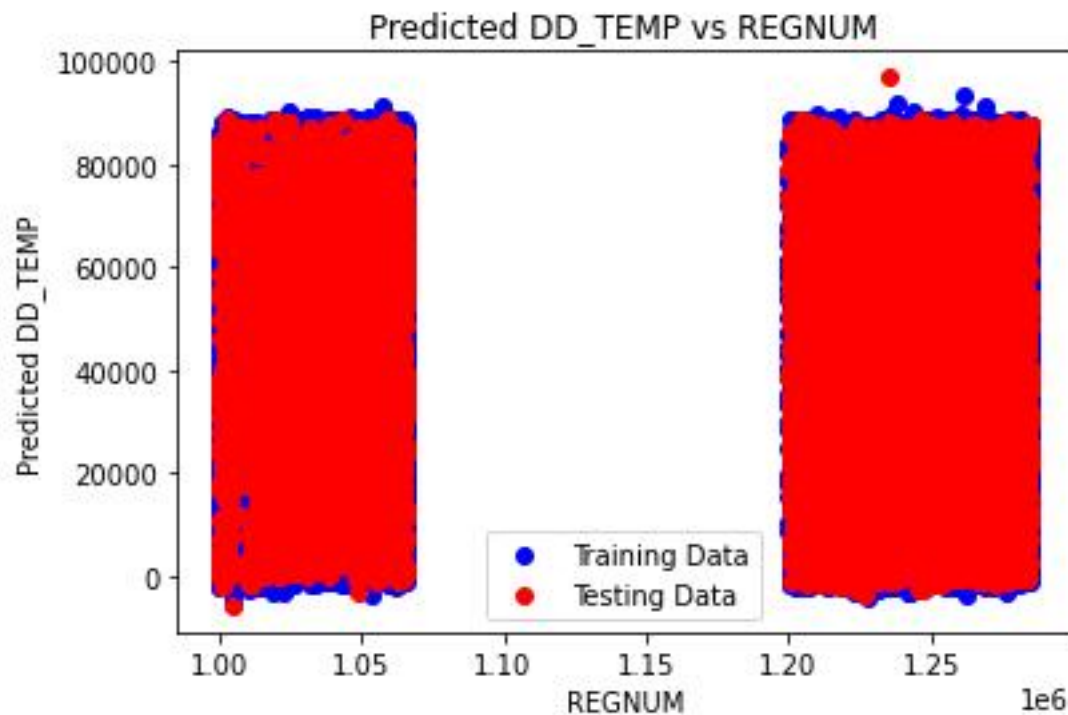
Model Complexity: If the model lacks complexity, it might struggle to capture the intricate relationships between FILENUM and DD\_TEMP, resulting in underestimation for certain FILENUM values.

Additional Considerations:

The plot does not display the actual range of DD\_TEMP values, making it challenging to ascertain the magnitude of the underestimation. Incorporating this information would provide context for understanding the difference between predicted and measured values.

The y-axis lacks units, which would offer crucial context for interpreting the difference between predicted and measured values (e.g., meters, feet).

Overall, the plot suggests a consistent underestimation in predicted DD\_TEMP values. Further investigation into the properties of the training data and model architecture is necessary to identify the precise cause of this bias.



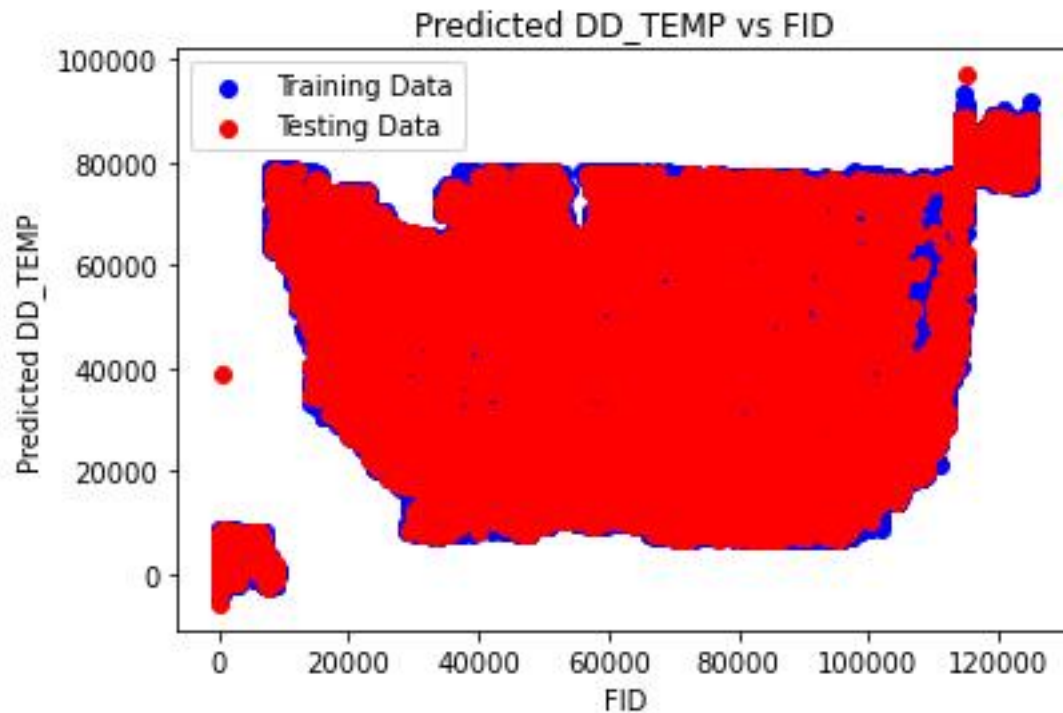
The plot illustrates the correlation between predicted elevation and actual elevation, with the x-axis likely denoting a reference elevation (REGNUM) and the y-axis representing the disparity between the predicted elevation (DD\_TEMP) and the actual elevation. The training data is depicted by the blue line, while the red line signifies the testing data.

#### Observation:

In contrast to an ideal scenario where both lines would perfectly align, indicating precise predictions, a positive bias is evident. This implies a consistent overestimation of elevation by the model. For instance, at a reference elevation of 1.10 (on the x-axis), the predicted elevation difference is approximately 20,000 (on the y-axis), suggesting that the model tends to forecast a higher elevation than the actual observation.

#### Potential Explanations:

1. **Training Data Bias:** The training dataset may be skewed towards higher elevations compared to lower ones, leading to an inherent overestimation bias in the model's predictions.
2. **Model Complexity:** An overly complex model might inadvertently incorporate noise from the elevation data, resulting in an exaggerated estimation of elevation differences.



Based on the provided image and the clarification that DD\_TEMP represents elevation, here's a interpretation of the plot:

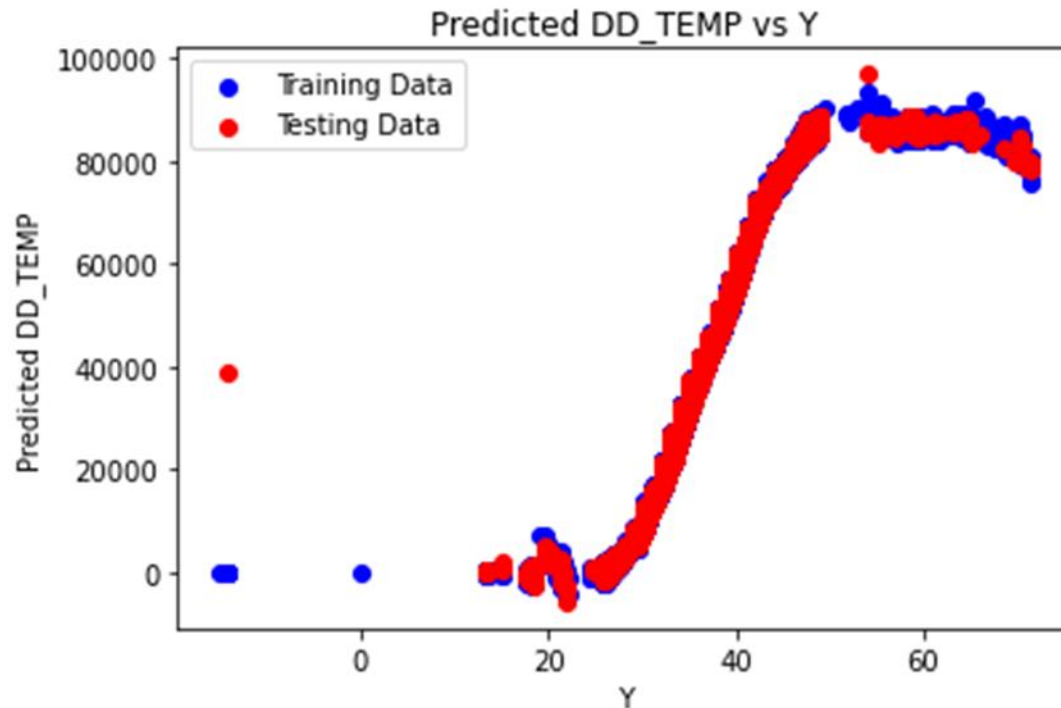
The plot depicts the disparity between predicted and actual elevations across the United States. The x-axis, labeled FID, likely serves as a unique identifier for individual data points. Meanwhile, the y-axis, labeled Predicted DD\_TEMP, represents the difference between the predicted elevation and the actual elevation. The blue line corresponds to the training data, while the red line signifies the testing data.

Observation:

In an ideal scenario, complete overlap between the training and testing data would signify optimal model performance. However, an evident positive bias is observed between the predicted and actual elevations. This indicates a consistent tendency of the model to overestimate elevation. For instance, at an FID value of approximately 60,000, the predicted difference in elevation exceeds 40,000 units, whereas the actual difference is closer to 0.

Possible Explanations:

1. Training Data Bias: It is plausible that the training data exhibits a bias towards higher elevations, leading to a systematic overestimation of elevation by the model.
2. Model Complexity: The model might be excessively complex, potentially fitting noise in the data and resulting in an exaggerated estimation of elevation differences.



Based on the provided image and the clarification that DD\_TEMP represents elevation, here is a interpretation of the plot:

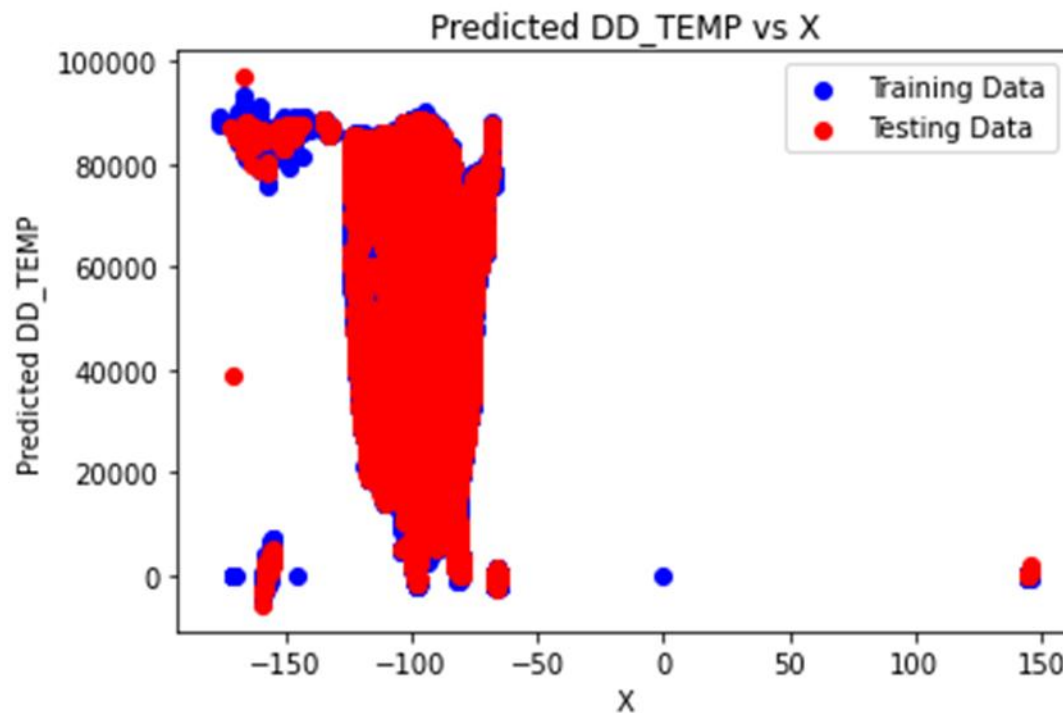
The plot illustrates the relationship between predicted elevation and actual elevation, where the x-axis, labeled as Y, likely denotes a reference elevation. The y-axis, labeled as Predicted DD\_TEMP, represents the predicted difference in elevation. The blue line corresponds to the training data, while the red line signifies the testing data.

Observation:

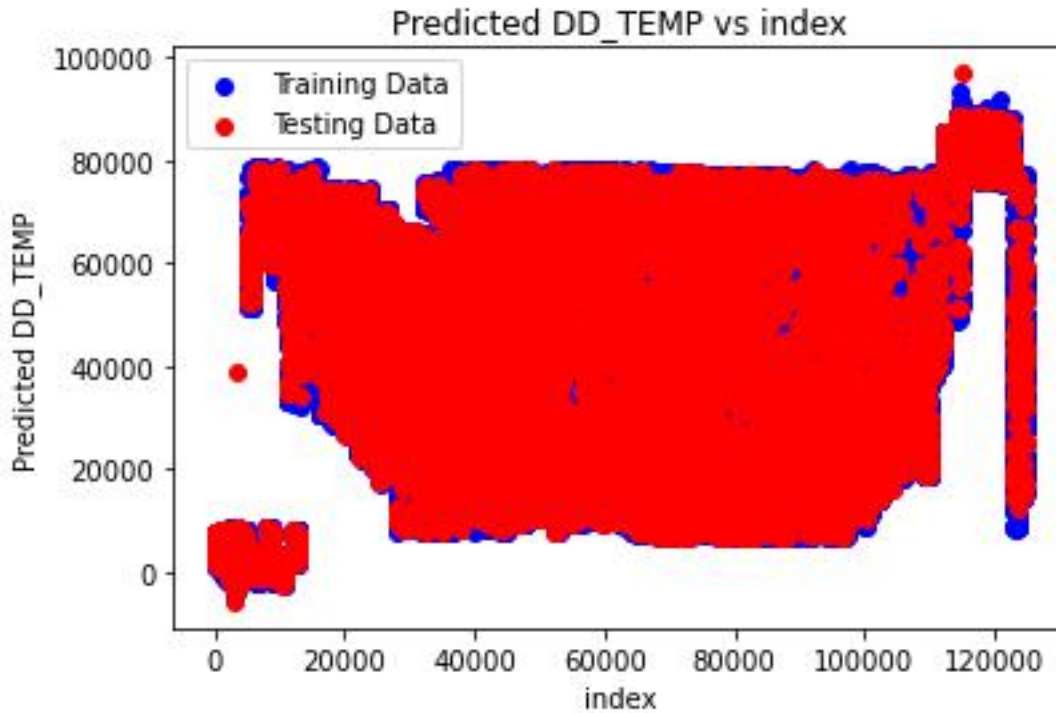
In an ideal scenario, complete overlap between the training and testing data would indicate optimal model performance. However, a discernible positive bias is observed between the predicted and actual elevations, suggesting a consistent overestimation of elevation by the model. For instance, at a reference elevation of 20 on the x-axis, the predicted difference in elevation exceeds 60,000 units, while the actual difference is closer to 0.

Possible Explanations:

1. Training Data Bias: It is conceivable that the training data exhibits a bias towards higher elevations, leading to a systematic overestimation of elevation by the model.
2. Model Complexity: The model might be overly complex, potentially fitting noise in the elevation data and resulting in an exaggerated estimation of elevation differences.



The plot visualizes the predicted DD\_TEMP versus X values. It shows distinct clusters of training data (blue) and testing data (red), indicating a model's performance in predicting temperatures. The clear separation and clustering of the data points suggest that the model may be performing well on the training data but not as well on the testing data. This could potentially indicate overfitting, where the model learns the training data too well and performs poorly on unseen data. However, without more context or data, this is just one possible interpretation.



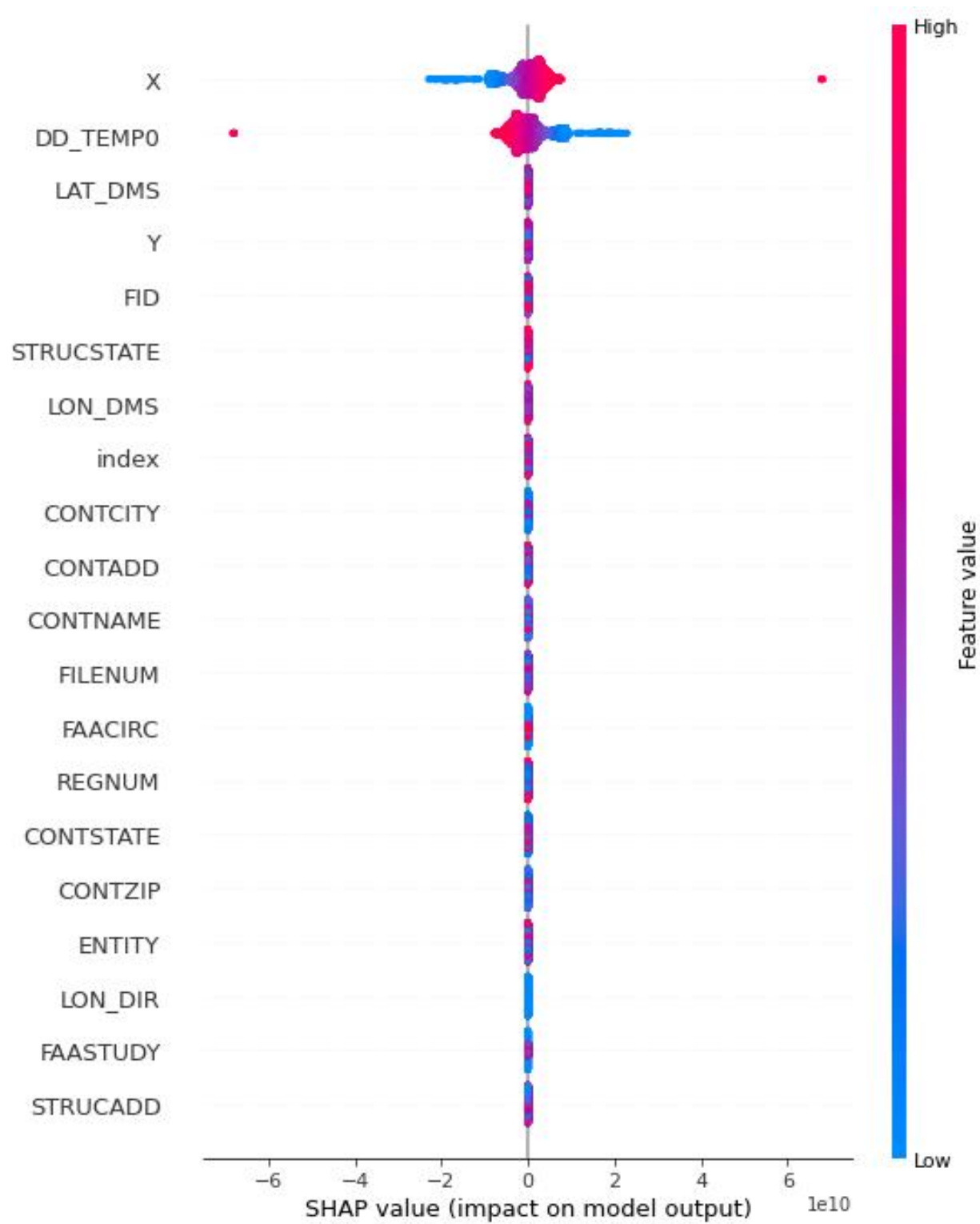
The plot provided offers a graphical representation of a machine learning model's performance. It juxtaposes predicted DD\_TEMP values against an index, with blue points denoting the training data and red points representing the testing data.

From the plot, it is apparent that the model has been trained on a dense set of data points, as evidenced by the clustering of blue points. The dispersion of red points across the plot illustrates how effectively the model predicts DD\_TEMP over various indices.

Such visualizations are commonly employed to assess a machine learning model's behavior and compare its performance on training versus testing data. They facilitate the identification of potential issues such as overfitting or underfitting, and provide insights into the model's generalization capabilities. However, to offer a more comprehensive interpretation, additional details or context regarding the data or the model would be necessary.

SHAP-INTERPRETATION:





### 1. DD\_TEMPO:

- This feature exhibits both positive and negative impacts on the model's output. Instances with higher DD\_TEMPO values contribute positively (shown in red), while lower values have a negative impact (in blue).

### 2. LAT\_DMS:

- Similar to DD\_TEMPO, LAT\_DMS influences the model in both directions. However, it tends to reduce the model's output more frequently.

### 3. Y:

- The Y feature demonstrates minimal influence, as its points predominantly cluster around zero. It does not significantly affect the model's predictions.

### 4. FID to STRUCADD:

- These features show little or no visible impact on the model's predictions. Their SHAP values are centered around zero.

### 5. Feature Value Gradient:

- A gradient bar on the right side represents feature values. Blue indicates low values, while red signifies high values.

Here's another analysis:

index	X	Y	OBJECTID	siteID	siteName	radarType	antennaElevation
0	98.413046	-45.455833	1	KABR	ABERDEEN	NEXRAD	Unknown
1	-	35.1497	2	KABX	ALBUQUERQUE	NEXRAD	Unknown

	106.8238 8	22					
2	77.00749 1	36.9838 89	3	KAKQ	NORFOLK	NEXRAD	Unknown
3	101.7092 69	35.2333 33	4	KAMA	AMARILLO	NEXRAD	Unknown
4	80.41304 8	25.6105 56	5	KAMX	MIAMI	NEXRAD	Unknown
5	84.71952 3	44.9063 5	6	KAPX	NCL MICHIGAN	NEXRAD	Unknown
6	91.19110 1	43.8227 78	7	KARX	LA CROSSE	NEXRAD	Unknown
7	122.4956 84	48.1946 11	8	KATX	SEATTLE	NEXRAD	Unknown
8	121.6316 58	39.4961 11	9	KBBX	BEALE AFB	NEXRAD	Unknown
9	75.98471 3	42.1996 94	10	KBGM	BINGHAMTON	NEXRAD	Unknown
10	124.2921 58	40.4983 33	11	KBHX	EUREKA (BUNKER HILL)	NEXRAD	Unknown
11	100.7602 68	46.7708 33	12	KBIS	BISMARCK	NEXRAD	Unknown
12	108.6067 96	45.8537 78	13	KBLX	BILLINGS	NEXRAD	Unknown
13	86.76971 3	33.1719 44	14	KBMX	BIRMINGHAM	NEXRAD	Unknown
14	71.13685 1	41.9557 78	15	KBOX	BOSTON	NEXRAD	Unknown
15	97.41860 3	25.9155 56	16	KBRO	BROWNSVILLE	NEXRAD	Unknown
16	78.73693 5	42.9486 11	17	KBUF	BUFFALO	NEXRAD	Unknown
17	-	24.5969	18	KBYX	KEY WEST	NEXRAD	Unknown

	81.70332 5	44					
18	81.11860 2	33.9486 11	19	KCAE	COLUMBIA	NEXRAD	Unknown
19	67.80640 7	46.0391 67	20	KCBW	CARIBOU	NEXRAD	Unknown
20	116.2360 23	43.4902 17	21	KCBX	BOISE	NEXRAD	Unknown
21	-78.00388	40.9230 56	22	KCCX	STATE COLLEGE	NEXRAD	Unknown
22	81.85999 1	41.4130 56	23	KCLE	CLEVELAND	NEXRAD	Unknown
23	81.04218 6	32.6555 28	24	KCLX	CHARLESTON, SC	NEXRAD	Unknown
24	97.45999 1	35.2383 33	25	KCRI	ROC FAA REDUNDANT (RDA 1)	NEXRAD	Unknown
25	97.51082 5	27.7838 89	26	KCRP	CORPUS CHRISTI	NEXRAD	Unknown
26	73.16637 9	44.5111 11	27	KCXX	BURLINGTON	NEXRAD	Unknown
27	104.8061 02	41.1519 44	28	KCYS	CHEYENNE	NEXRAD	Unknown
28	121.6778 24	38.5011 11	29	KDAX	SACRAMENTO	NEXRAD	Unknown
29	-99.96888	37.7608 33	30	KDDC	DODGE CITY	NEXRAD	Unknown
30	100.2802 7	29.2725	31	KDFX	LAUGHLIN AFB	NEXRAD	Unknown
31	89.98443 6	32.28	32	KDGX	JACKSON/BRANDON , MS	NEXRAD	Unknown
32	74.41071 3	39.9469 44	33	KDIX	PHILADELPHIA	NEXRAD	Unknown
33	92.20971 2	46.8369 44	34	KDLH	DULUTH	NEXRAD	Unknown

34	93.72285 2	41.7311 11	35	KDMX	DES MOINES	NEXRAD	Unknown
35	75.43999 1	38.8255 56	36	KDOX	DOVER AFB	NEXRAD	Unknown
36	83.47165 8	42.7	37	KDTX	DETROIT	NEXRAD	Unknown
37	90.58082 4	41.6116 67	38	KDVN	QUAD CITIES	NEXRAD	Unknown
38	99.25415 9	32.5383 33	39	KDYX	DYESS AFB	NEXRAD	Unknown
39	94.26446 3	38.8102 5	40	KEAX	PLEASANT HILL	NEXRAD	Unknown
40	110.6302 7	31.8936 11	41	KEMX	TUCSON	NEXRAD	Unknown
41	74.06407 4	42.5865 56	42	KENX	ALBANY	NEXRAD	Unknown
42	85.45938 1	31.4605 56	43	KEOX	FT RUCKER	NEXRAD	Unknown
43	106.6979 92	31.8730 56	44	KEPZ	EL PASO	NEXRAD	Unknown
44	114.8913 81	35.7011 11	45	KESX	LAS VEGAS	NEXRAD	Unknown
45	85.92165 9	30.5650 33	46	KEVX	EGLIN AFB	NEXRAD	Unknown
46	98.02860 3	29.7040 56	47	KEWX	AUSTIN/SAN ANTONIO	NEXRAD	Unknown
47	117.5607 41	35.0977 78	48	KEYX	EDWARDS AFB	NEXRAD	Unknown
48	80.27415 8	37.0241 67	49	KFCX	ROANOKE	NEXRAD	Unknown
49	98.97665 9	34.3621 94	50	KFDR	ALTUS AFB	NEXRAD	Unknown

50	103.6188 81	34.6341 67	51	KFDX	CANNON AFB	NEXRAD	Unknown
51	84.56582 5	33.3633 33	52	KFFC	ATLANTA	NEXRAD	Unknown
52	-96.72888	43.5877 78	53	KFSD	SIOUX FALLS	NEXRAD	Unknown
53	111.1984 35	34.5743 33	54	KFSX	FLAGSTAFF (RDA 1)	NEXRAD	Unknown
54	104.5457 97	39.7866 39	55	KFTG	DENVER	NEXRAD	Unknown
55	97.30313 1	32.5727 78	56	KFWS	DALLAS/FT WORTH	NEXRAD	Unknown
56	106.6246 83	48.2063 61	57	KGGW	GLASGOW	NEXRAD	Unknown
57	108.2137 52	39.0622 22	58	KGJX	GRAND JUNCTION (RDA 1)	NEXRAD	Unknown
58	101.7002 69	39.3669 44	59	KGLD	GOODLAND	NEXRAD	Unknown
59	88.11110 1	44.4986 33	60	KGRB	GREEN BAY	NEXRAD	Unknown
60	-97.38277	30.7216 67	61	KGRK	FT HOOD	NEXRAD	Unknown
61	-85.54488	42.8938 89	62	KGRR	GRAND RAPIDS	NEXRAD	Unknown
62	82.21982 5	34.8833 06	63	KGSP	GREER	NEXRAD	Unknown
63	88.32918 6	33.8969 17	64	KGWX	COLUMBUS AFB	NEXRAD	Unknown
64	70.25635 1	43.8913 06	65	KGYX	PORTLAND, ME	NEXRAD	Unknown
65	106.1200 24	33.077	66	KHDX	HOLLOMAN AFB	NEXRAD	Unknown
66	95.07888 1	29.4719 44	67	KHGX	HOUSTON	NEXRAD	Unknown

67	119.6321 3	- 36.3141 67	68	KHNX	SAN JOAQUIN VALY	NEXRAD	Unknown
68	87.28499 1	- 36.7366 67	69	KHPX	FT CAMPBELL	NEXRAD	Unknown

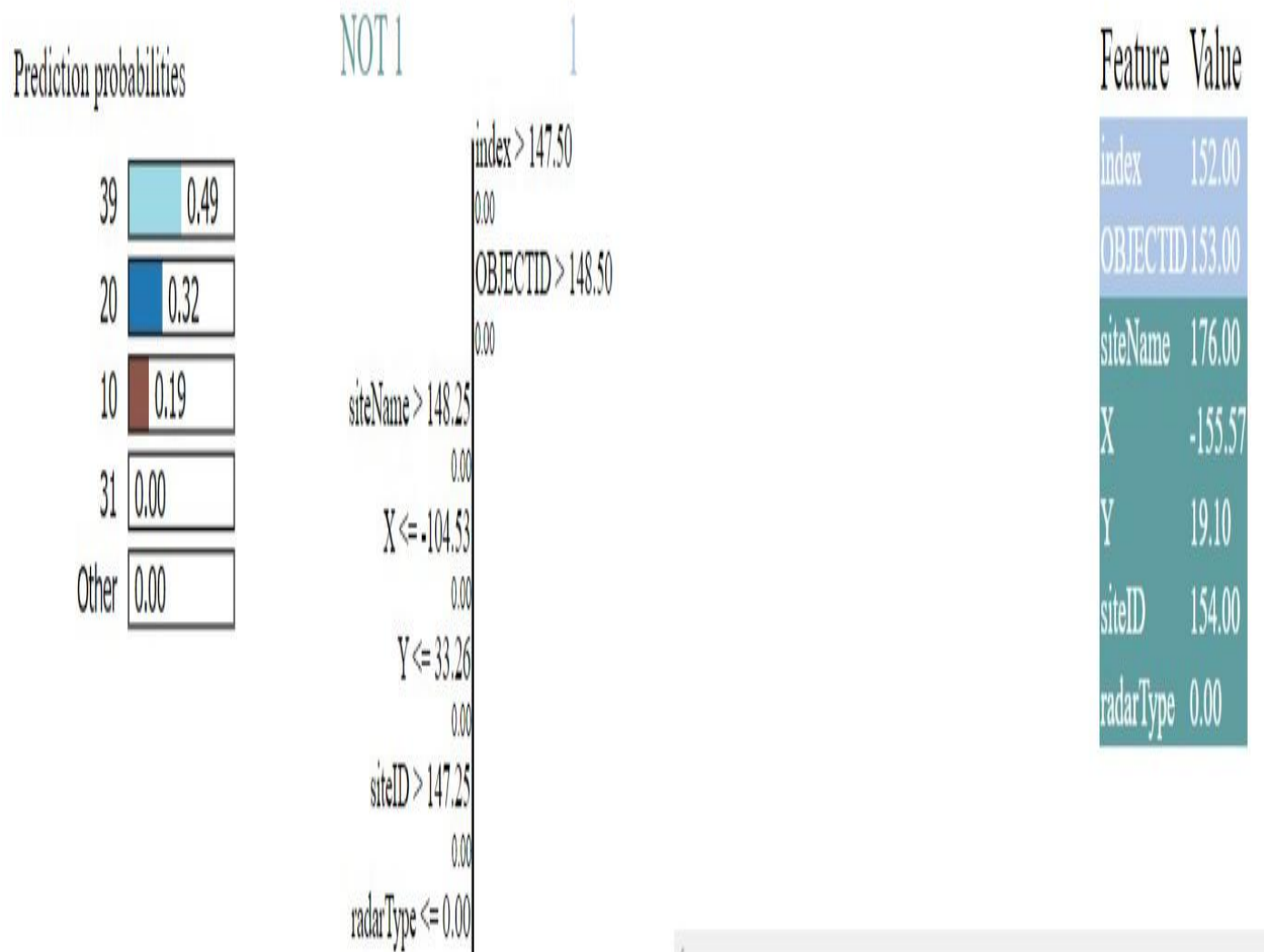
1. index: This feature likely represents a unique identifier or index for each data point. It serves as a reference point to uniquely identify each observation in the dataset.
2. X: This feature represents the longitude coordinate of the radar site. Longitude measures the east-west position on the Earth's surface, with values ranging from -180 degrees (West) to +180 degrees (East).
3. Y: This feature represents the latitude coordinate of the radar site. Latitude measures the north-south position on the Earth's surface, with values ranging from -90 degrees (South) to +90 degrees (North).
4. OBJECTID: This feature is likely another identifier for each radar site. It could serve a similar purpose as the index feature, providing a unique identifier for each observation.
5. siteID: This feature likely represents a standardized identifier for each radar site. It could be used for reference and identification purposes.
6. siteName: This feature contains the name or label of each radar site. It provides descriptive information about the location or purpose of each radar site.
7. radarType: This feature describes the type or classification of radar used at each site. It could indicate whether the radar is a NEXRAD (Next Generation Radar) or another type of radar system.

8. antennaElevation: This feature likely represents the elevation angle of the radar antenna. It describes the angle at which the radar antenna is tilted above the horizontal plane. This angle is important for determining the coverage area and range of the radar.

Each of these features provides valuable information about the radar sites included in the dataset, including their geographic coordinates, identifiers, names, radar types, and antenna elevations. Together, they help characterize and distinguish the radar sites for further analysis or modeling purposes.

LIME-INTERPRETATION:





ENCODING ONLY CATEGORICAL VARIABLE:

coefficient [-1.30815881e+09 8.31558601e-02 7.02519998e-01 1.30815880e+09

5.77362424e+00 2.88645349e-02 -5.45748342e+01 -8.12590325e-03

2.04384146e-02 1.03057639e-01 -1.79694672e-02 4.47181913e-02

8.36653864e-03 5.12392179e+00 -2.47773426e-04 -3.31388868e-03

2.07602797e-02 -4.12616490e-02 -6.13230685e-06 4.43982075e-02

-1.36522439e-02 1.01907210e-01 -2.02399002e-01 -8.98596183e-04

-3.53260874e-01 -1.77593608e-02 4.27486453e-02 1.33136138e-02

5.12299004e+00 -4.34691385e-02 -2.15692308e-02 -9.66311887e+00

1.18447754e-05 -7.28725887e-02 -5.45775914e+01]

intercept 37.48010491265191

Equation: antennaElevation= 37.480104913 + 0.083155860 \* X + 0.702519998 \* Y +  
1308158801.545084476 \* OBJECTID + 5.773624240 \* siteID + 0.028864535 \* siteName + -  
54.574834193 \* radarType + -0.008125903 \* index\*\*2 + 0.020438415 \* index\*\*1\*X\*\*1 +  
0.103057639 \* index\*\*1\*Y\*\*1 + -0.017969467 \* index\*\*1\*OBJECTID\*\*1 + 0.044718191 \*  
index\*\*1\*siteID\*\*1 + 0.008366539 \* index\*\*1\*siteName\*\*1 + 5.123921786 \*  
index\*\*1\*radarType\*\*1 + -0.000247773 \* X\*\*2 + -0.003313889 \* X\*\*1\*Y\*\*1 + 0.020760280  
\* X\*\*1\*OBJECTID\*\*1 + -0.041261649 \* X\*\*1\*siteID\*\*1 + -0.000006132 \*  
X\*\*1\*siteName\*\*1 + 0.044398207 \* X\*\*1\*radarType\*\*1 + -0.013652244 \* Y\*\*2 +  
0.101907210 \* Y\*\*1\*OBJECTID\*\*1 + -0.202399002 \* Y\*\*1\*siteID\*\*1 + -0.000898596 \*  
Y\*\*1\*siteName\*\*1 + -0.353260874 \* Y\*\*1\*radarType\*\*1 + -0.017759361 \* OBJECTID\*\*2 +  
0.042748645 \* OBJECTID\*\*1\*siteID\*\*1 + 0.013313614 \* OBJECTID\*\*1\*siteName\*\*1 +  
5.122990037 \* OBJECTID\*\*1\*radarType\*\*1 + -0.043469139 \* siteID\*\*2 + -0.021569231 \*  
siteID\*\*1\*siteName\*\*1 + -9.663118874 \* siteID\*\*1\*radarType\*\*1 + 0.000011845 \*  
siteName\*\*2 + -0.072872589 \* siteName\*\*1\*radarType\*\*1 + -54.577591419 \* radarType\*\*2

Accuracy: 0.7888502842920684

coefficient [ 3.75329801e+07 -1.54207065e+00 7.29509724e+00 -3.75329540e+07

-2.55545123e+01 -4.87990431e-01 2.38297252e+03 2.92878671e+01

2.88806925e-01 -4.05785883e+00 3.12871972e+01 -9.19288988e+01

9.72579098e-02 -5.46762464e+02 -4.98597419e-03 8.03254802e-02

-3.81138014e-01 9.71067970e-02 -6.21224863e-03 -6.57952062e+00

-8.91717912e-02 -2.60278571e+00 6.61479277e+00 6.01932367e-03

3.56128341e+01 3.20696139e+01 -9.13852980e+01 8.81768794e-01

-5.47434000e+02 9.06745307e+01 -9.71943652e-01 1.04368502e+03

6.46259519e-04 3.74094691e+00 2.38215057e+03 -6.83670603e-02

2.49423523e-01 1.56735277e-01 -6.74416497e-02 1.82456927e-01

-5.70986741e-02 -1.56108861e+02 -3.52238670e-01 -1.14267614e-01

2.48625681e-01 -8.20912246e-01 -2.82883263e-01 -2.12180225e+00

8.55237199e-02 1.56294571e-01 -3.39943631e-01 -1.29506032e-01

-3.35174963e+00 -6.73751812e-02 1.82774028e-01 -5.75523418e-02

-1.56108492e+02 -1.46272152e-01 1.70478227e-01 4.75919787e+02  
 -5.47206961e-04 -6.13659347e-01 -5.47425813e+02 4.79691662e-05  
 5.47171454e-04 3.63073561e-01 -1.07053742e-02 -6.92168251e-05  
 -2.25732489e-02 2.61704947e-04 1.15474661e-01 -1.07350061e-03  
 -1.73628796e-04 7.19036019e-02 7.54702059e-02 -3.03402949e-01  
 2.89774443e-01 -2.12181215e+00 5.50916890e-01 -6.83772843e-03  
 4.28730423e+00 -1.08210370e-05 -3.13421858e-02 -6.59326635e+00  
 9.58204335e-04 -4.75144924e-02 -3.74907728e-02 -3.05247842e-04  
 -5.86837255e-03 2.93530554e-01 -8.23195360e-01 1.31610143e-01  
 -3.35175955e+00 5.56841034e-01 -2.09999830e-03 6.28853021e+00  
 -5.69131225e-06 5.98111689e-02 3.56004957e+01 -6.74092923e-02  
 1.82773688e-01 -5.75301293e-02 -1.56108518e+02 -1.46266085e-01  
 1.70475719e-01 4.75919792e+02 -5.48862852e-04 -6.13651695e-01  
 -5.47425803e+02 1.51084326e-02 -1.68790098e-01 -4.83165789e+02  
 1.09285768e-03 1.15271875e+00 1.04368563e+03 -5.31226397e-06  
 8.30008037e-03 3.74162320e+00 2.38215100e+03]

intercept -75.53946827782525

Equation: antennaElevation= -75.539468278 + -1.542070646 \* X + 7.295097240 \* Y + -  
 37532954.032091662 \* OBJECTID + -25.554512324 \* siteID + -0.487990431 \* siteName +  
 2382.972522247 \* radarType + 29.287867121 \* index\*\*2 + 0.288806925 \* index\*\*1\*X\*\*1 + -  
 4.057858827 \* index\*\*1\*Y\*\*1 + 31.287197206 \* index\*\*1\*OBJECTID\*\*1 + -91.928898810 \*  
 index\*\*1\*siteID\*\*1 + 0.097257910 \* index\*\*1\*siteName\*\*1 + -546.762463931 \*  
 index\*\*1\*radarType\*\*1 + -0.004985974 \* X\*\*2 + 0.080325480 \* X\*\*1\*Y\*\*1 + -0.381138014  
 \* X\*\*1\*OBJECTID\*\*1 + 0.097106797 \* X\*\*1\*siteID\*\*1 + -0.006212249 \*  
 X\*\*1\*siteName\*\*1 + -6.579520619 \* X\*\*1\*radarType\*\*1 + -0.089171791 \* Y\*\*2 + -  
 2.602785706 \* Y\*\*1\*OBJECTID\*\*1 + 6.614792774 \* Y\*\*1\*siteID\*\*1 + 0.006019324 \*  
 Y\*\*1\*siteName\*\*1 + 35.612834085 \* Y\*\*1\*radarType\*\*1 + 32.069613912 \* OBJECTID\*\*2 +  
 -91.385297952 \* OBJECTID\*\*1\*siteID\*\*1 + 0.881768794 \* OBJECTID\*\*1\*siteName\*\*1 + -  
 547.434000108 \* OBJECTID\*\*1\*radarType\*\*1 + 90.674530689 \* siteID\*\*2 + -0.971943652 \*  
 siteID\*\*1\*siteName\*\*1 + 1043.685022464 \* siteID\*\*1\*radarType\*\*1 + 0.000646260 \*  
 siteName\*\*2 + 3.740946913 \* siteName\*\*1\*radarType\*\*1 + 2382.150571343 \* radarType\*\*2  
 + -0.068367060 \* index\*\*3 + 0.249423523 \* index\*\*2\*X\*\*1 + 0.156735277 \* index\*\*2\*Y\*\*1  
 + -0.067441650 \* index\*\*2\*OBJECTID\*\*1 + 0.182456927 \* index\*\*2\*siteID\*\*1 + -  
 0.057098674 \* index\*\*2\*siteName\*\*1 + -156.108860920 \* index\*\*2\*radarType\*\*1 + -

$$\begin{aligned}
&0.352238670 * \text{index}^{**1} * X^{**2} + -0.114267614 * \text{index}^{**1} * X^{**1} * Y^{**1} + 0.248625681 * \\
&\text{index}^{**1} * X^{**1} * \text{OBJECTID}^{**1} + -0.820912246 * \text{index}^{**1} * X^{**1} * \text{siteID}^{**1} + -0.282883263 \\
&* \text{index}^{**1} * X^{**1} * \text{siteName}^{**1} + -2.121802249 * \text{index}^{**1} * X^{**1} * \text{radarType}^{**1} + \\
&0.085523720 * \text{index}^{**1} * Y^{**2} + 0.156294571 * \text{index}^{**1} * Y^{**1} * \text{OBJECTID}^{**1} + - \\
&0.339943631 * \text{index}^{**1} * Y^{**1} * \text{siteID}^{**1} + -0.129506032 * \text{index}^{**1} * Y^{**1} * \text{siteName}^{**1} + - \\
&3.351749629 * \text{index}^{**1} * Y^{**1} * \text{radarType}^{**1} + -0.067375181 * \text{index}^{**1} * \text{OBJECTID}^{**2} + \\
&0.182774028 * \text{index}^{**1} * \text{OBJECTID}^{**1} * \text{siteID}^{**1} + -0.057552342 * \\
&\text{index}^{**1} * \text{OBJECTID}^{**1} * \text{siteName}^{**1} + -156.108492326 * \\
&\text{index}^{**1} * \text{OBJECTID}^{**1} * \text{radarType}^{**1} + -0.146272152 * \text{index}^{**1} * \text{siteID}^{**2} + 0.170478227 \\
&* \text{index}^{**1} * \text{siteID}^{**1} * \text{siteName}^{**1} + 475.919787338 * \text{index}^{**1} * \text{siteID}^{**1} * \text{radarType}^{**1} + - \\
&0.000547207 * \text{index}^{**1} * \text{siteName}^{**2} + -0.613659347 * \\
&\text{index}^{**1} * \text{siteName}^{**1} * \text{radarType}^{**1} + -547.425812986 * \text{index}^{**1} * \text{radarType}^{**2} + \\
&0.000047969 * X^{**3} + 0.000547171 * X^{**2} * Y^{**1} + 0.363073561 * X^{**2} * \text{OBJECTID}^{**1} + - \\
&0.010705374 * X^{**2} * \text{siteID}^{**1} + -0.000069217 * X^{**2} * \text{siteName}^{**1} + -0.022573249 * \\
&X^{**2} * \text{radarType}^{**1} + 0.000261705 * X^{**1} * Y^{**2} + 0.115474661 * \\
&X^{**1} * Y^{**1} * \text{OBJECTID}^{**1} + -0.001073501 * X^{**1} * Y^{**1} * \text{siteID}^{**1} + -0.000173629 * \\
&X^{**1} * Y^{**1} * \text{siteName}^{**1} + 0.071903602 * X^{**1} * Y^{**1} * \text{radarType}^{**1} + 0.075470206 * \\
&X^{**1} * \text{OBJECTID}^{**2} + -0.303402949 * X^{**1} * \text{OBJECTID}^{**1} * \text{siteID}^{**1} + 0.289774443 * \\
&X^{**1} * \text{OBJECTID}^{**1} * \text{siteName}^{**1} + -2.121812152 * X^{**1} * \text{OBJECTID}^{**1} * \text{radarType}^{**1} + \\
&0.550916890 * X^{**1} * \text{siteID}^{**2} + -0.006837728 * X^{**1} * \text{siteID}^{**1} * \text{siteName}^{**1} + \\
&4.287304227 * X^{**1} * \text{siteID}^{**1} * \text{radarType}^{**1} + -0.000010821 * X^{**1} * \text{siteName}^{**2} + - \\
&0.031342186 * X^{**1} * \text{siteName}^{**1} * \text{radarType}^{**1} + -6.593266349 * X^{**1} * \text{radarType}^{**2} + \\
&0.000958204 * Y^{**3} + -0.047514492 * Y^{**2} * \text{OBJECTID}^{**1} + -0.037490773 * \\
&Y^{**2} * \text{siteID}^{**1} + -0.000305248 * Y^{**2} * \text{siteName}^{**1} + -0.005868373 * Y^{**2} * \text{radarType}^{**1} \\
&+ 0.293530554 * Y^{**1} * \text{OBJECTID}^{**2} + -0.823195360 * Y^{**1} * \text{OBJECTID}^{**1} * \text{siteID}^{**1} + \\
&0.131610143 * Y^{**1} * \text{OBJECTID}^{**1} * \text{siteName}^{**1} + -3.351759552 * \\
&Y^{**1} * \text{OBJECTID}^{**1} * \text{radarType}^{**1} + 0.556841034 * Y^{**1} * \text{siteID}^{**2} + -0.002099998 * \\
&Y^{**1} * \text{siteID}^{**1} * \text{siteName}^{**1} + 6.288530210 * Y^{**1} * \text{siteID}^{**1} * \text{radarType}^{**1} + - \\
&0.000005691 * Y^{**1} * \text{siteName}^{**2} + 0.059811169 * Y^{**1} * \text{siteName}^{**1} * \text{radarType}^{**1} + - \\
&35.600495709 * Y^{**1} * \text{radarType}^{**2} + -0.067409292 * \text{OBJECTID}^{**3} + 0.182773688 * \\
&\text{OBJECTID}^{**2} * \text{siteID}^{**1} + -0.057530129 * \text{OBJECTID}^{**2} * \text{siteName}^{**1} + -156.108517557 * \\
&\text{OBJECTID}^{**2} * \text{radarType}^{**1} + -0.146266085 * \text{OBJECTID}^{**1} * \text{siteID}^{**2} + 0.170475719 * \\
&\text{OBJECTID}^{**1} * \text{siteID}^{**1} * \text{siteName}^{**1} + 475.919791938 * \\
&\text{OBJECTID}^{**1} * \text{siteID}^{**1} * \text{radarType}^{**1} + -0.000548863 * \text{OBJECTID}^{**1} * \text{siteName}^{**2} + - \\
&0.613651695 * \text{OBJECTID}^{**1} * \text{siteName}^{**1} * \text{radarType}^{**1} + -547.425802755 * \\
&\text{OBJECTID}^{**1} * \text{radarType}^{**2} + 0.015108433 * \text{siteID}^{**3} + -0.168790098 * \\
&\text{siteID}^{**2} * \text{siteName}^{**1} + -483.165788513 * \text{siteID}^{**2} * \text{radarType}^{**1} + 0.001092858 * \\
&\text{siteID}^{**1} * \text{siteName}^{**2} + 1.152718752 * \text{siteID}^{**1} * \text{siteName}^{**1} * \text{radarType}^{**1} + \\
&1043.685634689 * \text{siteID}^{**1} * \text{radarType}^{**2} + -0.000005312 * \text{siteName}^{**3} + 0.008300080 * \\
&\text{siteName}^{**2} * \text{radarType}^{**1} + 3.741623198 * \text{siteName}^{**1} * \text{radarType}^{**2} + 2382.151003692 * \\
&\text{radarType}^{**3}
\end{aligned}$$

Accuracy: 0.8559949888292026

ENCODING EVERY VARIABLE:

Equation: coefficient [7.15285855e-02 3.54303475e-02 -2.61882543e+09

-3.29718150e+00 -1.21567345e-03 -5.06867330e+01 -5.43255963e-02

-1.51496130e-02 5.92000916e-03 -6.23684678e-02 1.67640323e-01

3.37604862e-03 2.94709461e+00 -2.97894849e-04 2.11583434e-06

-8.30330430e-03 2.30727542e-02 1.65550422e-05 6.90031199e-02

-1.10687989e-04 -3.67287413e-03 -2.13581302e-03 -1.83949192e-04

3.87263064e-03 -5.63251231e-02 1.62487248e-01 -5.76348570e-03

2.94123911e+00 -1.56955974e-01 2.06984620e-03 -5.49952508e+00

1.92743967e-04 -8.42684431e-03 -5.06964870e+01]

intercept 39.903880479600694

Equation: antennaElevation= 39.903880480 + 0.071528585 \* X + 0.035430348 \* Y + -  
2618825427.105230808 \* OBJECTID + -3.297181504 \* siteID + -0.001215673 \* siteName + -  
50.686732964 \* radarType + -0.054325596 \* index^2 + -0.015149613 \* index^1\*X^1 +  
0.005920009 \* index^1\*Y^1 + -0.062368468 \* index^1\*OBJECTID^1 + 0.167640323 \*  
index^1\*siteID^1 + 0.003376049 \* index^1\*siteName^1 + 2.947094606 \* index^1\*radarType^1  
+ -0.000297895 \* X^2 + 0.000002116 \* X^1\*Y^1 + -0.008303304 \* X^1\*OBJECTID^1 +  
0.023072754 \* X^1\*siteID^1 + 0.000016555 \* X^1\*siteName^1 + 0.069003120 \*  
X^1\*radarType^1 + -0.000110688 \* Y^2 + -0.003672874 \* Y^1\*OBJECTID^1 + -0.002135813  
\* Y^1\*siteID^1 + -0.000183949 \* Y^1\*siteName^1 + 0.003872631 \* Y^1\*radarType^1 + -  
0.056325123 \* OBJECTID^2 + 0.162487248 \* OBJECTID^1\*siteID^1 + -0.005763486 \*  
OBJECTID^1\*siteName^1 + 2.941239105 \* OBJECTID^1\*radarType^1 + -0.156955974 \*  
siteID^2 + 0.002069846 \* siteID^1\*siteName^1 + -5.499525081 \* siteID^1\*radarType^1 +  
0.000192744 \* siteName^2 + -0.008426844 \* siteName^1\*radarType^1 + -50.696486974 \*  
radarType^2

Accuracy: 0.817827613511193

DEGREE-3:

coefficient [-3.38992552e+05 -8.90561425e-02 8.06656095e-04 3.19181853e+05

1.98106840e+04 -1.11738867e-01 1.58813842e+03 -9.89821913e+03  
-9.22377399e-02 3.51654352e-02 -9.89822208e+03 2.96947732e+04  
6.88866638e-02 1.19422955e+04 2.54298221e-04 -2.64671190e-05  
-9.24736799e-02 1.82484532e-01 2.02631503e-03 -1.27573786e-01  
-7.98099683e-04 2.81899747e-02 -6.25319000e-02 7.28663757e-04  
3.36444565e-01 -9.89821925e+03 2.96947753e+04 7.00773713e-02  
1.19422917e+04 -2.96948878e+04 -1.37353548e-01 -2.39120252e+04  
-2.96061374e-04 2.18922479e+00 1.58814125e+03 -2.47626460e+03  
1.37083053e-02 1.85483705e-02 -2.47626460e+03 9.90500531e+03  
-1.89343223e-02 3.58652538e+03 5.78146588e-04 -2.90548695e-04  
1.37086269e-02 -4.07191591e-02 1.33448357e-05 -1.11230523e-01  
-1.96423499e-04 1.85518211e-02 -5.49471393e-02 6.28408598e-05  
-8.74008192e-02 -2.47626460e+03 9.90500531e+03 -1.89337400e-02  
3.58652538e+03 -1.48574292e+04 5.57207054e-02 -1.07568024e+04  
-1.03175418e-04 -1.03465516e-01 1.19422916e+04 8.25348252e-08  
1.56437454e-06 5.85528469e-04 -1.15111213e-03 -7.54492794e-06  
-3.75079007e-03 -5.48097887e-07 -2.88763454e-04 5.73585790e-04  
-1.45615923e-06 2.25994412e-03 1.37066433e-02 -4.07197753e-02  
1.34431302e-05 -1.11230542e-01 4.03221680e-02 -2.90854241e-05  
2.26230035e-01 -1.08240238e-06 2.52219804e-04 -1.27563606e-01  
4.05707397e-06 -1.95810634e-04 3.88275307e-04 -2.11632869e-06  
1.14481659e-03 1.85511394e-02 -5.49470224e-02 6.09168710e-05  
-8.74010123e-02 5.42493512e-02 -1.23155278e-04 1.67387270e-01  
-2.15193722e-07 4.16567552e-04 3.36563836e-01 -2.47626460e+03  
9.90500531e+03 -1.89340995e-02 3.58652538e+03 -1.48574292e+04  
5.57207836e-02 -1.07568024e+04 -1.03456779e-04 -1.03464956e-01  
1.19422916e+04 9.90490094e+03 -5.46522443e-02 1.07541868e+04  
2.03655833e-04 1.80778116e-01 -2.39120252e+04 1.70675776e-06

2.82072518e-03 2.18922389e+00 1.58814125e+03]

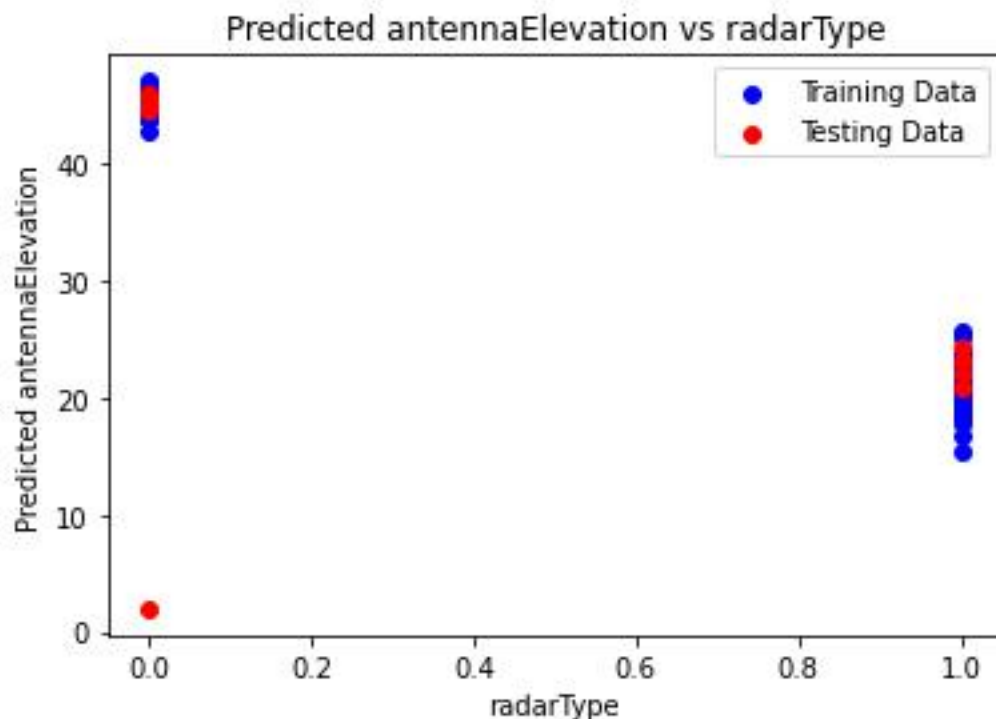
intercept 51.93620512220595

Equation: antennaElevation= 51.936205122 + -0.089056143 \* X + 0.000806656 \* Y +  
319181.852734038 \* OBJECTID + 19810.683996571 \* siteID + -0.111738867 \* siteName +  
1588.138424095 \* radarType + -9898.219131128 \* index^2 + -0.092237740 \* index^1\*X^1 +  
0.035165435 \* index^1\*Y^1 + -9898.222076919 \* index^1\*OBJECTID^1 + 29694.773209746  
\* index^1\*siteID^1 + 0.068886664 \* index^1\*siteName^1 + 11942.295462865 \*  
index^1\*radarType^1 + 0.000254298 \* X^2 + -0.000026467 \* X^1\*Y^1 + -0.092473680 \*  
X^1\*OBJECTID^1 + 0.182484532 \* X^1\*siteID^1 + 0.002026315 \* X^1\*siteName^1 + -  
0.127573786 \* X^1\*radarType^1 + -0.000798100 \* Y^2 + 0.028189975 \* Y^1\*OBJECTID^1 +  
-0.062531900 \* Y^1\*siteID^1 + 0.000728664 \* Y^1\*siteName^1 + 0.336444565 \*  
Y^1\*radarType^1 + -9898.219251254 \* OBJECTID^2 + 29694.775251924 \*  
OBJECTID^1\*siteID^1 + 0.070077371 \* OBJECTID^1\*siteName^1 + 11942.291721741 \*  
OBJECTID^1\*radarType^1 + -29694.887809176 \* siteID^2 + -0.137353548 \*  
siteID^1\*siteName^1 + -23912.025156738 \* siteID^1\*radarType^1 + -0.000296061 \*  
siteName^2 + 2.189224794 \* siteName^1\*radarType^1 + 1588.141252649 \* radarType^2 + -  
2476.264603361 \* index^3 + 0.013708305 \* index^2\*X^1 + 0.018548371 \* index^2\*Y^1 + -  
2476.264601003 \* index^2\*OBJECTID^1 + 9905.005306197 \* index^2\*siteID^1 + -  
0.018934322 \* index^2\*siteName^1 + 3586.525381385 \* index^2\*radarType^1 + 0.000578147  
\* index^1\*X^2 + -0.000290549 \* index^1\*X^1\*Y^1 + 0.013708627 \*  
index^1\*X^1\*OBJECTID^1 + -0.040719159 \* index^1\*X^1\*siteID^1 + 0.000013345 \*  
index^1\*X^1\*siteName^1 + -0.111230523 \* index^1\*X^1\*radarType^1 + -0.000196423 \*  
index^1\*Y^2 + 0.018551821 \* index^1\*Y^1\*OBJECTID^1 + -0.054947139 \*  
index^1\*Y^1\*siteID^1 + 0.000062841 \* index^1\*Y^1\*siteName^1 + -0.087400819 \*  
index^1\*Y^1\*radarType^1 + -2476.264602899 \* index^1\*OBJECTID^2 + 9905.005310254 \*  
index^1\*OBJECTID^1\*siteID^1 + -0.018933740 \* index^1\*OBJECTID^1\*siteName^1 +  
3586.525384435 \* index^1\*OBJECTID^1\*radarType^1 + -14857.429227533 \*  
index^1\*siteID^2 + 0.055720705 \* index^1\*siteID^1\*siteName^1 + -10756.802392854 \*  
index^1\*siteID^1\*radarType^1 + -0.000103175 \* index^1\*siteName^2 + -0.103465516 \*  
index^1\*siteName^1\*radarType^1 + 11942.291629467 \* index^1\*radarType^2 + 0.000000083  
\* X^3 + 0.000001564 \* X^2\*Y^1 + 0.000585528 \* X^2\*OBJECTID^1 + -0.001151112 \*  
X^2\*siteID^1 + -0.000007545 \* X^2\*siteName^1 + -0.003750790 \* X^2\*radarType^1 + -  
0.000000548 \* X^1\*Y^2 + -0.000288763 \* X^1\*Y^1\*OBJECTID^1 + 0.000573586 \*  
X^1\*Y^1\*siteID^1 + -0.000001456 \* X^1\*Y^1\*siteName^1 + 0.002259944 \*  
X^1\*Y^1\*radarType^1 + 0.013706643 \* X^1\*OBJECTID^2 + -0.040719775 \*  
X^1\*OBJECTID^1\*siteID^1 + 0.000013443 \* X^1\*OBJECTID^1\*siteName^1 + -0.111230542  
\* X^1\*OBJECTID^1\*radarType^1 + 0.040322168 \* X^1\*siteID^2 + -0.000029085 \*  
X^1\*siteID^1\*siteName^1 + 0.226230035 \* X^1\*siteID^1\*radarType^1 + -0.000001082 \*  
X^1\*siteName^2 + 0.000252220 \* X^1\*siteName^1\*radarType^1 + -0.127563606 \*  
X^1\*radarType^2 + 0.000004057 \* Y^3 + -0.000195811 \* Y^2\*OBJECTID^1 + 0.000388275 \*  
Y^2\*siteID^1 + -0.000002116 \* Y^2\*siteName^1 + 0.001144817 \* Y^2\*radarType^1 +  
0.018551139 \* Y^1\*OBJECTID^2 + -0.054947022 \* Y^1\*OBJECTID^1\*siteID^1 +

$$\begin{aligned}
&0.000060917 * Y^1 * OBJECTID^1 * siteName^1 + -0.087401012 * \\
&Y^1 * OBJECTID^1 * radarType^1 + 0.054249351 * Y^1 * siteID^2 + -0.000123155 * \\
&Y^1 * siteID^1 * siteName^1 + 0.167387270 * Y^1 * siteID^1 * radarType^1 + -0.000000215 * \\
&Y^1 * siteName^2 + 0.000416568 * Y^1 * siteName^1 * radarType^1 + 0.336563836 * \\
&Y^1 * radarType^2 + -2476.264602978 * OBJECTID^3 + 9905.005310053 * \\
&OBJECTID^2 * siteID^1 + -0.018934099 * OBJECTID^2 * siteName^1 + 3586.525384401 * \\
&OBJECTID^2 * radarType^1 + -14857.429226621 * OBJECTID^1 * siteID^2 + 0.055720784 * \\
&OBJECTID^1 * siteID^1 * siteName^1 + -10756.802392921 * \\
&OBJECTID^1 * siteID^1 * radarType^1 + -0.000103457 * OBJECTID^1 * siteName^2 + - \\
&0.103464956 * OBJECTID^1 * siteName^1 * radarType^1 + 11942.291629287 * \\
&OBJECTID^1 * radarType^2 + 9904.900935437 * siteID^3 + -0.054652244 * \\
&siteID^2 * siteName^1 + 10754.186798678 * siteID^2 * radarType^1 + 0.000203656 * \\
&siteID^1 * siteName^2 + 0.180778116 * siteID^1 * siteName^1 * radarType^1 + -23912.025226834 \\
&* siteID^1 * radarType^2 + 0.000001707 * siteName^3 + 0.002820725 * \\
&siteName^2 * radarType^1 + 2.189223888 * siteName^1 * radarType^2 + 1588.141248422 * \\
&radarType^3
\end{aligned}$$

Accuracy: 0.858191071825885

GRAPH:



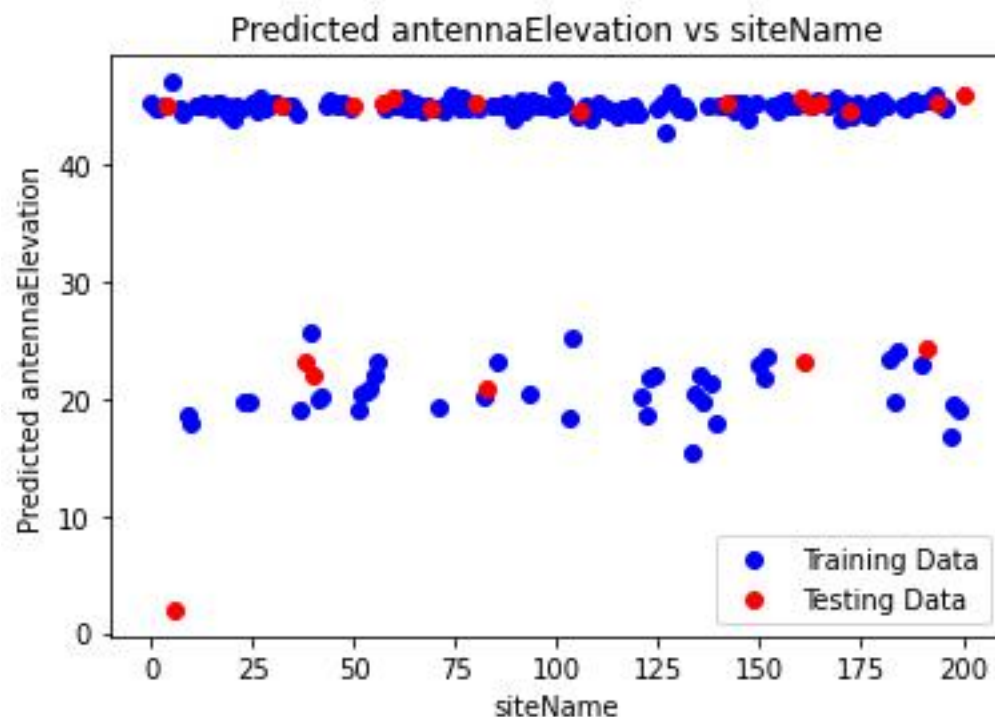
The plot provided illustrates the performance evaluation of a machine learning model deployed for a classification task, presumably predicting antenna elevation based on radar type.



On the x-axis, radar types are represented, ranging from 0.0 to 1.0, while the y-axis denotes the predicted antenna elevation. The blue line corresponds to the model's performance on the training data, reflecting its efficacy on the data it was trained on. Conversely, the red line depicts the model's performance on unseen testing data, showcasing its generalization ability.

Ideally, a close alignment between the blue and red lines would indicate robust generalization, suggesting that the model performs consistently well across both seen and unseen data. However, the noticeable gap between the blue and red lines suggests potential issues with generalization. This discrepancy implies that while the model may exhibit favorable performance on the training data, it fails to replicate this performance on unseen testing data, indicative of overfitting.

Overfitting occurs when a model excessively tailors itself to the idiosyncrasies of the training data, compromising its ability to discern broader patterns within the data. Consequently, despite performing well during training, overfitted models struggle to generalize effectively to new, unseen data. This discrepancy between training and testing performance underscores the need for model evaluation and potentially mitigative strategies to address overfitting.

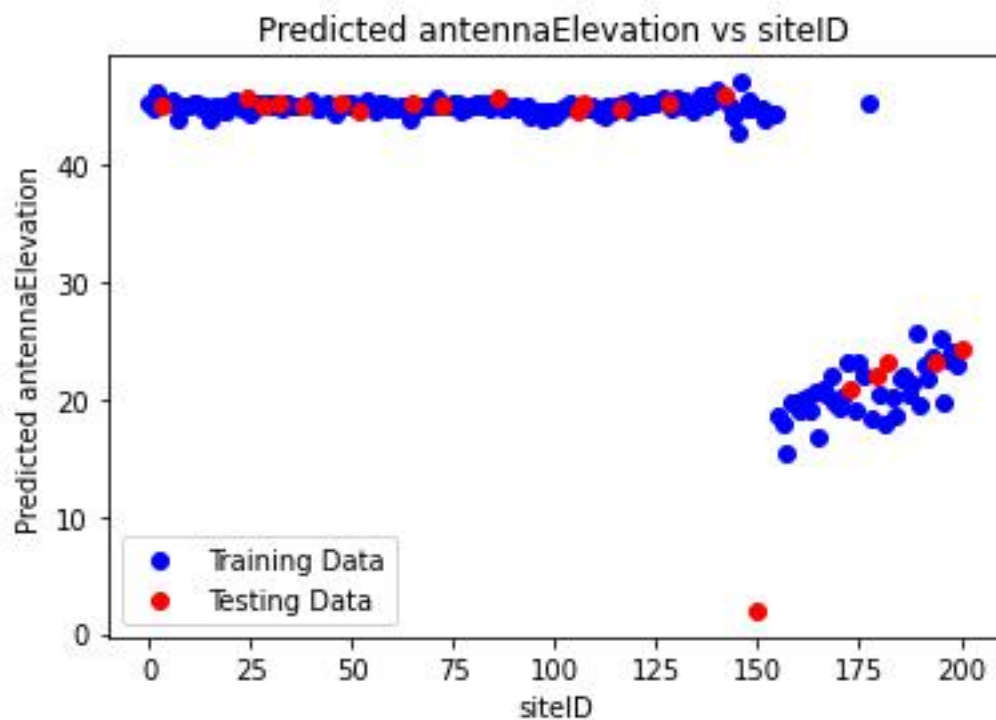


Based on the image provided, the plot illustrates the relationship between predicted antenna elevation and site names, with the training data represented in blue and the testing data in red.

Key observations from the plot include:

- The x-axis corresponds to the site names, indicating individual locations.
- Predicted antenna elevation is represented on the y-axis.
- Both the training and testing data exhibit a scattered distribution of points, indicating variability in predicted elevation across different sites.
- There is no discernible linear relationship between predicted antenna elevation and site name, as indicated by the lack of a clear trend in the data.
- The spread of data points appears wider for sites with higher predicted antenna elevation, suggesting greater variability in elevation predictions for these locations.
- Some overlap in data points between training and testing data suggests that the model predicts similar antenna elevation values for certain sites.

Overall, while the plot provides insights into the relationship between predicted antenna elevation and site names, it does not reveal a straightforward pattern or linear correlation. The presence of variability and overlap in data points suggests that site names may contribute to predicting antenna elevation, but other factors likely play a role as well. Further analysis and consideration of additional features may be necessary to fully understand the predictive relationship between site names and antenna elevation.

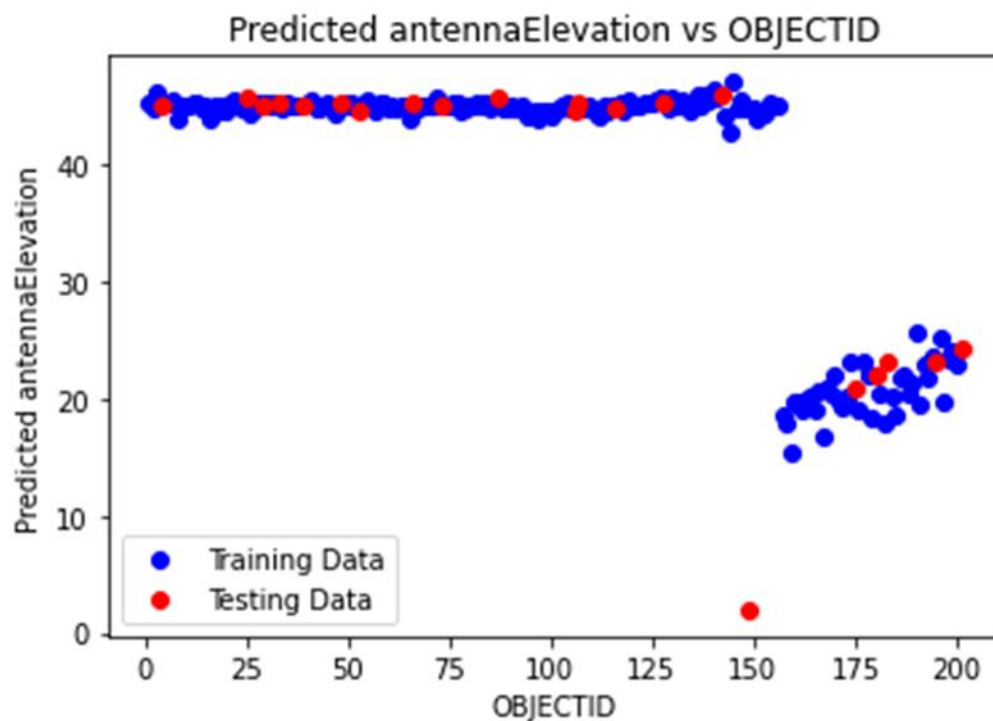


Based on the image provided, the scatter plot illustrates the relationship between predicted antenna elevation and siteID, with training data represented in blue and testing data in red.

Key observations from the plot include:

- The x-axis represents siteID, serving as a unique identifier for each site.
- Predicted antenna elevation is depicted on the y-axis.
- The plot does not exhibit a clear linear relationship between predicted antenna elevation and siteID, evident from the scattered distribution of data points across the plot.
- The spread of data points appears consistent across the range of siteIDs, suggesting uniform variability in predicted antenna elevation across different sites.
- Some overlap in data points between training and testing data indicates similarity in predicted antenna elevation values for certain sites.

Overall, while the plot provides insights into the relationship between predicted antenna elevation and siteID, it does not reveal a discernible pattern or linear correlation. This suggests that siteID alone may not be a significant predictor of antenna elevation. It is likely that other factors not depicted in this plot contribute more prominently to the model's predictions. Further analysis incorporating additional features may be necessary to better understand the predictive relationship between siteID and antenna elevation.

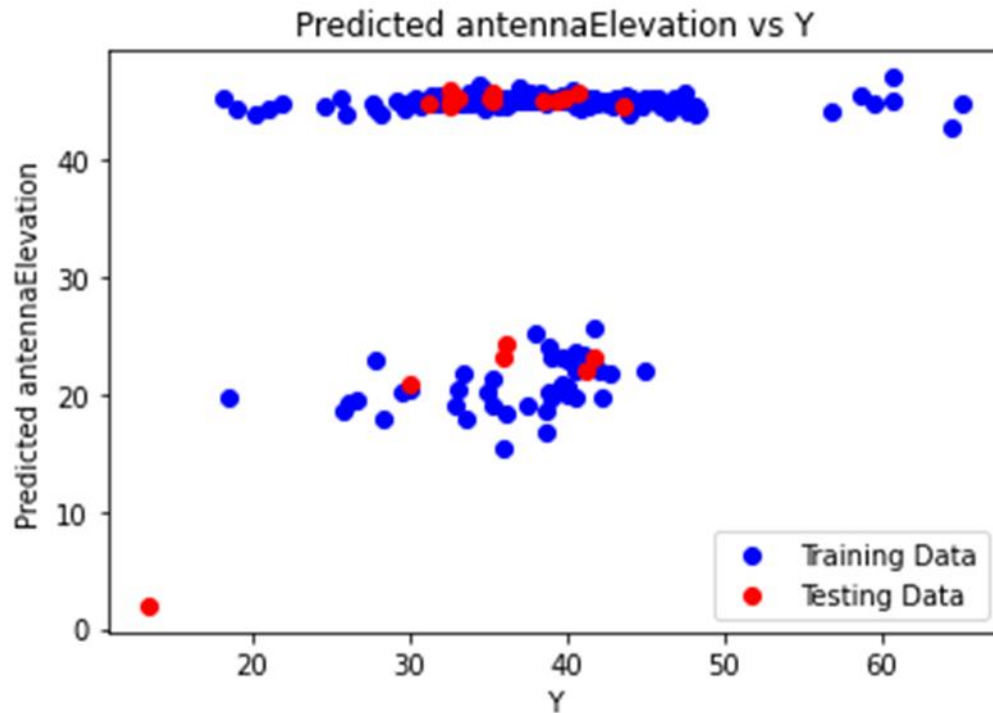


Based on the image you provided, the scatter plot illustrates the difference between predicted antenna elevation and objectid, with the predicted antenna elevation plotted on the y-axis and objectid on the x-axis. The training data is represented in blue, while the testing data is depicted in red.

Here are some observations from the plot:

- The x-axis displays the objectid, likely serving as a unique identifier for each data point.
- The y-axis represents the disparity between the predicted antenna elevation and the actual antenna elevation, indicated by objectid. Positive values denote instances where the model predicted a higher antenna elevation than the actual value, while negative values indicate instances where the model predicted a lower antenna elevation.
- The plot does not reveal a discernible pattern for either the training or testing data, suggesting that the model's predictions are not consistently biased towards over or underestimating antenna elevation.
- A spread of data points is observed around the zero line, indicating instances where the model's predictions closely align with the actual antenna elevation. However, deviations from the zero line suggest inaccuracies in the model's predictions.
- Some data points exhibit significant deviations from the zero line, both in the training and testing data, signifying substantial errors in the model's predictions for these specific sites.

Overall, the plot suggests that while the model's predictions of antenna elevation are not consistently accurate, it also does not exhibit a systematic bias towards over or underestimation. However, notable errors are evident for certain sites, indicating areas where the model's performance could be improved.



Based on the image provided, the plot illustrates the disparity between predicted and actual antenna elevations for both the training and testing datasets of a machine learning model.

- The x-axis denotes Y the difference between the predicted antenna elevation and the actual elevation, with positive values indicating overestimation by the model and negative values representing underestimation.
- The y-axis represents the predicted antenna elevation frequency or count of data points falling within each difference interval.

Here are key observations:

#### 1. Concentration Around Zero Difference:

- A substantial concentration of data points is observed around the zero difference mark on the x-axis for both the training (blue) and testing (red) datasets. This indicates instances where the model's predictions closely aligned with the actual antenna elevations.

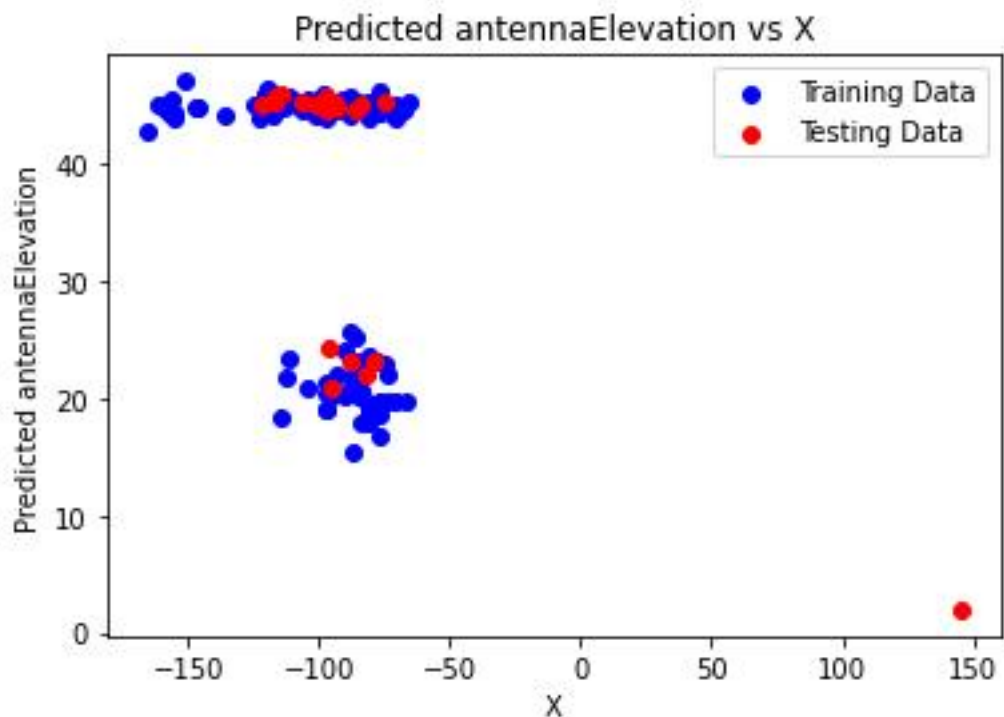
#### 2. Spread of Data Points:

- The distribution of data points appears to be wider for the testing set compared to the training set. This suggests that the model's predictions exhibit more variability when applied to unseen data (testing set) as opposed to the data it was trained on (training set).

### 3. Assessment of Model Performance:

- Overall, the model seems to perform reasonably well, as evidenced by the concentration of data points around zero difference. However, the wider spread of points in the testing set raises concerns about the model's generalization capability.

- The wider spread observed in the testing set could potentially indicate overfitting, where the model fits the training data too closely and struggles to generalize to new, unseen data.



The plot provided illustrates the comparison between predicted antenna elevation and a variable X, with the training data depicted in blue and the testing data in red.

Key observations from the plot include:

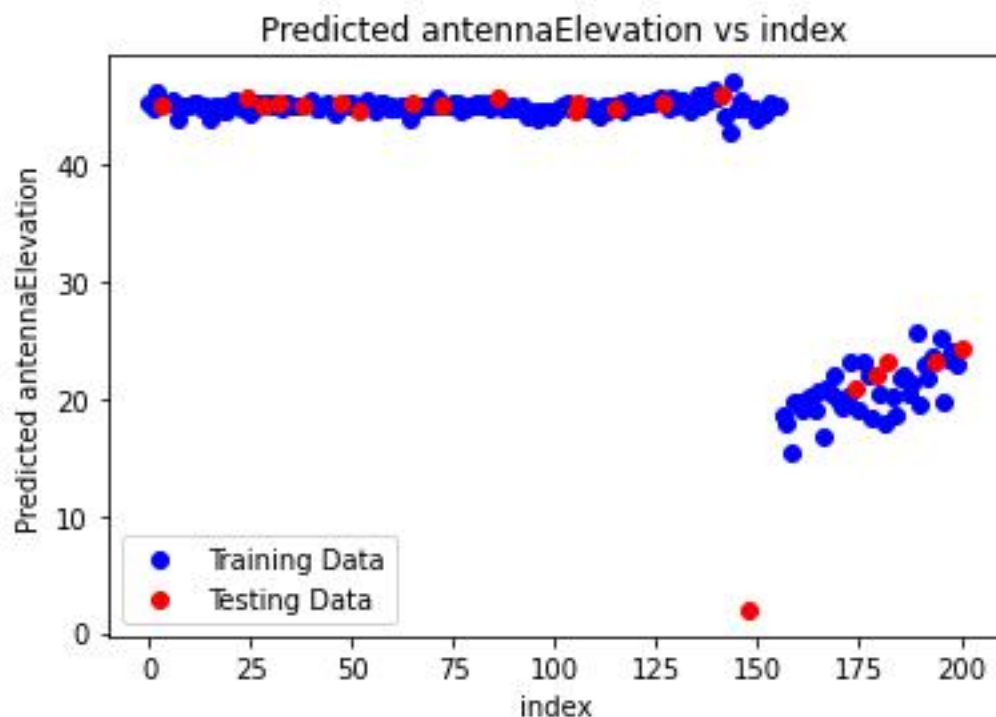
1. Training vs. Testing Performance: A notable distinction is apparent between the performance of the model on the training data (blue) versus the testing data (red). While the model appears to align closely

with the training data, its performance on the testing data seems to deviate, indicating potential disparities in predictive accuracy between the two datasets.

2. Potential Overfitting: The discrepancy in performance between the training and testing datasets suggests the possibility of overfitting. Overfitting occurs when a model captures noise or idiosyncrasies present in the training data, leading to reduced performance when applied to unseen data. The disparity observed in the plot could signify that the model has learned the training data too well, resulting in a lack of generalization to the testing data.

3. Dataset Disparities: Alternatively, differences in the characteristics or distribution of the training and testing datasets may contribute to the observed performance gap. If the datasets exhibit varying features or statistical properties, the model may struggle to accurately generalize from the training to the testing data.

while the plot provides valuable insights into the model's performance, further investigation into the cause of the observed disparities between the training and testing datasets is warranted. Understanding whether the discrepancies arise from overfitting, dataset disparities, or other factors is essential for refining the model and enhancing its predictive capabilities.



The provided plot depicts the relationship between predicted antenna elevation and an index variable. The blue line represents the predicted antenna elevation, while the red line represents the testing data.

Key observations from the plot include:

- The x-axis represents the index, which likely corresponds to a specific feature or variable utilized in predicting antenna elevation.

- The y-axis denotes the predicted antenna elevation.

- Training Data (Blue): The blue data points, representing the training data, are dispersed around the diagonal line. However, there appears to be a slight bias towards the upper left corner, indicating a tendency of the model to underestimate antenna elevation for the training data.

- Testing Data (Red): In contrast, the red data points, representing the testing data, exhibit greater dispersion and deviation from the diagonal line compared to the training data. This suggests that the model's performance on unseen data is less consistent, indicating potential issues with generalization.

the plot suggests that the model may exhibit a bias towards underestimating antenna elevation, and it demonstrates suboptimal generalization to unseen data. Possible reasons for these discrepancies could include inadequate training data or model complexity exceeding the variability present in the dataset.



# SHAP-INTERPRETATION:

